Multi-NFP Utilization in the Fifth Generation and Beyond Systems

by

HUDA YOUSEF ALSHEYAB

Graduate Program

in

Department of Electrical and Computer Engineering

A thesis submitted in partial fulfillment of the requirements

for the degree of Doctor of Philosophy (Ph.D.)

The Faculty of Graduate Studies

Lakehead University

Thunder bay, Ontario, Canada

May 2021

I hereby confirm that the entirety of the work contained therein is my own, original work, that I am the owner of the copyright thereof (unless to the extent explicitly otherwise stated).

I understand that my thesis may be made electronically available to the public.

Abstract

Over the past few years, wireless communication needs have experienced continuous growth. There is now a great demand for more sophisticated infrastructure to cope with the fifth generation and beyond (5G+) systems. 5G+ systems promise to provide better real-time services, more efficient spectrum utilization, increased energy efficiency, and enhanced coverage. 5G+ systems are expected to adopt several adaptations in their network architecture, construction, and deployment. The integration of Network Flying Platforms (NFPs) with 5G+ capabilities will allow much higher connectivity, lower latency, and quicker transfer of high-precision data. This aggregation of 5G+ networks and NFPs is robust, paving the way to the introduction of many new capabilities and improvements in wireless applications.

Resource allocation in wireless communication systems is one of the most critical issues when it comes to utilizing systems efficiently. In 5G+ cellular technology, the main research focus is on spectral efficiency, network throughput, and communication delays. Furthermore, this focus will continue to the next generation cellular systems. To support the communication of various internet of things (IoT) devices, especially unmanned aerial drones and balloons, next-generation cellular systems (5G+) will play a vital role. However, resource allocation will be a significant determinant in the effective use of such communications. Increasing network capacity while minimizing interference will be a significant research challenge. A different level of Quality of Service (QoS) for individual user levels will also need to be satisfied.

In this thesis, NFPs as aerial hubs are considered in future 5G+ networks to provide fronthaul connectivity to small cells (SCs)/ user equipment (UE). This thesis has different objectives. The first objective is to find the near optimal association between the NFPs and SCs to maximize the total sum rate subject to QoS, bandwidth, and the supported number of links constraints. The second objective is to study the association problem of SCs with NFPs in order to minimize the system interference while taking into consideration the number of NFP links, the NFP's maximum bandwidth, and the target data rate. The final objective is to deploy multiple UAVs for serving a group of UEs on the ground to maximize the total uploaded rate among all UEs by jointly optimizing the UAVs-UEs association, the UEs transmit power, and the UAVs trajectory.

Dedication

This thesis is dedicated to the memory of my beloved father '**Yousef ALSheyab**'. To whom I promised to dedicate this thesis before he left this world. I am forever grateful for his believing in my ability to succeed, more than myself, and for providing his endless support and love.

To my mother for her prayers and Dua.

To my husband and son for their support and endless love.

To my sisters, brothers and friends for their support.

To everyone who believes in me, I dedicate this thesis.

Acknowledgements

First and foremost, I thank Allah (SWT) for making me able to do this work "Alhamdullah".

This thesis would have never been made possible without the invaluable support of many people to whom these few lines will try to thank.

I would like to express my sincere gratitude to my supervisor, Dr. Salama Ikki, and my co-supervisors, Dr. Salimur Choudhary and Dr. Ebrahim Bedeer, for the trust they have given me by accepting to supervise this work as well as for their continued support, invaluable advice and encouragement throughout my PhD period. This work would have not been brought to completion without their expertise in formulating the research questions and methodology. Their insightful feedback pushed me to sharpen my thinking and brought my work to a higher level.

I warmly express my thanks to the committee members, Prof. Sanaa Sharafeddine , Prof. Rachid Benlamri, and Dr. Waleed Ejaz for agreeing to judge this work as reviewers and to give me constructive remarks that allow me to improve this thesis.

Last but not least, big thanks to my late father Yousef ALSheyab and my mother Aishah ALSheyab for their wise counsel, sympathetic ear, unconditional encouragement and their sacrifices. You were always there for me. I could have not completed this thesis without the support of my husband, Omar Qananeweh and my son Taim Qananeweh, who helped me to be strong enough to complete what I started. Finally, I would like to thank my brothers Mane'e, Wasel, Ma'amon and Hasan, sisters Bothaina, Ghadeer and Ghaidaa, my father-in-law, my mother-in-law, as well as my friends, for their love, support and prayers.

There are challenging moments in day to day living, while learning and achieving my goals. I built good working relationships which supported me during such moments. I learned to encourage myself and will stay determined in life. I am grateful for what I have achieved.

Table of Contents

List of Tables

List of Figures

Abbreviations

(DM)²S distributed maximal demand minimum servers algorithm 39, 54–56, 58, 60, 62

3D three dimensional 124, 125

4G fourth-generation 1

5G Fifth-generation 1, 25, 26, 32, 33, 63, 65, 124

5G+ fifth-generation and beyond 1, 2, 4–6, 25, 27, 29, 55, 63–65, 122

ABS Aerial Base Station 26

ATG air-to-ground 35, 36, 69, 124

BSs base stations 3, 22–24, 26, 93, 94, 96, 122

CHs cluster heads 116

CoMP coordinated multi-point 66

eMBB Enhanced mobile broadband 1

HAPs High-altitude platforms 24

HBCA Hungarian based centralized algorithm 40–45, 52–56, 58, 60–62, 87, 88, 92

HBIMTI Hungarian based initial minimum total interference 75, 76, 79, 81, 84–87, 91

HCN eterogeneous cellular networks 66

uMUB ubiquitous mobile ultra-broadband 1

URLLCs ultra rate low latency communication 1

Chapter 1

Introduction

1.1 Background and Motivation

The key drivers of conventional cellular systems, such as the fourth-generation (4G) of cellular systems and their predecessors, were designed to bear the challenges and performance of the human-centric applications, such as voice calls and mobile broadband connectivity. 4G was capable of providing high-speed connectivity to a specified number of users.

Fifth-generation (5G) was derived based on addressing the problems of the previous generations along with the purpose of providing connectivity for machine-centric applications. Thus, the core requirements for fifth-generation and beyond (5G+) are Enhanced mobile broadband (eMBB), ultra rate low latency communication (URLLCs), and massive machine-type communication (mMTC). The key-driven of 5G and 5G+ is the intelligence and the industrial revolution. Hence, the core requirements for 5G+ are the service classes of ubiquitous mobile ultra-broadband (uMUB), ultra high-speed-with-low-latency communications (uHSLLC), and ultra high data density (uHDD). While uMUB enables 5G+ systems to deliver any required performance within the space-aerial-terrestrial-sea area, uHSLLC provides ultra high speed with low latency communication, and uHDD meets the data density and high-reliability requirements [1].

5G+ cellular networks are anticipated to fulfill the presumptions and challenges of the near future and meet high-end user requirements. Thus, 5G+ networks are expected to bring extremely efficient mobile Internet, and better optimized networks, by capitalizing the ability to transfer large amounts of data with exceptional speed. 5G+ is predicted to increase the number of connected devices, and the network coverage, as well as increase their availability. There will also be significant enhancement in the battery life for low power devices, and a reduction of the energy consumed by network. New technologies are therefore necessary towards the realization of these goals [2].

The key technologies that can be used in 5G+ wireless systems to satisfy the expected performance are massive multiple-input and multiple-output (mMIMO), device to device communication, spectrum sharing with cognitive radio, ultra dense networks, multi-radio access technology, full duplex communication, millimeter wave communication, energy harvesting communication and cloud technologies [3, 4]. Fiber has been used for fronthaul links in the previous cellular networks; however, it has disadvantages including high cost and the need to minimize time-to-market [5, 6]. On the other hand, free-space optical (FSO)/microwave links are cost-effective, easy to deploy and carry traffic for small cell (SCs) from the core network. Unfortunately, FSO/microwave systems lead to less coverage due to short-range communication, and are affected by any obstacles or animals in the environment, consequently hindering transmission. Furthermore, FSO is affected by weather such as rain, snow, and fog. In contrast to fiber and FSO, network flying platforms (NFPs), such as (unmanned aerial vehicles (UAVs)), drones, and unmanned balloons are cost-effective and scalable.

The use of NFP is rapidly growing. NFPs are functional, reliable, and affordable, and as a result, NFP-based solutions for new markets have started becoming more and more competitive. The previous features make it possible to widely deploy NFPs, such as drones, small aircrafts, balloons, and airships, for wireless communication purposes [7, 8, 9, 10].

NFPs are capable of hovering at an altitude ranging from a few hundred meters to about 20 km to mitigate unfavorable weather conditions [11], which cannot be achieved using a fixed FSO/microwave. In terms of communication, NFPs can be used as flying aerial base stations to support the connectivity of existing terrestrial wireless networks.

Compared to terrestrial base stations, NFPs are able to avoid obstacles, adjust their location (including relative altitude), and enhance the solidification of the probability of line-of-sight (LoS) communication links to ground users. Moreover, NFPs have attracted industrial and academic attention during the past couple of years [12, 13] as candidate solutions to support the coverage of dense networks.

Due to the UAVs mobility, flexibility, and ability of adapting their altitude, the advantage of using UAVs as flying base stations (BSs) compared to conventional/terrestrial base stations, is the ability of UAVs to avoid obstacles and enhance the capability of establishing LoS communication links to ground users. Therefore, UAV base stations equipped with existing terrestrial cellular systems can effectively provide additional capacity for urban areas and network coverage in hard-to-reach rural areas.

In the one hand, NFPs can be used as BSs that provide power-efficient, cost-effective, reliable on-demand wireless connectivity for ground users as alternative future technology. NFPs as BSs can be used for the dynamic network, deploying network quickly in emergency, or temporarily provide coverage for an area. On the other hand, NFPs can act as flying user equipment (UE). For instance, an NFP equipped with necessary sensors can be a cost-efficient solution for surveillance, inspection, and delivery.

NFPs can be used in Internet of things (IoT) applications where the devices have small transmit power and are able to communicate over a short range. Thus, UAVs can be used as wireless relays to improve the connectivity and coverage of the ground wireless devices [14, 15, 16, 17]. Moreover, building a complete cellular infrastructure in some regions and countries can be very expensive; therefore; deploying UAVs, instead of expensive towers and infrastructure deployment, is highly advantageous.

1.2 Objectives and Contributions of the Thesis

The main objective of this thesis is to efficiently utilize NFPs as flying aerial base stations to support the connectivity of existing terrestrial wireless networks in future cellular systems, such as 5G+ systems. This thesis addresses some of the main challenges of utilizing the NFPs in cellular systems. In addition, it proposes new solutions and enhancements for achieving better communication system. The main contributions of the thesis can be summarized as follows:

1. Near-Optimal resource allocation algorithms for 5G+ cellular networks. A heterogeneous network that consists of SCs, NFPs, and the ground core network was studied along with the association problem between NFPs with SCs to maximize the network total sum rate. Two algorithms (centralized and distributed) are proposed, where each NFP is associated with one or more SCs, while ensuring that necessary quality-of-service (QoS) requirements are met. Thus, a centralized resource allocation is designed based on a weighted bipartite matching algorithm (Hungarian algorithm) to find the best association between NFPs and SCs that maximizes the system's total sum rate subject to QoS constraints (the SINR). Moreover, a distributed algorithm based on a stable marriage matching scheme is designed to maximize the total sum rate, while requiring only local information of NFPs and SCs, subject to QoS constraints.

2. Interference minimization algorithms for 5G+ systems. An ultra-dense SCs network is an approach to serve 5G+ systems requirements including higher data rate, energy efficiency, and spectrum utilization. However, this large number of SCs will increase the overall system interference. Therefore, achieving a target data rate with minimal total system interference is an important research problem.

The research community has addressed several 5G+ issues, such as the total sum rate, total consumed power and coverage. However, the interference minimization

issue was often overlooked. 5G+ systems need to provide high data rates for an ultra-dense network of SCs along with low interference and widespread coverage. Interference minimization is an important research problem in the 5G+ systems.

3. Studying a multi-UAV enabled wireless communication system, where multiple UAVs are operated to serve a group of UEs on the ground, with the goal of maximizing the total uploaded rate among all UEs by jointly optimizing the UAVs-UEs association, the UEs transmit power control, and the UAVs trajectory in a given period of time. Two scenarios are considered, namely, offline and online. In the offline scenario, we propose an iterative algorithm to optimize the UAVs-UEs association using a modified Hungarian algorithm. Next, the UEs transmit power is optimized using a logarithmic approximation and the Lagrange equation. Finally, the UAVs trajectory is optimized using the UAVs trajectory in an interior-point algorithm alternately over all the time slots. However, in the online scenario, we assume fixed transmit power of UEs and find closed-form expressions of the optimal UAVs-UEs associations. The simulation results show that the performance of the online solution approaches its counterpart of offline solution with lower computational complexity.

1.3   Thesis Outline

The structure of the thesis is organized as follows:

Chapter 2 introduces some relevant background on NFPs. In particular, the NFPs classifications are explained. Then, the wireless networking with NFPs is elucidated. After that, the research tools are introduced.

Chapter 3 considers resource allocations for SCs with NFPs in order to maximize the system total sum rate subject to QoS. An introduction, followed by the related work are presented. Then, chapter 3 presents the system model and problem formulation. After that, chapter 3 talks about an existing work and proposes better solutions. The proposed solutions time and message are analysed. The performance of the proposed solutions is

presented. Finally, chapter 3 provides a brief conclusion.

Chapter 4 presents the interference minimizing algorithms for 5G+ while satisfying a minimum data rate target. In this regard, in chapter 4 the introduction and prior research and the contributions of the research are discussed. After that, chapter 4 proposes the system model and the problem formulation. Then, the proposed solutions are illustrated. The following section evaluated and presented the complexity performance of the proposed solutions. After that, the proposed system performance evaluation is exhibited. Finally, the conclusion of chapter 4 is presented.

Chapter 5 discuss the multi-UAV enabled wireless networks user association and power allocation with trajectory optimization. Chapter 5 starts with an introduction. After that, the used system model is presented and the problem of maximizing the total uploaded rate for a multi-UAV enabled wireless network is formulated. Then, two efficient iterative algorithms are proposed to solve the "offline" and "online" scenarios. In addition, numerical results are presented to demonstrate the performance of the proposed algorithms. Finally, we conclude chapter 5.

In Chapter 6, we introduce a summary of our investigation and work conclusions. We also put forward number of remaining future research challenges that we did not solve yet.

1.4 List of Publications

1. H. Y. AlSheyab, S. Choudhury, E. Bedeer and S. Ikki, "Near-Optimal Resource Allocation Algorithms for 5G+ Cellular Networks," *IEEE Transactions on Vehicular Technology*, vol. 68, no. 7, pp. 6578-6592, Jul. 2019.

2. H. Y. AlSheyab, S. Choudhury, E. Bedeer, S. Ikki, "Interference minimization algorithms for fifth generation and beyond systems", *Elsevier Computer Communications*, Special Issue on Unmanned Aerial, vol. 156, pp. 145-158, Apr.2020.

3. H. Y. AlSheyab, E. Bedeer, S. Choudhury, S. Ikki, "Joint User Association and Power Allocation with Trajectory Optimization for Multi-UAV Enabled Wireless Networks", Submitted to *IEEE Transactions on Signal and Information Processing over Networks*, 2021.

7

Chapter 2

Background

2.1 Global vs Local Optimal Solution

A global optimum is the minimum or maximum of the objective function for the entire input search space. A local optimal solution is the minimum or maximum of the objective function for a given region of the input space. An objective function may have many local optimal solution. However, it can have a single global optimal solution.

In fact, every local optimal solution is globally optimal in convex optimization. This is not true with non-convex optimization in general. For an optimization problem to be convex, the objective function to be minimized (maximized) and the inequality constraint functions should be convex (concave), and the equality constraint functions should be affine. Generally, the optimal solution for the non-convex optimization problems are hard to find, and there may exist many local optimal solutions which are not global optimal. It is theoretically and practically difficult to check whether a given local optimal solution is globally optimal, and this prevents the development of efficient solution methods [18].

2.2 Integer Linear Programming (ILP)

Integer Linear Programming (integer linear program (ILP)) is a mathematical optimization technique that be used to describe a large number of optimization problems. ILP

models have two parts: a cost function and a set of constraints. Both the cost function and the constraints are a linear function of integer.

ILP is a variant of linear programming (LP). In LP, the variables can take any real values not only an integer values. ILP and LP models can be solved optimally. Regrettably, ILP is NP-complete and it's take up to an exponential execution times in worst case. Therefore, ILP technique is useful for solving the optimization problems. Thus, the execution times depend on the number of variables and on the number and structure of the constraints [19]. The ILP can be written on the form

$$\max_x \quad cx,$$

$$\text{subject to} \quad Ax \leq b,$$

$$x \geq 0,$$

where A is $m \times n$ matrix , c is n-dimensional row vector, b is m-dimensional column vector, and x n-dimensional column vector of unknown variables. If some but not all variables x are integer, we have a mixed integer linear program (MILP). If all variables are integer, we have an ILP.

There are different algorithms use to solve ILP, such as cutting plane methods which first solves the LP relaxation, after that adds linear constraints to find the integer solution without missing any integer feasible points [20]. Another algorithm uses to solve ILP is the branch and bound method. Branch and bound algorithms more beneficial than cutting plan method, since it can be ended early when at least one feasible integral solution is found [21, 22]. Moreover, branch and bound methods can return optimal solutions.

To understand the ILP, consider in the following example of formulating an ILP problem.

2.2.1 Integer Linear Program Example

Consider the example of a manufacturer of babies feed who is producing food mix for babies. The food mix contains two active ingredients and water. Each one kg of the food mix should include a minimum quantity of each of the four nutrients shown in Table 2.1:

Table 2.1: The Nutrients

Nutrients	A	B	C	D
gram	90	50	20	2

The ingredients nutrient values and costs are shown in Table 2.2. Therefore, what is

Table 2.2: The Ingredients Values and Costs

	A	B	C	D	Cost/kg
Ingredient 1	100	80	40	10	40
Ingredient 2	200	150	20	-	60

the amounts of active ingredients and water in one kg of food mix?

- Mixing problem Variables

  To solve this problem each food mix kilogram is made up of three parts - ingredient 1, ingredient 2 and water, therefore, x_1 = amount (in kg) of ingredient 1 in one kg of food mix, x_2 = amount (in kg) of ingredient 2 in one kg of food mix, x_3 = amount (in kg) of water in one kg of food mix, where $x_1 >= 0$, $x_2 >= 0$ and $x_3 >= 0$.

- Objective "minimize the cost"

  minimise $40x_1 + 60x_2$

- Constraints

  1. Balancing constraint $x_1 + x_2 + x_3 = 1$

  2. Nutrients constraints

     $100x_1 + 200x_2 \geq 90$ (Nutrients A)

$$80x_1 + 150x_2 \geq 50 \text{ (Nutrients B)}$$

$$40x_1 + 20x_2 \geq 20 \text{ (Nutrients C)}$$

$$10x_1 \geq 2 \text{ (Nutrients D)}$$

3. Additional conditions

   (a) If we use any of ingredient 2 we incur a fixed cost of 15

   (b) We need to satisfy three of the nutrients constraints

   These new two constraints give the complete MILP formulation of the problem.

- Mixing problem formulation

  To deal with the condition that if $x_2 \geq 0$ we incur a fixed cost of 15, we have introducing a zero-one variable y defined by

$$y = \begin{cases} 1, & \text{if } x_2 \geq 0, \\ 0, & \text{Otherwise,} \end{cases}$$

  and add a term $+15y$ to the objective function and add the additional constraint $x_2 \leq$[largest value x_2 can take]y.

  We can see that x_2 can never be greater than one, therefore, the additional constraint is $x_2 \leq y$.

  To deal with the condition that we need only satisfy three of the four nutrients constraints we introduce four zero-one variables z_i, $i \in 1, 2, 3, 4$ where

$$z_i = \begin{cases} 1, & \text{if nutrients constraint } i \in 1, 2, 3, 4 \text{ is satisfied,} \\ 0, & \text{Otherwise,} \end{cases}$$

  and add the constraint

  $z_1 + z_2 + z_3 + z_4 \geq 3$.

  Then, change the nutrients constraints to be:

  $100x_1 + 200x_2 \geq 90z_1$,

$$80x_1 + 150x_2 \geq 50z_2,$$

$$40x_1 + 20x_2 \geq 20z_3,$$

$$10x_1 \geq 2z_4.$$

If a $z_i = 1$ then the constraint becomes the original nutrients constraint which needs to be satisfied. However, if $z_i = 0$ then the original nutrient constraint becomes greater than or equal to zero, which is always true and so can be neglected. Hence, the complete problem formulation of the problem is given by

$$
\begin{aligned}
\textbf{Objective:} \quad \min \quad & 40x_1 + 60x_2 + 15y, \\
\textbf{subject to} \quad & x_1 + x_2 + x_3 = 1, \\
& 100x_1 + 200x_2 \geq 90z_1, \\
& 80x_1 + 150x_2 \geq 50z_2, \\
& 40x_1 + 20x_2 \geq 20z_3, \\
& 10x_1 \geq 2z_4, \\
& z_1 + z_2 + z_3 + z_4 \geq 3, \\
& x_2 \leqslant y, \\
& z_i \in 0, 1, i \in 1, 2, 3, 4, \\
& y \in 0, 1, \\
& x_i \geq 0, i \in 1, 2, 3, 4.
\end{aligned}
$$

2.3 Local Search

Local search is a heuristic solution for finding a locally optimal solution to the optimization problems. Local search algorithm tries to find improved solutions by considering perturbations "neighbors" of the current solution.

The local search algorithm's main idea is to start with an initial solution and move from neighbor to neighbor solution as long as the neighbor solution is better. The neighborhood

relation should be defined on the search space. Normally, every expected solution has more than one neighbor solution; therefore, the information about the solutions in the neighborhood of the current one is used to choose which neighbor solution to move to.

The local search solver tries to move to every neighbor to the current solution and picks the best accepted neighbor as the next solution. The algorithm stops either when it finds a global optimal solution, in this case the problem is solved, or if all neighboring solution is worse than the current solution, then the current solution is locally optimal. In the latter case the algorithm may be restarted from a different initial random feasible point [23, 24].

2.4 Hungarian Algorithm

Hungarian algorithm is a combinatorial optimization algorithm, where it has been used to solve the assignment problem in polynomial time to find maximum-weight matching [25]. The Hungarian algorithm consists of four steps. The first two steps are executed one time, while steps 3 and 4 are repeated until an optimal assignment is found. The input of the algorithm is an $n \times n$ square matrix with a non-negative elements.

1. Subtract row minima: for each row, find the lowest element and subtract it from each element in that row.

2. Subtract column minima: similarly, for each column, find the lowest element and subtract it from each element in that column.

3. Cover all zeros with a minimum number of lines: cover all zeros in the resulting matrix using a minimum number of horizontal and vertical lines. If n lines are required, an optimal assignment exists among the zeros. The algorithm stops. If less than n lines are required, continue with the next step.

4. Create additional zeros: find the smallest element (call it k) that is not covered by a line in step 3. Subtract k from all uncovered elements, and add k to all elements

that are covered twice.

Note that for an input of $n \times n$ square matrix the Hungarian algorithm is an optimal one to one matching algorithm, and its worst computational complexity is $O(n^3)$. To understand the Hungarian algorithm, consider the numerical example in the the following subsection.

2.4.1 Hungarian Algorithm Example

We consider an example where four jobs (J_1, J_2, J_3, J_4) need to be executed by four workers (W_1, W_2, W_3, W_4), as one job per worker. The matrix below shows the cost of assigning a certain worker to a certain job. This problem objective is to minimize the total cost of the jobs-workers assignment.

	J_1	J_2	J_3	J_4
W_1	82	83	69	92
W_2	77	37	49	92
W_3	11	69	5	86
W_4	8	9	98	23

The following steps explain the Hungarian algorithm using this example.

- Step 1: subtract row minima. We start with subtracting the row minimum element from each row. The smallest element in the first row is 69. Therefore, we subtract 69 from each element in the first row. The resulting matrix is

	J_1	J_2	J_3	J_4
W_1	13	14	0	23
W_2	40	0	12	55
W_3	6	64	0	81
W_4	0	1	90	15

- Step 2: subtract column minima. Same as step 1, we subtract the column minimum element from each column, which giving the following matrix

	J_1	J_2	J_3	J_4
W_1	13	14	0	8
W_2	40	0	12	40
W_3	6	64	0	66
W_4	0	1	90	0

- Step 3: cover all zeros with a minimum number of lines. Determine the minimum number of lines (horizontal or vertical) that are required to cover all zeros in the matrix. In this example all zeros can be covered using 3 lines

	J_1	J_2	J_3	J_4
W_1	13	14	0	8
W_2	40	0	12	40
W_3	6	64	0	66
W_4	0	1	90	0

Since the required number of covering line is less than the size of the matrix (3 covering lines $<$ n=4), we continue with step 4.

- Step 4: create additional zeros. Start by finding the smallest uncovered number which is 6. Then, subtract this number from all uncovered elements and add it to all elements, which lie at the intersection of two lines. Thus, we obtain another reduced matrix as follows repeat Step 3.

	J_1	J_2	J_3	J_4
W_1	7	8	0	2
W_2	40	0	18	40
W_3	0	58	0	60
W_4	0	1	96	0

- Step 3: cover all zeros with a minimum number of lines. Again, We determine the minimum number of lines required to cover all zeros in the matrix.

Since the required number of covering lines (4) equals to the size of the matrix (n=4), an optimal jobs-workers assignment is among the zeros in the matrix. Therefore, the algorithm stops.

	J_1	J_2	J_3	J_4
W_1	7	8	0	2
W_2	40	0	18	40
W_3	0	58	0	60
W_4	0	1	96	0

- The optimal assignment. The following zeros cover an optimal assignment:

	J_1	J_2	J_3	J_4
W_1	7	8	0	2
W_2	40	0	18	40
W_3	0	58	0	60
W_4	0	1	96	0

This corresponds to the following optimal assignment in the original cost matrix:

	J_1	J_2	J_3	J_4
W_1	82	83	69	92
W_2	77	37	49	92
W_3	11	69	5	86
W_4	8	9	98	23

Thus, worker 1 should perform job 3, worker 2 job 2, worker 3 job 1, and worker 4 should perform job 4. The total cost of this optimal assignment is $69+37+11+23 = 140$.

2.5 Gale–Shapley Algorithm (Stable Marriage Problem)

The stable marriage problem is the problem of finding the preferable match for each element of two equally sized sets. The matching is different from the elements of one set to the elements of the other set. the Gale–Shapley algorithm is an algorithm for solving the stable matching problem.

To understand Gale–Shapley algorithm, suppose that we have two equally sized sets of men and women and each one of them looking for his/her best match. Thus, the

Gale–Shapley algorithm comprises a number of repeated steps

1. Each un-engaged man proposes to the woman he prefers most, then the woman replies "maybe" to her most prefers man and "no" to all other men. Therefore, she will be engaged to her most prefers man so far, and that man is likewise engaged to her.

2. Each un-engaged man proposes to the most-preferred woman whom he has not yet proposed (regardless of whether the woman is already engaged). Then, each woman replies "maybe" if she is not engaged or if she prefers this man more than her current partner (thus, she rejects her current partner and he becomes un-engaged).

3. This process is repeated until everyone is engaged.

The computational complexity of this algorithm is $O(n^2)$ where n is the number of men or women [26]. To understand the Gale–Shapley algorithm, consider the numerical example in the the following subsection.

2.5.1 Gale–Shapley Algorithm Example

Consider the problem of matching 4 men with 4 women. Each man has an ordered preference list of the 4 women, and each woman has a similar list of the 4 men.

Member	Preferable list			
M_1	W_1	W_2	W_3	W_4
M_2	W_2	W_1	W_4	W_3
M_3	W_2	W_3	W_4	W_1
M_4	W_3	W_1	W_4	W_2
W_1	M_1	M_3	M_4	M_2
W_2	M_1	M_2	M_3	M_4
W_3	M_1	M_2	M_3	M_4
W_4	M_4	M_3	M_2	M_1

- Step 1: Since M_1 is the first free man, M_1 browse through his women preference list. He find that his first choice W_1 is still free. So M_1 and W_1 get engaged.

Member	Preference list			
M_1	W_1	W_2	W_3	W_4
M_2	W_2	W_1	W_4	W_3
M_3	W_2	W_3	W_4	W_1
M_4	W_3	W_1	W_4	W_2
W_1	M_1	M_3	M_4	M_2
W_2	M_1	M_2	M_3	M_4
W_3	M_1	M_2	M_3	M_4
W_4	M_4	M_3	M_2	M_1

- Step 2: Next free man is M_2. M_2 go through his preferences list. He find that his most preference is W_2 who still free. Therefore, M_2 and W_2 get engaged.

Member	Preference list			
M_1	W_1	W_2	W_3	W_4
M_2	W_2	W_1	W_4	W_3
M_3	W_2	W_3	W_4	W_1
M_4	W_3	W_1	W_4	W_2
W_1	M_1	M_3	M_4	M_2
W_2	M_1	M_2	M_3	M_4
W_3	M_1	M_2	M_3	M_4
W_4	M_4	M_3	M_2	M_1

- Step 3: The next free man is M_3. M_3 first preference is W_2 who is engaged. To resolve this, W_2 go through the her preferences. W_2 prefers M_1, who is already engaged to another woman. Then, W_2 is already engaged to M_2 and prefers M_2 more than M_3. Therefore, M_3 check the next woman in his preference list. He find that W_3 is the next one. Note that W_3 is free so M_3 and W_3 get engaged.

Member	Preference list			
M_1	W_1	W_2	W_3	W_4
M_2	W_2	W_1	W_4	W_3
M_3	W_2	W_3	W_4	W_1
M_4	W_3	W_1	W_4	W_2
W_1	M_1	M_3	M_4	M_2
W_2	M_1	M_2	M_3	M_4
W_3	M_1	M_2	M_3	M_4
W_4	M_4	M_3	M_2	M_1

- Step 4: The last free man is man 4. His preferences is W_3 who is engaged and prefers her partner more than M_4. Then, M_4 check his next preferred who is W_1. W_1 is also engaged and prefers her partner. Therefore, M_4 check the next woman in his preference list, who is W_4. W_4 is free. Hence, M_4 and W_4 get engaged.

Member	Preference list			
M_1	W_1	W_2	W_3	W_4
M_2	W_2	W_1	W_4	W_3
M_3	W_2	W_3	W_4	W_1
M_4	W_3	W_1	W_4	W_2
W_1	M_1	M_3	M_4	M_2
W_2	M_1	M_2	M_3	M_4
W_3	M_1	M_2	M_3	M_4
W_4	M_4	M_3	M_2	M_1

- Now all men and women are engaged. Therefore, the optimal solution of the given problem in the following table.

Man	Woman
M_1	W_1
M_2	W_2
M_3	W_3
M_4	W_4

2.6   The Lagrangian Method

The Lagrangian multiplier method is a strategy for finding the local maxima and minima of a multi-variable function $f(x, y)$, subject to equality constraints $g(x, y) = c$ [27]. The Lagrangian method can be briefly explained as follows. To find the maximum or minimum of a function $f(x)$ subjected to the equality constraint $g(x) = 0$,

1. Define a new variable λ, and define a new function $\mathcal{L}$ as follows:

$$\mathcal{L}(x, y, \lambda) = f(x, y) - \lambda(g(x, y) - c), \tag{2.3}$$

where the function $\mathcal{L}$ is called the Lagrangian function and λ is the Lagrangian multiplier.

2. Set the gradient of $\mathcal{L}$ equal to the zero vector to find the critical points of $\mathcal{L}$.

$$\nabla \mathcal{L}(x, y, \lambda) = \mathbf{0}, \tag{2.4}$$

3. Take into consideration all returned solutions (x_0, y_0, λ_0) and substitute it in f, after removing the λ_0 since function f does not have λ as input. Any one gives the greatest (or smallest) value is the maximum (or minimum) point we are seeking. Note that the Lagrangian method does not guarantee global optimal solution. In the following subsection, we consider an numerical example to understand the Lagrange multiplier method.

2.6.1 Lagrangian Method Example

Consider the problem of maximizing $f(x, y) = x + y$ subject to the constraint $x^2 + y^2 = 1$. The feasible set is the unit circle, and the level sets of f are diagonal lines. Therefore, the maximum occurs at $\left(\frac{\sqrt{2}}{2}, \frac{\sqrt{2}}{2} \right)$ and the minimum occurs at $\left(-\frac{\sqrt{2}}{2}, -\frac{\sqrt{2}}{2} \right)$.

The problem can be written as follows

$$\max \quad f(x, y) = x + y \tag{2.5a}$$

$$\text{subject to} \quad g(x, y) = x^2 + y^2 = 1 \tag{2.5b}$$

- Step 1: For using the Lagrangian method we can rewrite the constraint as follows

$$g(x, y) = x^2 + y^2 - 1 = 0. \tag{2.6}$$

- Step 2: Define the Lagrangian multiplier λ and the Lagrangian function $\mathcal{L}$ as

follows

$$\mathcal{L}(x, y, \lambda) = f(x, y) + \lambda g(x, y) \tag{2.7}$$

$$= x + y + \lambda(x^2 + y^2 - 1) \tag{2.8}$$

- Step 3: Calculate the gradient of $\mathcal{L}$ and set it equal to zero vector to find the critical points of $\mathcal{L}$.

$$\nabla_{x,y,\lambda}\mathcal{L}(x, y, \lambda) = \left(\frac{\partial \mathcal{L}}{\partial x}, \frac{\partial \mathcal{L}}{\partial y}, \frac{\partial \mathcal{L}}{\partial \lambda} \right) \tag{2.9}$$

$$= (1 + 2\lambda x, 1 + 2\lambda y, x^2 + y^2 - 1) \tag{2.10}$$

Therefore,

$$\nabla_{x,y,\lambda}\mathcal{L}(x, y, \lambda) = 0 \Leftrightarrow \begin{cases} 1 + 2\lambda x = 0, \\ 1 + 2\lambda y = 0, \\ x^2 + y^2 - 1 = 0. \end{cases} \tag{2.11}$$

Thus, from the $1 + 2\lambda x = 0$ and $1 + 2\lambda y = 0$ we can see that

$$x = y = \frac{1}{2\lambda}, \quad \lambda \neq 0, \tag{2.12}$$

by substituting x and y into $x^2 + y^2 - 1 = 0$ we find:

$$\lambda = \pm\frac{1}{\sqrt{2}}. \tag{2.13}$$

Hence, the stationary points of $\mathcal{L}$ are

$$\left(\frac{\sqrt{2}}{2}, \frac{\sqrt{2}}{2}, -\frac{1}{\sqrt{2}} \right), \left(-\frac{\sqrt{2}}{2}, -\frac{\sqrt{2}}{2}, \frac{1}{\sqrt{2}} \right). \tag{2.14}$$

21

4. Step 4: Substitute the stationary points in the objective function. Thus,

$$f\left(\tfrac{\sqrt{2}}{2}, \tfrac{\sqrt{2}}{2}\right) = \sqrt{2}, \quad f\left(-\tfrac{\sqrt{2}}{2}, -\tfrac{\sqrt{2}}{2}\right) = -\sqrt{2}. \tag{2.15}$$

Therefore, the constrained maximum is $\sqrt{2}$ and the constrained minimum is $-\sqrt{2}$.

2.7   NFP Classifications

NFPs are available in different sizes and specifications. In this section, the classifications, characteristics, and features of NFPs are summarized and explained with particular focus on their impact on NFP-aided cellular communications. NFPs can be assorted into different categories according to various criteria such as functionality, weight/payload, size, endurance, wing, configuration, control methods, cruising range, flying altitude, maximum speed, and energy supplying methods.

2.7.1   Payload

Payload refers to the maximum weight the NFP can carry, and essentially measures its carriage ability. NFP payload can be a few grams or up to hundreds of kilograms [28]. As the payload increases, the size of NFP needs to be larger, which requires higher battery capacity, and which leads to shorter duration in the air. Usually the payloads are used to carry video cameras and sensors; and this allows for usage in exploration, surveillance and commercial purposes [29]. On the other hand, payloads can be used to assist cellular communications. They can carry mobile phones or tablets, with weights less than one kilogram [30]. Moreover, NFPs can carry BSs or remote radio heads (RRHs). In this case, the payload of NFPs are at least a few kilograms.

2.7.2   Flying Mechanism

Based on their flying mechanisms (or wings), UAVs can be categorized into three types:

- **Rotary Wings**: rotary-wing drones use vertical take-off and landing, can hover over a fixed location to provide continuous cellular coverage for certain areas. This ability makes them suitable for the deployment of BSs at specific locations with high precision or to fly in a specified trajectory while carrying the BSs . However, they have limited mobility and experience high power consumption, since they fly against gravity all the time.

- **Fixed Wings**: fixed-wing drones can fly off over the air, which makes them more energy-efficient while carrying a heavier payload, and they can also fly at faster speeds. On the other hand, the drawbacks of this type are that they require a runway to take off and land [31], they cannot hover over a fixed location, and they are more expensive than rotary-wings UAVs.

- **Hybrid Fixed/Rotary Wing**: hybrid fixed/rotary wing drones are a combination between the two above-mentioned drone types. They can take off vertically, they are very fast and can reach their destination by gliding in the air. Then, they can switch to hovering over designated locations using the rotors.

2.7.3   Altitude

The altitude is the maximum height a drone can reach, regardless of the regulations. The flying altitude of an NFP is an important parameter for utilizing NFP cellular communications, since an NFP BS needs to change its attitude to maximize the ground coverage and satisfy the different QoS requirements [32]. Hence, NFPs can be classified into two types depending on their altitude:

- **Low-altitude platforms (LAPs)**: LAPs are more cost-effective and allow fast deployment. Hence, they are utilized to assist cellular communications. LAPs provide short-range Line-of-Sight (LoS) links that can considerably enhance communication performance [33, 34, 35].

- **High-altitude platforms (HAPs)**: HAPs can also provide cellular connectivity. HAPs have wider coverage and can stay much longer in the air, compared to LAPs. However, the deployment of HAPs is more complex. HAPs used to provide Internet coverage to large regions of the world that were not served by cellular networks. Using HAPs in cellular communications is more susceptible to a network outage, on account of considerably large inter-cell interference [36, 37]. Therefore, they are rarely examined in the UAV-aided cellular networks in previous works.

2.7.4 Speed and Flying Time

NFP speeds vary between 15 m/s for the smaller sizes and a maximum speed of 100 m/s for larger ones [33, 38]. When utilizing NFPs as BSs, NFPs fly in a specific trajectory to enhance their energy and spectral efficiency; therefore if an NFP requires frequent turns, the trajectory and the speed need to be carefully considered [39]. NFP flight time (or endurance) is the maximum time an NFP can spend in the air without needing to recharge or refuel.

NFP flight times range between 20-30 minutes for small commercial NFPs and a few hours for large NFPs [40]. The new technologies have extended the endurance of small NFPs to achieve an endurance of up to 4.5 hours with hybrid-electric power sources [41]. The endurance of NFPs is one of the most important factors that restrict their full-scale deployment in cellular networks.

2.7.5 Power Supply

NFP endurance depends on its power supply. On one hand, NFPs can use rechargeable battery power like most commercial NFPs. On the other hand, NFPs can use fuels such as gas as a source of power for longer endurance like the large NFP [42]. Another technique that can be used in powering the NFP is by employing solar energy [43]. For BS NFPs, the power supply needs to support the functionality of both drone flying and its equipment

such as antenna array, amplifier, circuits, etc. [44, 45, 46].

The widespread use of NFP technologies increases the concerns regarding privacy, data protection, and public safety [47, 48, 49]. These concerns, express the need to develop the NFP Regulations.

NFP regulations are formed and developed, based on the aforementioned concerns. Current NFP regulations are mainly based on the applicability, technical requirements, operational limitations, administrative procedures, and implementation of ethical constraints [50].

2.8   Wireless Networking with NFPs

5G and 5G+ aim for systems with higher capacity, increased data rate, and reduced latency. Moreover these systems are expected to be energy efficient and capable of handling massive device connectivity [51]. The intensive distributed terrestrial networks in urban areas require high data rate access. Recently, it is widely believed that the existing networks cannot meet the need to process enormous volumes of data and execute fundamental applications such as IoT, cloud computing, and big data.

The expectation of 5G and 5G+ to transfer high data demand a large bandwidth. Demanding a high-bandwidth solution require using lower wavelength waves, which can be achieved by utilizing LoS propagation. Having LoS is challenging compared with lower frequency propagation. Thus, the terrestrial systems are used to provide network in complex propagation areas. On the other hand, satellite links are used in areas can not be covered by the terrestrial systems.

NFPs at high altitudes provide line of sight propagation. NFPs can serve broadband wireless service. NFPs can cover an area with a radius up to 30Km which help to reduce the number of terrestrial base stations in suburban and rural areas. NFPsis cost effective when compared with satellite, which require an expensive lunching[52].

Therefore, developing an integrated network architecture from the air-based network (using NFP) and the ground-based network is the growing trend among research communities. Using NFPs in wireless communications supports the existing cellular communications with cost efficiency to fulfill the hurried service recovery and offer the traffic offloading of the highly congested areas [53].

Carrying telecommunications equipment on NFPs allows NFPs to act as flying cell sites for mobile cellular communication networks. These cell sites have all the capabilities of a conventional mobile cell, and add new capacity. NFP cell sites can be deployed quickly and conveniently. Thus, NFP cells can play an important role in the early stages of restoring communications in the damaged areas.

NFPs can be used as flying UEs. The flying UEs can take advantage of existing infrastructure (such as cellular networks) to communicate with the ground operator with certain reliability, throughput and delay, depending on the application requirements. This leads to address new challenges such as studying the flying UEs optimal height to maximize the coverage of the flying UEs, minimizing the required transmitted power for covering a target area as well as investigating the optimal deployment of the flying UEs [54].

Furthermore, NFPs can be used as BSs that provide power-efficient wireless connectivity for ground users in the alternative future technology. Aerial Base Station (ABS) mobility and flexibility help to provide additional capacity-on-demand. ABS can be used by service providers for the dynamic network, deploying network quickly in emergency, or coverage temporarily providing for an area. ABS complements the existing cellular systems to expand the capacity and provides coverage in difficult-to-reach rural areas. The cell planning problem in 5G to determine the number and the location of ABS is an important challenge. Research works to minimize deployment costs to meet coverage and capacity constraints with the minimum number of ABS [55].

Moreover, the regulators of drone operations can dictate when to operate the NFPs depending on the weather conditions. An example of practical applications for NFPs

that are capable of operating in different weather conditions is weather hyphen resistant drones equipped with a built-in WiFi chip to support all-time connectivity even during rainy, snowy, stormy, and/or windy weather [56].

Furthermore, artificial intelligence can be used to predict weather conditions and improve the operation of NFPs [57]. As can be seen from the previous discussion, the effect of poor weather conditions on the NFPs can be reduced or at least controlled, which is not the case in the FSO/ microwave links. Another advantage of NFPs is that they can be considered an affordable solution to extend coverage in rural areas that do not have the required infrastructure [58]. NFPs also assist in maintaining communication in case of failure of the existing infrastructure as a result of disasters such as: earthquakes, tsunamis, flooding, and land sliding [59, 60, 61]. It is expected that NFPs can overcome the shortcomings of the fiber and FSO in 5G+ systems [11].

The integration of NFPs with 5G+ capabilities will allow much greater connectivity, lower latency, and quicker transfer of high-precision data. This aggregation of 5G+ networks and NFPs is powerful, giving way to many new capabilities and improvements in wireless applications. In comparison with the static ground macro base station, NFPs are more scalable. The integration of NFPs into wireless and mobile networks is expected to bring higher spectral efficiency and solutions to many communication challenges. The rapid and dynamic deployment of NFPs and their reliable LoS communication links are the main advantages of NFP-based communications. NFPs also assist in maintaining the communications in case of failure of the existing infrastructure that may happen in case of disasters such as: earthquakes, tsunami, flooding, and land sliding [59, 60, 61].

Wireless communication with NFPs is significantly different from its terrestrial counterparts due to the high probability of NFP-ground LoS channels, the high altitude and high mobility of UAVs, the size, weight and power (SWAP) constraints of NFPs, as well as the QoS requirements. The differences between NFP based networks and terrestrial networks can be summarized as shown in Table 2.3

Table 2.3: NFP Network versus terrestrial network.

	Terrestrial System	NFP System
Mobility	• Nodes usually move randomly (e.g., in a MANET) • Nodes move with predetermined path (e.g., mobile robotics) • Very restrictive path planning • Mostly fixed and static. • No timing constraints, BS always there.	• NFP mobility highly controllable/ predictable • More flexible path adaptation in 3D space • Mobility dimension. • Hover and flight time constraints.
Communication channel	• Difficult to predict offline • Suffer more severe path loss due to shadowing and multi-path fading effects	• UAV-BSs/relays are more likely to have LoS connection with their ground users • More reliable links for communication as well as multiuser scheduling and resource allocation. • Less shadowing and fading • More predictable • Air-ground channel
Coverage	• 2D coverage for terrestrial users. • Mainly static association.	• Coverage support of the NFP communications beyond the terrestrial coverage of cellular network. • The high NFP altitude requires cellular BSs to offer 3D aerial coverage for users • Changing cell association.
Deployment	• Difficult to deployed • 2D point deployment for terrestrial BSs. • Mostly long-term, permanent deployments. • Few, selected locations.	• NFP BSs can be freely deployed in 3D space • NFP-mounted BSs/relays can be swiftly deployed on demand • NFP-BSs/relays possess an additional degree of freedom (DoF) for communication performance enhancement, by dynamically adjusting their locations in 3D • Short-term, frequently changing deployments. • Mostly unrestricted locations.
Energy consumption	• Polynomial and increasing function of speed • Well-determined energy limitations and models.	• More complicated • Limited onboard energy of NFPs • Proper modelling for NFP energy consumption is crucial. • NFPs are subject to the additional propulsion energy consumption to remain aloft and move freely. • Detailed and strict energy limitations and models.

The importance of developing the air-ground network in 5G+ wireless communications is increasingly growing. However, its realization is facing a lot of challenging tasks including air-to-ground channel modelling, resource allocation, optimal deployment, energy efficiency, path planning, and network security. This work formulates and attempts to solve some of the most pressing challenges in the following chapters.

Chapter 3

Near-Optimal Resource Allocation Algorithms for 5G+ Cellular Networks

3.1 Introduction

Few algorithms (centralized and distributed) have been proposed to connect air drones and balloons with traditional small cells of the cellular network while maximizing the system capacity. In this work, a heterogeneous network that consists of SCs, NFPs, and the ground core network is studied as well as the association problem between NFPs with SCs to maximize the network total sum rate is also studied. Two algorithms (centralized and distributed) are proposed, where each NFP is associated with one or more SCs. We ensure that necessary QoS requirements are met.

Practical constraints were included in our optimization problem, such as considering interference between NFPs and SCs, the maximum number of links and the maximum bandwidth that the NFP can support. NFPs act as a hub to provide fronthaul connectivity between the SCs and the core network. Hence, the association problem of SCs

and NFPs is an important problem to enhance the performance of the system. These algorithms enhance the running time speed and perform a greedy search with higher data rate demands.

The main contributions of this work can be summarized as follows.

- We design a centralized resource allocation based on a weighted bipartite matching algorithm (Hungarian algorithm) to find the best association between NFPs and SCs that maximizes the system's total sum rate subject to QoS constraints signal to noise and interference ratio (SINR). This guarantees the performance while satisfying all constraints and notably outperforming other existing algorithms.

- We design a distributed algorithm based on a stable marriage matching scheme to maximize the total sum rate, while requiring only local information of NFPs and SCs, subject to QoS constraints. The main advantage of this distributed algorithm is the reduction of the necessary feedback overhead, hence reducing the system complexity.

- Furthermore, we compare our work with what is studied in [62]. Indeed, our solution is different from [62] and this difference can be explained as follows. The SCs in [62] send association requests to the NFP with the highest SINR. Each NFP selects the SCs depending on its available bandwidth and number of links. The distributed algorithm in [62] does not re-associate the rejected SCs with other NFPs. To overcome this drawback, in our proposed distributed algorithm we used the staple marriage matching algorithm which guarantees that each SC is matched with one NFP (either real or dummy).

- Finally, we provide extensive simulation results to assess the performance of the proposed algorithms in realistic conditions.

31

3.2 Related Work

A few years ago, the NFPs utilization in wireless communication starts to attract research and industry. Thus, Mozaffari *et al.* [63] proposed an approach for deploying UAVs to provide wireless service to ground users while minimizing the overall UAV transmit power needed to satisfy the users' data rate. Hence, they tried to derive the optimal coverage area and locations of UAVs that minimize the required transmit power. The power allocation problem for the downlink transmission in a spectrum sharing multi-tier 5G environment was studied in [64]. They proposed an online learning based approach to assigning transmission power to reduce the overall power consumption while maintaining QoS. Also, the scheme employed an approximation mechanism for the Q-value, which reduced the state/action space and accelerate the speed of convergence.

A framework for optimizing UAV-enabled wireless networks was proposed in [65]. The authors took into consideration the flight time constraints of UAVs. They had investigated two UAV-based communication scenarios. First, they maximized the average data service to ground users, taking into consideration the maximum possible hover times of UAVs. Second, they minimized the average hover time of UAVs needed to completely serve the users given the load requirements.

In one hand, Ghanavi *et al.* [66] used NFP as an aerial-base station (BS). They attempted to find the optimal placement of the aerial-BS to improve the system performance. Additionally, the SINR was considered the only QoS of the system. On the other hand, the authors in [67], found the 3D placement and solved the association problem of the drone-BS. They took into consideration some constraints such as the data rate, maximum bandwidth of each drone-BS, and path loss. They provided two approaches: the network-centric approach to maximize the total number of served users regardless of their required rates, and the user-centric approach which maximizes the sum rate.

The association problem of NFPs and SCs for the network is one of the most impor-

tant issues of using NFPs in wireless communication. In one hand, serving the maximum number of SCs without any consideration (like the total sum rate) was proposed in [68]. Their work presented two simple greedy algorithms, centralized and distributed algorithms. Thus, centralization was used when the system needed to decrease power consumption and distribution was used when it needed to reduce latency. On the other hand, a fully distributed algorithm to maximizes the number of associated users was designed in [69] while taking into consideration the QoS requirements in a heterogeneous and small cells network (HetSNet). This piece of work proposed a completely distributed algorithm which assumes no coordination between the base stations. Furthermore, The association problem of NFP-hubs and SCs to find the maximum total sum rate of the system was studied in [62]. They took into consideration some constraints like maximum supported bandwidth and number of links per NFP. Moreover, the association problem of UAVs and users was investigated in [70], to maximize the sum data rate along with minimize the inter-cell interference. Thus, they considered interference between UAVs instead of users. Furthermore, they included a practical constraint involving backhaul data rate. They presented a heuristic algorithm to solve the presented NP-hard problem.

As shown, there are a lot of works that tried to solve different resource allocation problems in 5G. However, they had a different system model and problem formulation than here, and their solutions may not suit our problem. Most of the work related to NFPs use them to enhance network coverage and other arguments.

The rest of this chapter is organized as follows: Section 3.3 describes the proposes system model. Section 3.4 provides the proposed solution and existing work. Section 3.5 discusses the computational complexity analysis. Section 3.6 discusses the performance analysis and results. Finally, Section 3.7 concludes this chapter.

3.3 System Model

The intensive distributed terrestrial networks in urban areas assist the high data rate
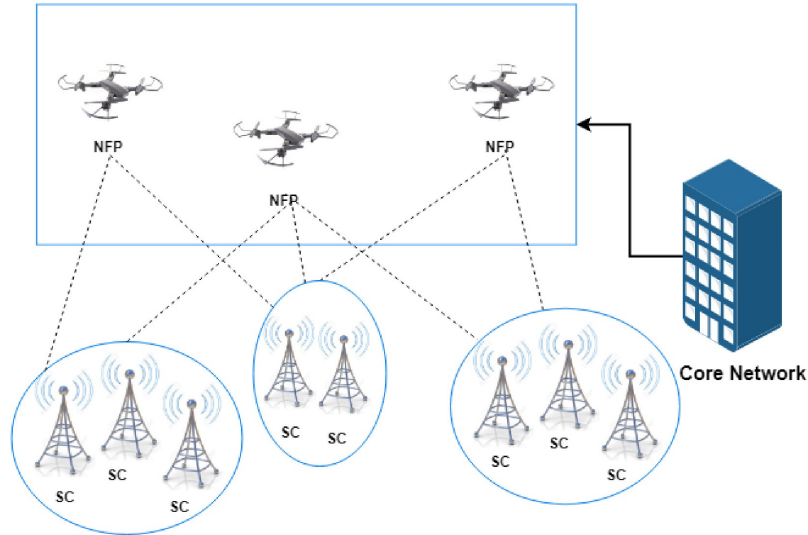
Figure 3.1: Graphical illustration of NFPs and SCs in 5G+.

access. Using NFPs communications can support the existing cellular communications with cost efficiency to fulfil the hurried service recovery and offer traffic offloading of highly congested areas [53]. Presently, it is widely believed that the existing network cannot meet the need to process enormous volumes of data and execute fundamental applications such as IoT, cloud computing, and big data. Therefore, developing an integrated network architecture from the air-based network (using NFPs) and ground-based network is a growing trend among scientific communities.

This section presents the system model of the NFPs and SCs association which has been used in this chapter.

As shown in Fig. 3.1, a heterogeneous network is investigated, which includes three categories of wireless nodes: ground SCs, NFP-hubs, and the ground core network. The SCs carry the traffic directly between the end users and the core network using fronthaul links; while the NFPs act as a hub to provide additional fronthaul connectivity between SCs and the core network. The system model in [68] and [62] is considerably similar to ours, but it is worth mentioning that our proposed algorithms are divergent. In particular, [62] proposed a distributed algorithm to solve the association problem between NFPs and SCs; however, in our work we proposed a more efficient distributed algorithm and a

centralized algorithm to address the same association problem.

On the other hand, the problem formulation in [68] maximizes the number of associated SCs and NFPs which is different than our problem formulation that targets maximizing the total sum rate. NFPs can be considered an affordable solution to extend coverage in rural areas that do not have the required infrastructure [58].

It is assumed that the NFPs are placed at a pre-defined height h_D (i.e., LAP, MAP, and HAP) according to safety and security policies [62] and uniformly distributed on a horizontal plane parallel to the ground; while, SCs are uniformly distributed on the ground level. This section considers a system with I NFPs and J SCs pairs ($I << J$) where the set of NFPs is represented as $F = \{f_1, f_2, ..., f_I\}$ and the set of SCs is represented as $S = \{s_1, s_2, ..., s_J\}$. NFPs are denoted as f_i, $1 \leq i \leq I$ and SCs are denoted as s_j, $1 \leq j \leq J$. To facilitate the implementation of the centralized algorithm, NFPs can share the control information (required bandwidth, required data rate, and SINR) with the core network for association purposes. Based on the control information, the system can specify the association between SCs and NFPs. However, this does not include the data information.

In this system model, the s_j requested bandwidth the from f_i can be represented as $b_{i,j}$. It has also been assumed that each NFP has a different number of links to support the communication with SCs, i.e., each NFP can serve one or more SCs depending on the number of links L_i, and maximum bandwidth it can support B_i,

Since NFPs are spread in a horizontal parallel plane to the SCs at a height h_d from ground level, we use the air-to-ground path loss channel model; this is in contrary to the conventional terrestrial communications that use log-distance path loss model. Thus, the wireless link between NFPs and SCs is mainly vertical. Hence, in the following subsection, the air-to-ground (ATG) path loss model is discussed.

3.3.1 Air-to-Ground Path Loss Model

The same ATG path loss (PL) model is used as in [62], which is widely adopted in the NFP literature [11]. The adopted ATG model considers two propagation groups: *i*) LoS receivers where the SCs are placed in LoS / near-LoS to the NFPs and *ii*) Non-line-of-sight (NLoS) receivers where SCs depend on reflections and refraction for coverage. One factor that plays an important role in determining the PL in the ATG model is the probability of LoS. This depends on the surrounding environment (urban, rural, etc.) and the orientation of NFPs and SCs. Hence, the probability of LoS is formulated as in [62]

$$P(\text{LoS}) = \frac{1}{1 + \alpha \exp[-\beta(\frac{180}{\pi}\theta - \alpha)]}, \tag{3.1}$$

where α and β are constants depending on the environment (rural, urban, etc) and $\theta = \arctan(\frac{h_D}{s})$ is the angle between the SC and the NFP, where $s = \sqrt{(x - x_D)^2 + (y - y_D)^2}$ is the horizontal distance between the SC and the NFP. The locations of the SCs and NFPs in the Cartesian coordinate are given as (x, y) and (x_D, y_D, h_D), respectively. The average PL is given as

$$PL(d)|_{\text{dB}} = 10 \log \left(\frac{4\pi f_c d}{c} \right)^{\gamma} + \eta_{\text{LoS}} \, P(\text{LoS}) + \eta_{\text{NLoS}} \, P(\text{NLoS}), \tag{3.2}$$

where $PL(d)|_{\text{dB}}$ represents the free space path loss in dB, f_c is the carrier frequency, c is the speed of light, γ is the PL exponent, and $d = \sqrt{h_D^2 + s^2}$ is the distance between the NFP and SC. η_{LoS} and η_{NLoS} represent the additional losses of the LoS and NLoS links, and $P(\text{NLoS}) = 1 - P(\text{LoS})$.

This system model denotes the requested data of the s_j associated with the f_i by $r_{i,j}$, where Shannon capacity formula is used to compute $r_{i,j}$ in bps, and we denote the association between the s_j and the f_i by $A_{i,j}$ that can be formally defined as

$$A_{i,j} = \begin{cases} 1, & \text{if } f_i \text{ is connected with } s_j, \\ 0, & \text{Otherwise.} \end{cases}$$

36

Thus, the data rate supported by the f_i is $\sum_{j=1}^{J} r_{i,j}.A_{i,j}$ and the total sum rate over all NFPs is $\sum_{i=1}^{I} \sum_{j=1}^{J} r_{i,j}.A_{i,j}$.

The SINR between the s_j and the f_i is defined as

$$\text{SINR}_{i,j} = \frac{P_{i,j}PL(d_{i,j})}{\sum_{k=1,k \neq i}^{I} P_{k,j}PL(d_{k,j}) + \sigma_i^2}, \tag{3.3}$$

where $P_{k,j}$ is the transmit power from f_k to s_j and σ_i^2 represents the received noise power at the f_i and $d_{i,j}$ is the distance between f_i and s_j. The Interference depend on path loss in equation (3.2).

3.3.2 Problem Formulation

This work aims to find the optimal association between SCs and NFPs to maximize the total sum rate subject to constraints on the QoS and the maximum number of links and bandwidth supported by each NFP. The QoS constraint should guarantee that the $\text{SINR}_{i,j}$ is greater than a minimum required value $\text{SINR}_{\min}$. Hence, the QoS constraint can be expressed as

$$A_{i,j}.\text{SINR}_{\min} \leq \text{SINR}_{i,j}, \quad \forall\, i, j. \tag{3.4}$$

The bandwidth constraint can be formulated as

$$\sum_{j=1}^{J} A_{i,j}.b_{i,j} \leqslant B_i, \quad \forall\, i. \tag{3.5}$$

The maximum number of links that the f_i can support is declared as L_i. Hence, the number of NFP links constraint can be expressed as

$$\sum_{j=1}^{J} A_{i,j} \leqslant L_i, \quad \forall\, i. \tag{3.6}$$

The maximum number of links that the s_j can support is one link. Hence, the number

of SC links constraint can be formulated as

$$\sum_{i=1}^{I} A_{i,j} \leqslant 1 \ , \quad \forall \, j. \tag{3.7}$$

Taking into consideration all constraints mentioned previously, for a specific time when NFPs and SCs have fixed positions, this work seeks to find the association between the SCs and the NFPs in order to maximize total sum rate of the system. The SC association with NFP problem can be formulated as

$$\max_{A_{i,j}} \ \sum_{i=1}^{I} \sum_{j=1}^{J} r_{i,j}.A_{i,j} \tag{3.8a}$$

$$\text{subject to} \tag{3.8b}$$

$$A_{i,j}.\text{SINR}_{\min} \leq \text{SINR}_{i,j}, \quad \forall \, i,j. \tag{3.8c}$$

$$\sum_{j=1}^{J} A_{i,j}.b_{i,j} \leqslant B_i \ , \quad \forall \, i. \tag{3.8d}$$

$$\sum_{j=1}^{J} A_{i,j} \leqslant L_i \ , \quad \forall \, i. \tag{3.8e}$$

$$\sum_{i=1}^{I} A_{i,j} \leqslant 1 \ , \quad \forall \, j. \tag{3.8f}$$

$$A_{i,j} \in \{0,1\} \ , \quad \forall \, i,j. \tag{3.8g}$$

This is an integer linear program that can be solved numerically to get the optimal solution. However, in worst case the system will try to connect each NFP with all SCs to find the best association and this can take exponential time [71]. Therefore, this is an NP-hard problem as explained in [72], which proves that the provided association problem is equivalent to NLoS. Using this relation with the NLoS, they show the NP-hard complexity of the association problem (the problem can be reduced to a maximum knapsack problem [73]). In the coming section, two polynomial-time algorithms to obtain sub-optimal solutions are proposed.

3.4 Proposed and Existing Solutions

3.4.1 Existing Solution

A distributed maximal demand minimum servers algorithm ($(\mathbf{DM})^2\mathbf{S}$) is proposed in [62] to provide an efficient solution of the optimization problem (3.8). They have proposed a greedy method to solve the association problem. The major steps of the algorithm are:

1. Each SC sends a message to the NFP with the maximum SINR. Basically, each SC wants to connect that NFP which will give it the best SINR value.

2. Once an NFP receives messages (an NFP can get messages from more than one SC), it selects that SC to be connected with which will maximize the total sum rate along with satisfying maximum NFP bandwidth and links constraints.

Lemma 1 In the worst case, the performance of $(\mathbf{DM})^2\mathbf{S}$ is unbounded.

Proof Consider a scenario where there is J SCs ($s_1, s_2, ...s_J$) and 2 NFPs (f_1, f_2). Now, if SINR of each SCs and f_1 is the same say, $\text{SINR}_{1,j}$, for all j. And for all j, $\text{SINR}_{2,j}$ is same too as shown in Fig. 3.2. Now, if $\text{SINR}_{2,j} = \text{SINR}_{1,j} - \epsilon$ where ϵ is a very small constant, then all SCs will send message to f_1 as shown in Fig. 3.3 .

Assume that f_1 has only one link available and f_2 has $(J-1)$ available links. After sending messages from all SCs, f_1 eventually will only consider one small cell. Now, if all SCs provide the same data rate (say r for every connection) and f_1 picks one of them (say s_1). Hence, at the end of the algorithm, only one SC will be connected as shown in Fig. 3.3. No small cell will be connected with f_2 since no message was sent to f_2.

The total sum rate of this solution will be r. On the other hand, as one can see in Fig. 3.4, in an optimal solution, total $J * r$ can be obtained by connecting one small cell to f_1 and the rest with f_2. Hence, the performance ratio of $(\mathbf{DM})^2\mathbf{S}$ is $\frac{r}{J*r}$ which $\frac{1}{J}$ which is unbounded (will be increase with the increase of small cells).
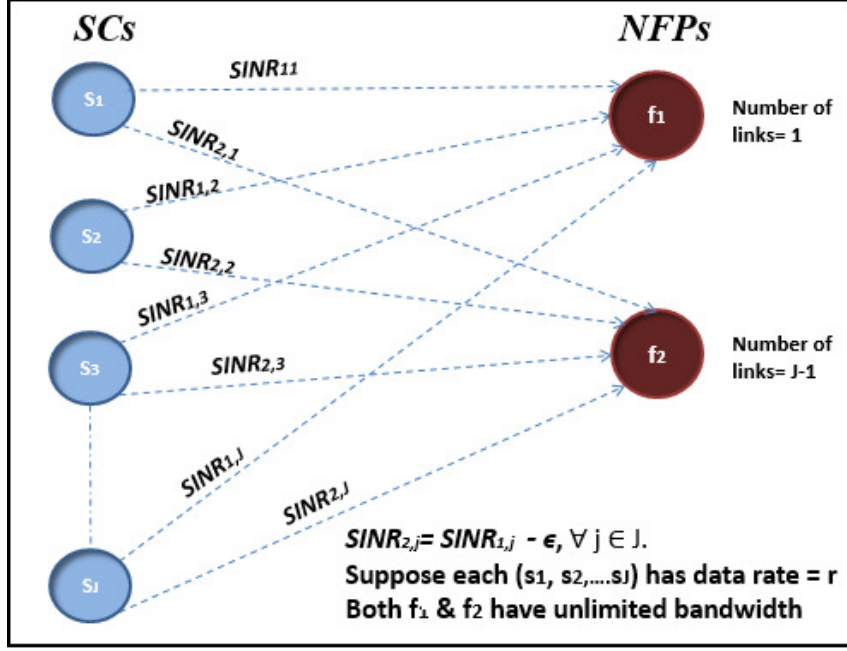
Figure 3.2: Example of the SINR and data rate between SCs and NFPs

3.4.2 Proposed Solutions

In this section, two efficient algorithms are proposed to solve the SCs and NFPs association problem in (3.8) in polynomial time complexity. The first algorithm works in a centralized manner; while the second one provides a distribution solution.

Proposed HBCA

The centralized solutions are designed to move all processing work to a central location in support of multiple remote radio heads. The central location could store both the communication and the user account information, as well as all the necessary information from the SCs and NFPs. The proposed Hungarian based centralized algorithm (HBCA) maximizes the total sum rate after receiving all necessary information about both SCs and NFPs, such as $r_{i,j}$, $b_{i,j}$, $\text{SINR}_{i,j}$, $\text{SINR}_{\min}$, L_i, and B_i. The main idea of the proposed HBCA is based on extending the Hungarian algorithm to handle the unbalanced association problem between SCs and NFPs, where the number of SCs is much larger than the number of NFPs. The Hungarian algorithm gives the optimal solution in case of

40
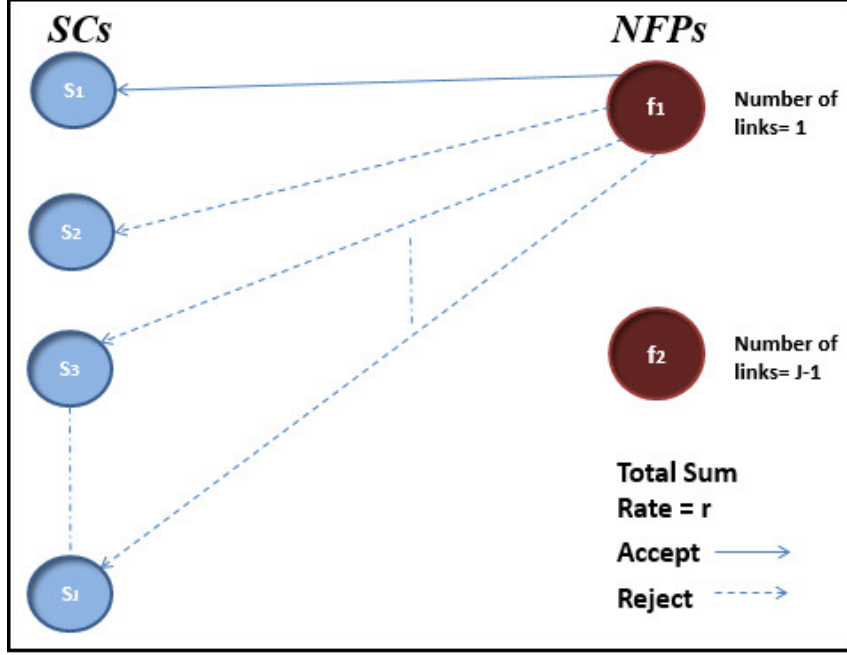
Figure 3.3: SCs ask NFPs to associate using $(\mathbf{DM})^2\mathbf{S}$ algorithm

one-to-one matching (which is not the case in our SCs-NFPs association problem). The first part of the proposed HBCA, i.e., HBCA - part 1, can be briefly explained as follows.

- The algorithm starts by checking if there is a free NFP (has remaining links and enough bandwidth), then fills the W matrix of the SCs and NFPs with $r_{i,j}$ or zero based on the constraints. (lines 4-12).

- Since the Hungarian algorithm accepts only a squared matrix and the number of SCs is much larger than the number of NFPs, a number of dummy NFPs is added that represents the difference between the number of SCs and NFPs. (lines 13-15).

- The Hungarian algorithm returns the association between SCs and NFPs, and then, the available bandwidth and number of remaining links for non-dummy NFPs is updated accordingly. (lines 16-26).

- This process will repeat until all SCs are assigned or there are no free NFPs.

The simulation results presented in Section VI show a gap between the performance of the proposed HBCA - part 1 and the optimal solution. In the following, the performance

41
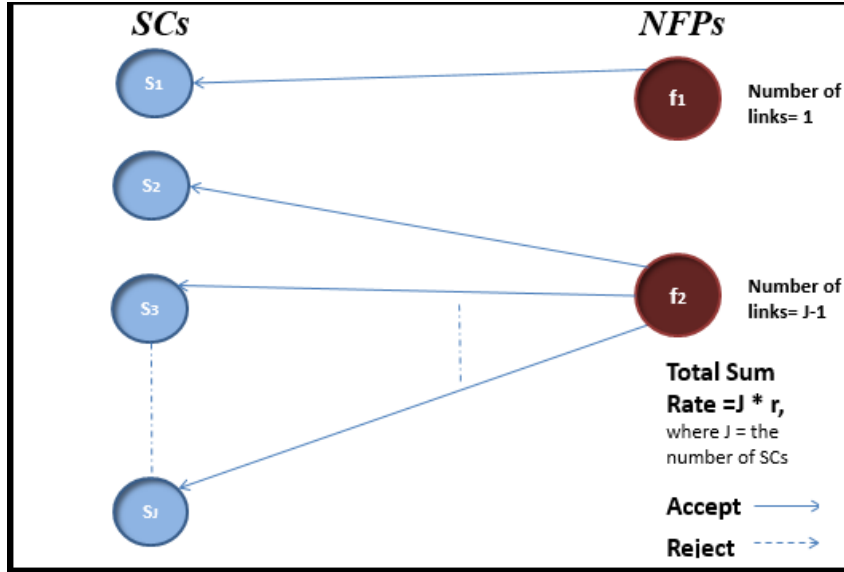
Figure 3.4: Optimal solution

of HBCA - part 1 is improved by introducing HBCA - part 2 to reduce the gap to the optimal solution. The basic idea of HBCA - part 2 can be explained as follows. HBCA - part 2 checks if swapping the already existing association between SCs and NFPs obtained from HBCA - part 1 can further lead to a higher total sum rate. If yes, HBCA - part 2 swaps the association; otherwise, the association kept as in HBCA - part 1. It is worth mentioning that if algorithm HBCA - part 2 swapped the association then the new matrix will be used to find the total sum rate.

The performance of the HBCA can be further improved as shown in HBCA - part 3. The basic idea of HBCA - part 3 is to check if any NFP has free links and if so, then dissociating one SC and associating it with the free NFP can lead to higher total sum rate.

Fig. 3.5 shows an example that helps illustrate the HBCA algorithm more clearly. We have two NFPs f_1 and f_2, where f_1 has one link and f_2 has 2 links. We also have three SCs and each SC requires a specific data rate from each NFP as shown in Fig. 3.5. Please note that we suppose all links between SCs and NFPs satisfy the minimum SINR and each NFP has enough bandwidth. Since the Hungarian algorithm accept only a square

---

Hungarian based centralized algorithm (HBCA) - part 1

1: **Input:** $(S, F, \text{SINR}, \text{SCLink}, \text{SINR}_m, L, B, b, r)$
2: Let $W_{J \times J}$ be a new Matrix $\qquad \triangleright W_{i,j}$ is the weight of the edge between f_i and s_j
3: **while** there is free $f_i \in F$ **do**
4: $\quad$ **for** each $f_i \in F$ **do**
5: $\qquad$ **for** each $s_j \in S$ **do**
6: $\qquad\quad$ **if** $SCLink_j > 0$ and $L_i > 0$ **then**
7: $\qquad\qquad$ **if** $B_i - b_{i,j} \geq 0$ and $\text{SINR}_{i,j} \geq \text{SINR}_m$ **then**
8: $\qquad\qquad\quad W_{i,j} = r_{i,j}$
9: $\qquad\qquad$ **end if**
10: $\qquad\quad$ **end if**
11: $\qquad$ **end for**
12: $\quad$ **end for**
13: $\quad$ **for** each $J - I$ dummy NFP pair **do**
14: $\qquad W_{i,j} = 0$
15: $\quad$ **end for**
16: $\quad$ Let $H_{J \times J}$ be a new matrix $\quad \triangleright$ a boolean matrix, a true value in i, j index depicts, f_i is assigned to s_j $H = \text{HUNGARIAN}(W)$ $\qquad \triangleright$ Hungarian Algorithm is the bipartite matching algorithm which will return a boolean matrix
17: $\quad$ **for** each $f_i \in F$ **do**
18: $\qquad$ **for** each $s_j \in S$ **do**
19: $\qquad\quad$ **if** $H_{i,j} = 0$ **then**
20: $\qquad\qquad$ Associate s_j with f_i
21: $\qquad\qquad L_i = L_i - 1$
22: $\qquad\qquad B_i = B_i - bi, j$
23: $\qquad\qquad SCLink_j = SCLink_j - 1;$
24: $\qquad\quad$ **end if**
25: $\qquad$ **end for**
26: $\quad$ **end for**
27: **end while**

---

matrix, the HBCA starts by adding a dummy NFPs to create and fill a $3X3$ W matrix with the requested $r_{i,j}$ if all constraints are satisfied and with zero otherwise.

After that, HBCA sends the matrix to the Hungarian algorithm to get the optimal one-to-one match between the SCs and the NFPs as shown in Fig. 3.6. Each SC that has a real association drops from the W matrix. This process repeats until all the NFPs links are used, all the NFPs bandwidth are used or all SCs are associated. Fig. 3.7 shows the initial association between the SCs and the NFPs at the end of HBCA - part 1. Fig. 3.8 shows the association between the SCs and the NFPs at the end of HBCA- part 2,

---

HBCA - part 2

1: **Input:** (S, F)
2: Improve=true
3: **while** Improve **do**
4:     Improve=false
5:     **for** each pair $(f_i, f_j) \in F$ **do** ▷ where $i \neq j$ ▷ $s_i, s_j \in S$ are assigned with f_i and f_j
   respectively
6:         Find Total Sum rate : SumRate
7:          Swap association (f_i, s_j) , (f_j, s_i)
8:         Find Total Sum rate: SumSwap
9:         **if** $SumSwap > SumRate$ && all constraints still satisfied **then**
10:             Swap association (f_i, s_j) , (f_j, s_i)
11:             Improve=true
12:         **end if**
13:     **end for**
14: **end while**

---

where some swapping between the associated SCs and NFPs has been done to enhance the total sum rate and the new associations should satisfy all constraints.

There is a swap here, where the association between (s_1 associates instead with f_1) and (s_2 associates with f_2) to be (s_1 associates with f_2) and (s_2 associates with f_1) enhances the total sum rate. Finally if there is available any free links HBCA- part 3 checks if dropping some SCs association and associate it with the free NFPs can improve the total sum rate or not. However, in this example there are no free links; therefore we give another example to explain HBCA- part 3 as shown in Fig. 3.9. We have two NFPs f_1 and f_2, where f_1 has one link and f_2 has 2 links, we also have two SCs and each SC requires a specific data rate from each NFP as shown in Fig. 3.9.

Please note that we assume all links between SCs and NFPs satisfy the minimum SINR and each NFP has enough bandwidth. Fig. 3.10 shows the initial association between the SCs and NFPs after HBCA- part 1, HBCA- part 2 does not change the association in this case. On the other hand, HBCA- part 3 disassociates s_1 from f_1 and associates it with f_2, since f_2 satisfy all constraints and has a free link. This process enhances the total sum rate as shown in Fig. 3.11.

44

1: **Input:** (S, F)
2: Improve=true
3: **while** Improve **do**
4:     **for** each pair $(f_i, f_j) \in F$ **do** $\triangleright$ where $i \neq j$ $\triangleright$ $s_j \in S$ are assigned with f_j
5:        Improve=false
6:       **if** f_i is free **then**
7:           Find Total Sum rate : SumRate
8:           Unassigned s_j from f_j and assigned it to f_i
9:           Find Total Sum rate: SumSwap
10:           **if** $SumSwap > SumRate$ && all constraints still satisfied **then**
11:              Unassigned s_j from f_j and assigned it to f_i
12:              Improve=true
13:           **end if**
14:       **end if**
15:     **end for**
16: **end while**
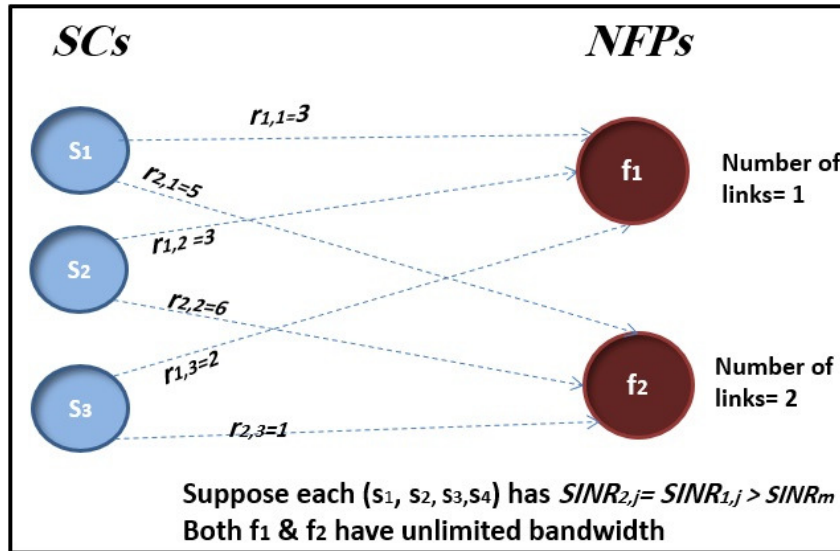
Figure 3.5: SCs ask NFPs to associate

Staple Marriage based Distributed Algorithm (SMBDA)

The stable marriage algorithm is the problem of finding a stable matching between two equally sized sets of elements given an ordering of preferences for each element [74]. A matching is a mapping from the elements of one set to the elements of the other set. Matching is not stable if there is an element A of the first matched set that prefers some given element B of the second matched set over the element to which A is already
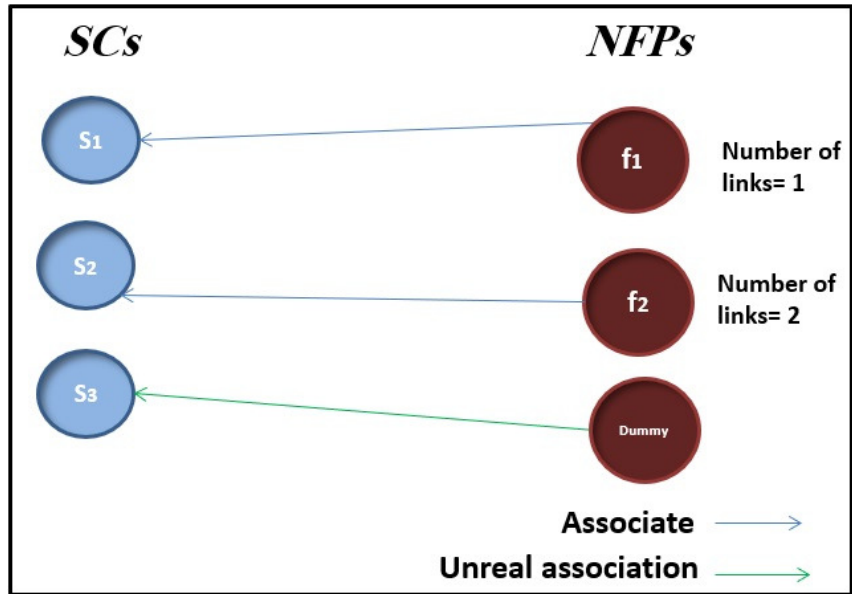
Figure 3.6: Hungarian algorithm returned matching
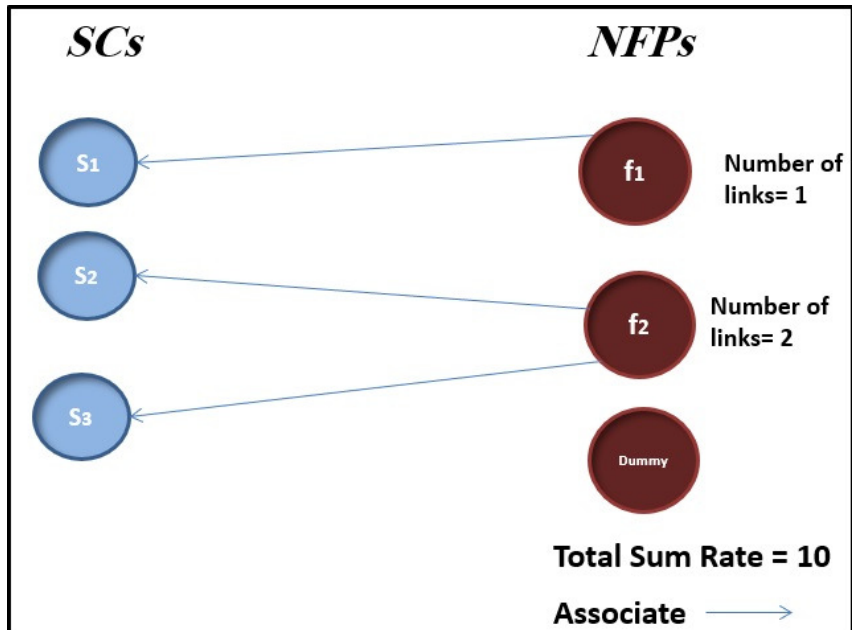
Figure 3.7: SCs and NFPs association at the end of HBCA-part 1

matched, or if B prefers A over the element to which B is already matched. In the end, each element in both lists will have a matched element from the other list.

In this section, a stable marriage based distributed algorithm (stable marriage based distributed algorithm (SMBDA)) is proposed to efficiently solve the SCs and NFPs as-
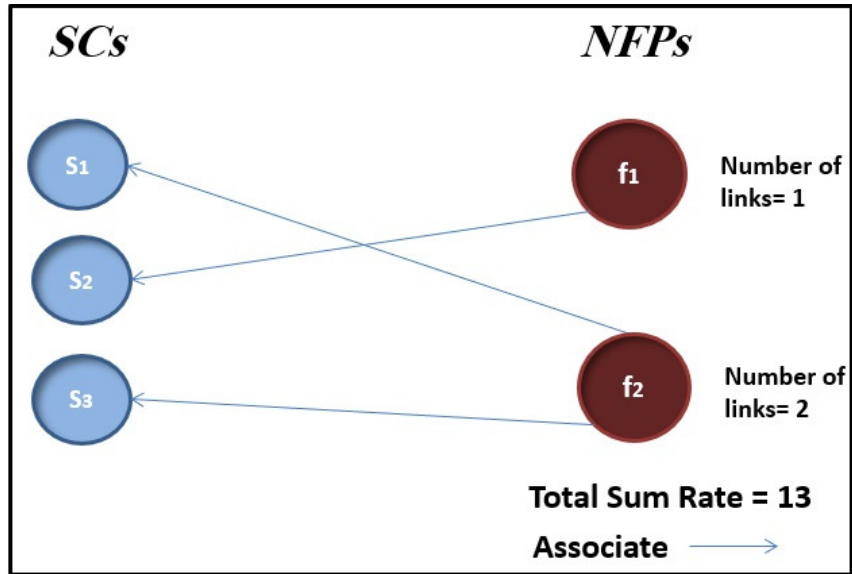
Figure 3.8: SCs and NFPs association at the end of HBCA
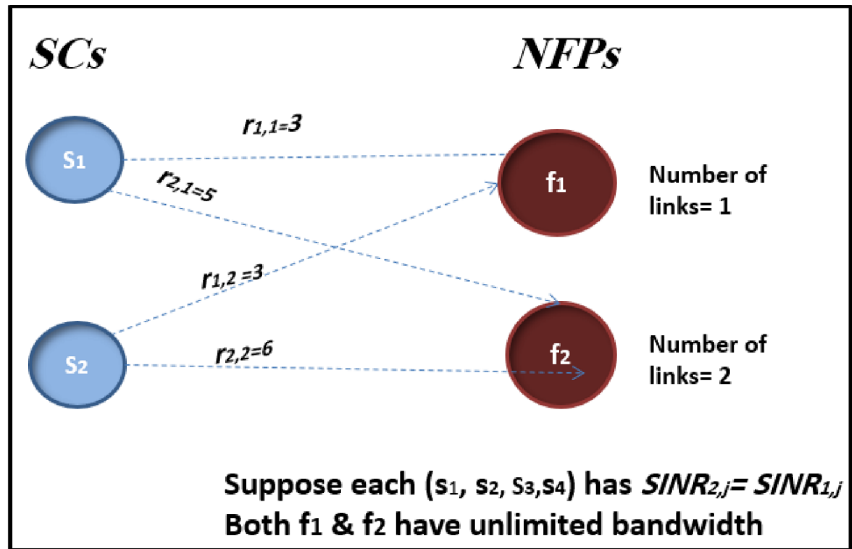
Figure 3.9: SCs ask NFPs to associate

sociation problem in low complexity. In the distributed algorithm, each SC and NFP stores only local information. This means that each SC and NFP is responsible for its association, where SC sends the request to associate with NFP or vice-versa.

In a preferable list algorithm, each SC and NFP are filled a preferable list, based on the maximum data rate between SC and NFP, starting from the most preferable down to least preferred. As previously mentioned, the number of SCs is much larger than the

47
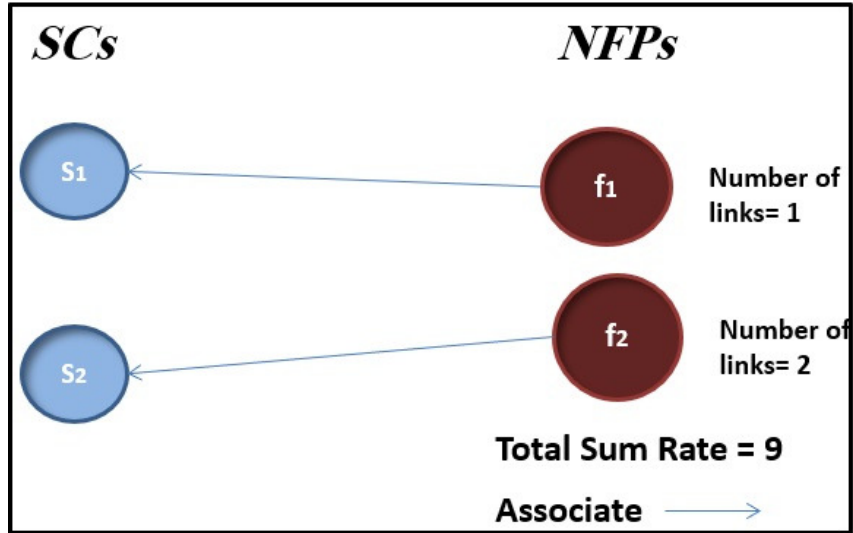
Figure 3.10: SCs and NFPs association at the end of HBCA-part 1
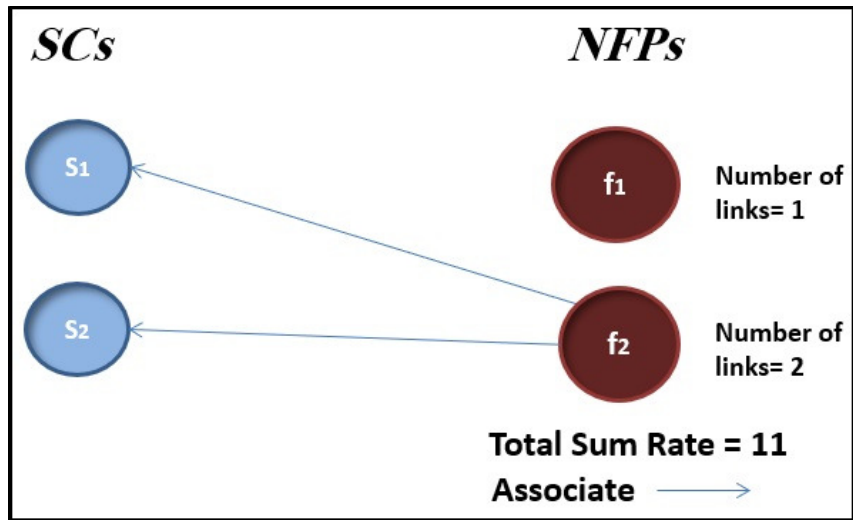
Figure 3.11: SCs and NFPs association at the end of HBCA

number of NFPs and considering the fact that the size of the first list and second list in the stable marriage algorithm should be the same, we added dummy NFPs. The preferable list will help each SC to connect with the most appropriate NFP which is done in the SMBDA algorithm.

SMBDA Algorithm starts at the beginning with all SCs and NFPs are free, (line 2). Each NFP and SC broadcasts its local information; after that the NFP f_i first selects the preferable SC s_j from it's $PrefNFP$ and if the constraints are satisfied, f_i sends a

48

1: **Input:** (S, F, r)
2: Each free $f_i \in F$ will broadcast B_i to all $s_j \in S$
3: Each s_j calculate $\text{SINR}_{i,j}$ and $b_{i,j}$
4: Each s_j will broadcast it's local information to all $f_i \in F$
5: Each s_j will fill it's $PrefSC$ with the indices of the preferred NFPs based on $r_{i,j}$ from max to min
6: Each f_i will fill it's $PrefNFP$ with the indices of the preferred SCs based on $r_{i,j}$ from max to min

association request to that s_j, (lines 3-7). There are three cases:

- Case 1: SC s_j is free and it sends accept and call Accept$(s_j, f_i, L_i, B_i, b_{i,j})$, (lines $8 - 9$).

- Case 2: SC s_j is engaged (no final association) to NFP f_k and SC s_j prefers NFP f_i more, then SC s_j sends disassociate message to NFP f_k and sends accept message to NFP f_i and call Accept$(s_j, f_i, L_i, B_i, b_{i,j})$, (lines $10 - 12$).

- Case 3: SC s_j is engaged (no final association) to NFP f_k and SC s_j prefers NFP f_k more, then SC s_j sends Reject message to NFP f_i. after that, NFP f_i selects the next SC in its $PrefNFP$ list, (lines $13 - 15$).

After that, the SC married (final associated) with NFP, that provide it a stable matching.

As can be seen in Accept algorithm, when s_j calls Accept$(s_j, f_i, L_i, B_i, b_{i,j})$, then SC s_j and NFP f_i local information will be updated as following:

- Associate SC s_j with NFP f_i

- Decrease B_i by $b_{(i,j)}$

- Decrease L_i by 1

- if L_i less than or equal to zero, set f_i to be not free.

1: **Input:** $(S, F, \mathrm{PrefNFP}, \mathrm{PrefSC}, L, B, b)$
2: At the beginning All $f_i \in F$ and $s_j \in S$ are free
3: Each free f_i broadcasts B_i to all s_j
4: Each s_j calculates $\mathrm{SINR}_{i,j}$ and $b_{i,j}$
5: Each s_j broadcasts it's local information to all f_i
6: $s_j = PrefNFP_i$
7: If all constraints are satisfied f_i Sends Request to associate with s_j
8: **Case 1: s_j is free**
9:   Calls Accept$(s_j, f_i, L_i, B_i, b_{i,j})$
10: **Case 2: s_j is engaged to f_k and f_i is more preferable, as in $PrefSC_j$, for s_j than f_k**
11: Calls Accept$(s_j, f_i, L_i, B_i, b_{i,j})$
12: Calls Disassociate$(s_j, f_k, L_k, B_k, b_{k,j})$
13: **Case 3: s_i prefers f_k more than f_i as in $PrefSC_j$ list**
14:   s_i Rejects to associate with f_i
15:   Go to the next preferred SC in $PrefSC_j$ preferable list

---

Accept

Input: $(s_j, f_i, L_i, B_i, b_{i,j})$
s_j connect with f_i
$L_i = L_i - 1$
$B_i = B_i - b_{i,j}$
if $L_i == 0$ **then**
    set f_i is not free
end if

On the other hand, in the Disassociate algorithm, when s_j calls Disassociate $(s_j, f_i, L_i, B_i, b_{i,j})$, then SC s_j, NFP f_i local information will be updated as followed:

- Disassociate SC s_j with NFP f_i

- Increase B_i by $b_{(i,j)}$

- Increase L_i by 1

- Set f_i to be free.

Using SMBDA we found the best association for the fig. 3.5 example. In this example there are three SCs and two NFPs with three Free links. Fig. 3.12 shows each SC and NFP with its preferable lists. For example, as can be seen from Fig. 3.12, s_1 prefers f_2

1: **Input:** $(s_j, f_i, L_i, B_i, b_{i,j})$
2: s_j disconnect from f_i
3: $B_i = B_i + b_{i,j}$
4: set f_i is free
5: $L_i = L_i + 1$
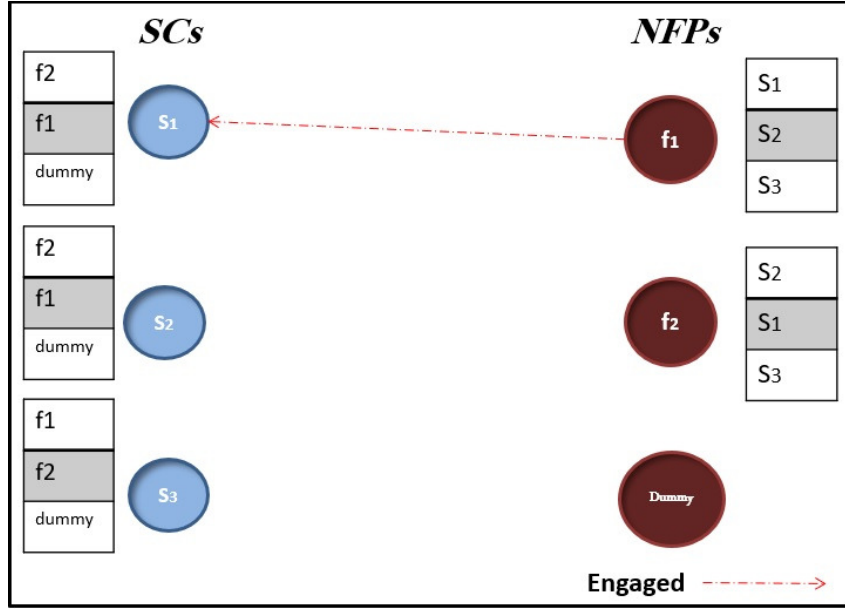
Figure 3.12: NFP f_1 is engages to s_1

then f_1; however, f_1 prefers s_1 first then s_2 and finally s_3. SMBDA starts when f_1 sends request to s_1, which accepts to engage (not fixed associates) with f_1.

After that, as shown in Fig. 3.13, f_2 sends request to s_2 which accepts to engage to f_2. Since f_2 has 2 links and enough bandwidth f_2 sends request to the second SC in its preferable list which is s_1. Therefore, s_1 disengages from f_1 and engages to f_2 as shown in Fig. 3.14. Again f_1 becomes free. Hence, f_1 sends request to s_2 which is reject, since s_2 is engaged to f_2 and it prefers f_2 more than f_1. Hence, f_1 sends request to s_3 which accepts to engage with f_1 as shown in Fig. 3.15. At the end there are no free links, and all SCs and NFPs have stable match. Fig. 3.16 shows the final association between the SCs and the NFPs.
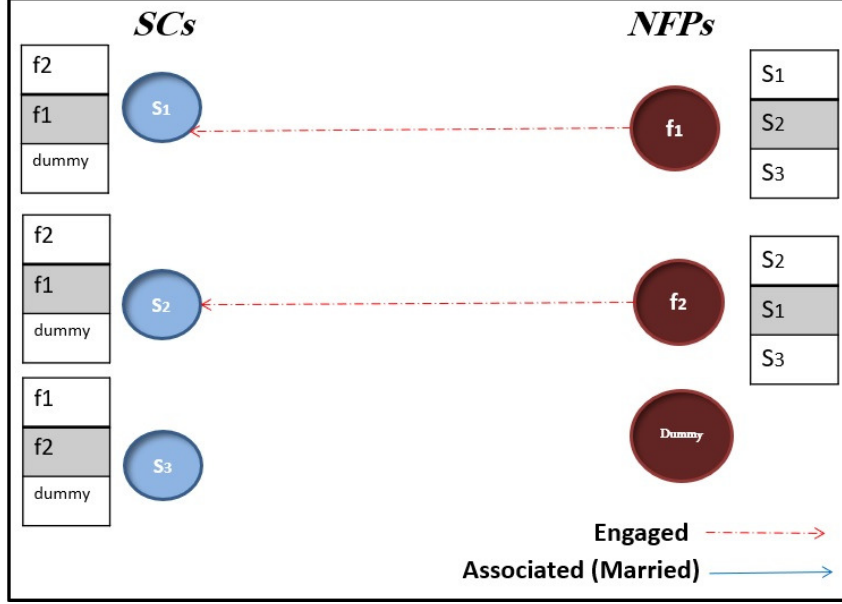
Figure 3.13: NFP f_2 engages to s_2

3.5 Complexity Analysis

In this subsection, the worst case complexity analysis of the proposed algorithms is provided. We find that the time complexity of HBCA - part 1 in the worst case is $O(IJ^3)$. This can be explained as follows:

- The while loop in line 3 requires a complexity of $O(I)$

- The for loops in lines 4 and 5 require a complexity of $O(I)$ and $O(J)$, respectively.

- The for loop in line 13 requires a complexity of $O(J-I)$, and the Hungarian algorithm in line 16 requires a complexity of $O(J^3)$.

- The for loops in lines 17 and 18 require a complexity of $O(I)$ and $O(J)$, respectively.

Hence the worst case complexity of HBCA - part 1 is:

$O(I)\left(O(IJ) + O(J-I) + O(J^3) + O(IJ)\right) = O(IJ^3)$.

For HBCA - part 2 time complexity can be clarified as follows:

- The while loop in line 3 requires a complexity of $O(W)$ where $W = \sum_{i=1}^{I} \sum_{j=1}^{J} r_{i,j}$.

52
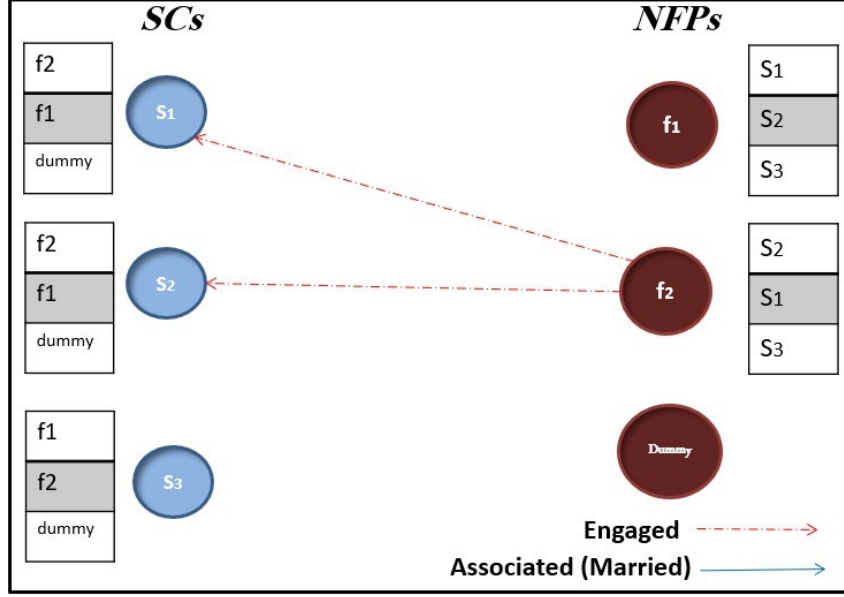
Figure 3.14: NFP f_2 engages to s_1

- The for loop in line 5 requires a complexity of $O(IJ)$.

- The SumRate and SumSwap in lines 6 and 8 both require a complexity of $O(IJ)$.

Hence, HBCA - part 2 time complexity in worst case is $O(W)(O(IJ)O(IJ)) = O(WI^2J^2)$. Similarly the worst case computational complexity of HBCA - part 3 is $O(WI^2J^2)$. Finally, the overall time complexity for the HBCA algorithm will be $O(IJ^3) + O(WI^2J^2) + O(WI^2J^2) = O(WI^2J^2)$.

Regarding the time complexity of SMBDA, it is found that in the worst case each NFP at maximum sends requests to all SCs. Therefore, the time complexity in the worst case occurs when all NFPs send to all SCs, is $O(IJ)$. Furthermore, in the worst case, each SCs rejects all NFPs. Hence, the time complexity in the worst case occurs when all SCs reject all NFPs, is $O(IJ)$. Subsequently, the worst time complexity of SMBDA is $O(IJ)$. This explains that SMBDA termination is assured, as each NFP at maximum sends request to all SCs depend on each NFP $PrefNFP$ list, and each SC at maximum sends reject or accept to all NFPs depend on each SC $PrefSC$ list.

Table 3.1 summaries the worst case time complexity of the proposed algorithms with
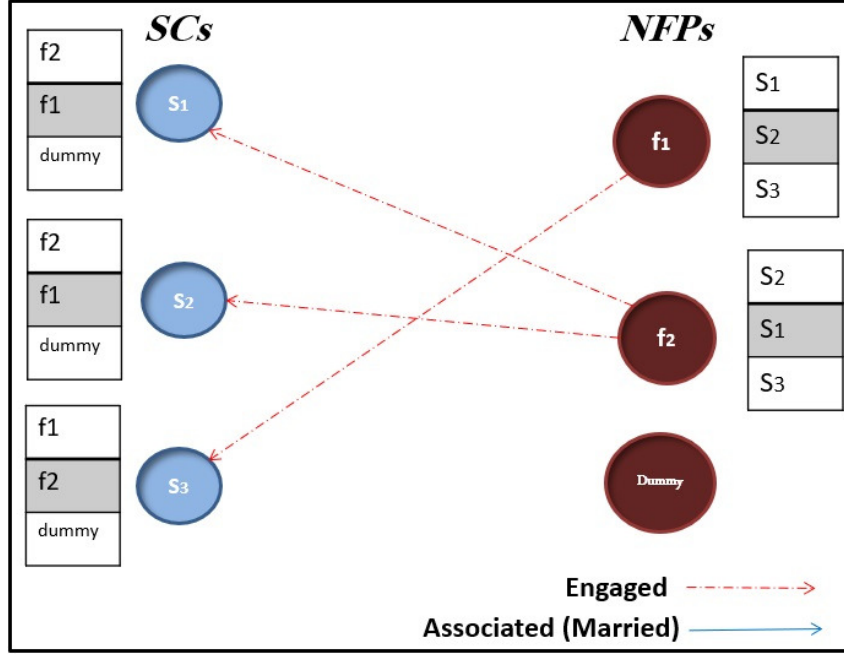
Figure 3.15: NFP f_1 engages to s_3

the $(\mathbf{DM})^2\mathbf{S}$ algorithm. It can be noticed that the proposed algorithms are slightly more computationally expensive than the $(\mathbf{DM})^2\mathbf{S}$ algorithm in the worst case. However, the proposed algorithms are computationally acceptable and are practically applicable.

Table 3.1: Computational time complexity of the proposed algorithms.

Algorithm	Time Complexity Order
HBCA	$O(WI^2J^2)$
SMBDA	$O(IJ)$
$(DM)^2S$	$O(IJ)$

Additionally, the message complexity of the SMBDA distributed algorithm is found. The NFP message complexity in worst case happens when the NFP sends a request message to each single SC. Therefore, the NFP message complexity is $O(IJ)$ in worst case. The SC message complexity in the worst case happens when the SC sends accept or reject message to each single f. Therefore, the SC message complexity is $O(IJ)$ in the worst case. Hence, the SMBDA message complexity is $O(IJ) + O(IJ) = O(IJ)$.

Table 3.2 compares the worst case time complexity of the proposed SMBDA algorithm
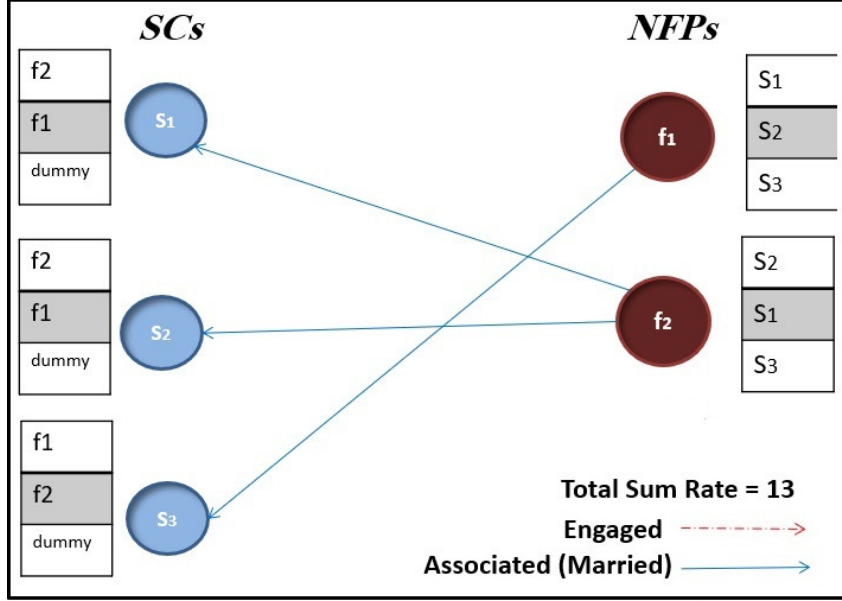
Figure 3.16: NFP f_1 fix associates to s_3 and f_2 fix associates to both s_1 and s_2

and the $(\mathbf{DM})^{\mathbf{2}}\mathbf{S}$ algorithm. It can be noticed that the proposed SMBDA algorithm message complexity is the same as its counterpart of the $(\mathbf{DM})^{\mathbf{2}}\mathbf{S}$ algorithm.

Table 3.2: Computational message complexity of the algorithms.

Algorithm	Message Complexity Order
SMBDA	$O(IJ)$
$(\mathbf{DM})^{\mathbf{2}}\mathbf{S}$	$O(IJ)$

3.6 Performance Evaluation

We use the Gurobi optimization tool [75] to find the ILP solution for problem (3.8), which takes an exponential time. In this section, the performance of the proposed HBCA and SMBDA algorithms are investigated and the results with their counterparts obtained from the optimal solution of ILP of the problem in (3.8) are compared with the proposed distributed algorithm $(\mathbf{DM})^{\mathbf{2}}\mathbf{S}$ in [62].

A 5G+ system is considered, where the SCs and NFPs are uniformly distributed within a 4 km by 4 km area. The data rates used in [62] is considered, then the bandwidth $b_{i,j}$

and $\text{SINR}_{i,j}$ are calculated. Without loss of generality, we assume that all NFPs have the same hight, $h_{d_i} = h_d = 300$ m $\forall i$, and all NFPs have the same bandwidth $B_i = B = 250$ MHz $\forall i$. Following [62], the rest of parameters are defined in Table 3.3.

Table 3.3: Simulation Parameters

Parameter	Value	Parameter	Value
α	9.61	β	0.16
η_{LoS}	1 dB	η_{NLoS}	20 dB
f_c	2 GHz	P_t	5 Watts
σ_j	1 dB	h_d	300 m
J	$(50 - 100)$ $(60 - 200)$	I	$(20 - 50)$ $(50 - 100)$
SINR_{min}	-5 dB	L_i	$2 - 5$

.

Fig. 3.17 shows the total sum rate of the proposed HBCA, SMBDA, ILP, $(\mathbf{DM})^\mathbf{2}\mathbf{S}$ versus the number of SCs at 30 NFPs. As can be seen, the HBCA and the SMBDA performances approach that of the optimal results of the ILP. One can also see from Fig. 3.17 that the proposed SMBDA outperforms the $(\mathbf{DM})^\mathbf{2}\mathbf{S}$. As previously discussed in the $(\mathbf{DM})^\mathbf{2}\mathbf{S}$ algorithm, the SC sends a request to associate with the NFP of the highest SINR, and if rejected then that SC will not associate with another NFP. Even more, as shown in Fig. 3.17, the total sum rate in both proposed HBCA and SMBDA along with the ILP increases when the number of SCs increases, on the other hand, the total sum rate of $(\mathbf{DM})^\mathbf{2}\mathbf{S}$ has a little increment.

Fig. 3.18 shows the total sum rate of the proposed HBCA, SMBDA, ILP, $(\mathbf{DM})^\mathbf{2}\mathbf{S}$ versus the number of NFP at 100 SCs. Again as shown in Fig. 3.18, the HBCA and the SMBDA performances approach that of the optimal results of the ILP. Further, Fig. 3.18 shows that the proposed SMBDA outperforms the $(\mathbf{DM})^\mathbf{2}\mathbf{S}$ as discussed in Fig. 3.17. Additionally, as shown in Fig. 3.18, the total sum rate of the proposed HBCA and SMBDA along with the ILP at the beginning increases with the increase of NFP. After that, the total sum rate saturates or slightly increases. This can be explained as when the number of NFPs reaches 40, almost all SCs are associated which causes the total sum

Figure 3.17: Total Sum Rate versus the number of SCs for the proposed HBCA, SMBDA, ILP, and $(\mathbf{DM})^{\mathbf{2}}\mathbf{S}$ at 30 NFPs.

Figure 3.18: Total Sum Rate versus the number of NFPs for the proposed HBCA, SMBDA, ILP, and $(\mathbf{DM})^{\mathbf{2}}\mathbf{S}$ at 100 SCs.

rate to saturate. However, the total sum rate of $(\mathbf{DM})^2\mathbf{S}$ almost unchanged.

Figure 3.19: Total Sum Rate versus the number of SCs for the proposed HBCA, SMBDA, ILP, and $(\mathbf{DM})^2\mathbf{S}$ at 50 NFPs.

Fig. 3.19 shows the total sum rate of the proposed HBCA, SMBDA, ILP, $(\mathbf{DM})^2\mathbf{S}$ versus the number of SCs at 50 NFPs. As can be seen, the HBCA and the SMBDA performances approach that of the optimal results of the ILP. However the ILP takes around 46882 second running time, which is a very long time comparing to HBCA which takes around 138 second and the SMBDA which takes around 48 seconds. where is the used computer processor is Intel core i7-8750h 2.20 GHz and the ram is 16 GB. As shown in Fig. 3.19, the proposed SMBDA outperforms the $(\mathbf{DM})^2\mathbf{S}$. Even more, the total sum rate in both proposed HBCA and SMBDA along with the ILP highly increases when the number of SCs increase in contradiction with $(\mathbf{DM})^2\mathbf{S}$ where the total sum rate is slightly increased.

Fig. 3.20 shows the total sum rate of the proposed HBCA, SMBDA, ILP, $(\mathbf{DM})^2\mathbf{S}$ versus the number of NFP at 200 SCs. As shown in Fig. 3.20, the HBCA and the SMBDA performances approach that of the optimal results of the ILP. Fig. 3.20 shows that the
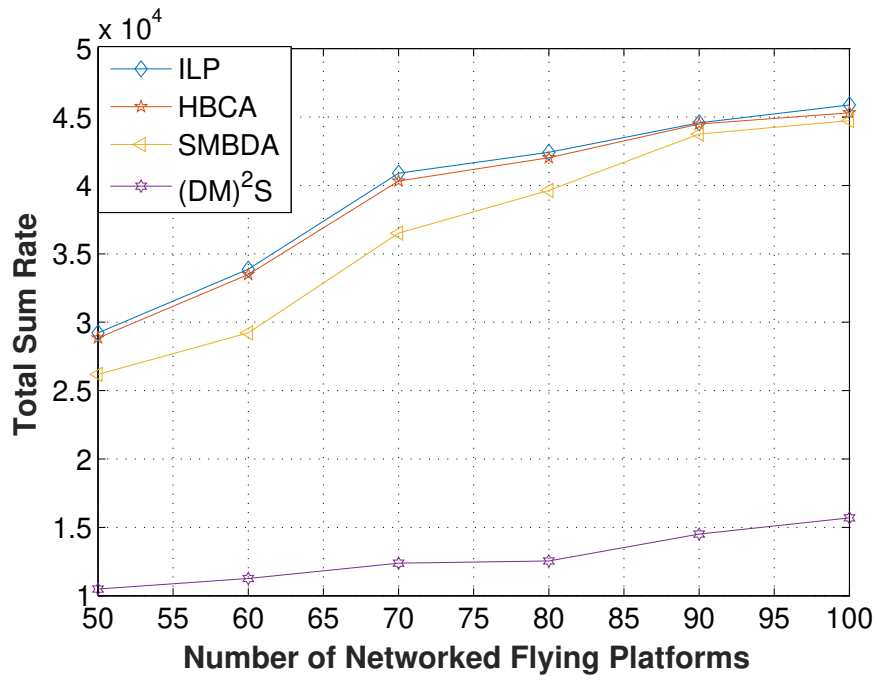
Figure 3.20: Total Sum Rate versus the number of NFPs for the proposed HBCA, SMBDA, ILP, and $(DM)^2S$ at 200 SCs.
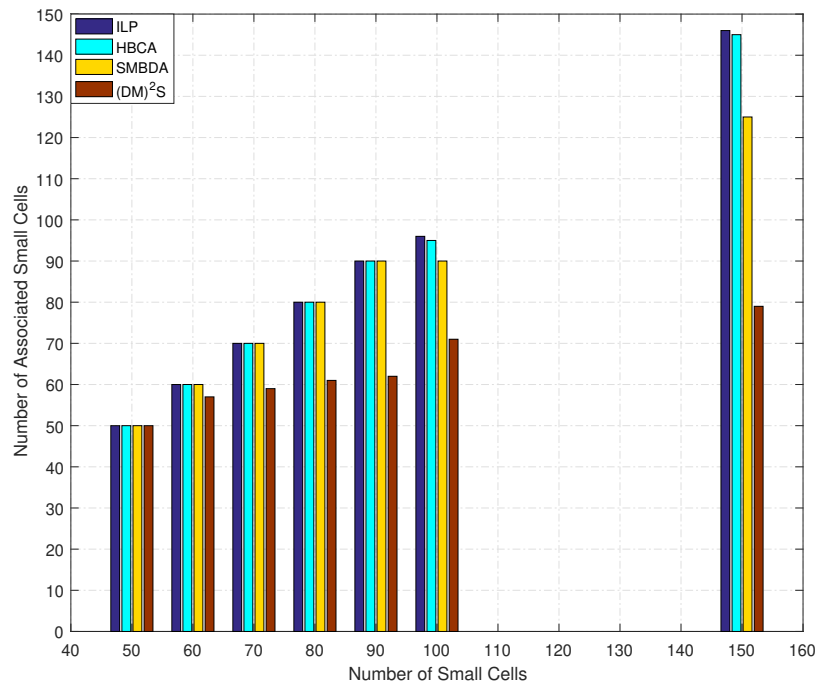
Figure 3.21: Total Number of associated SC versus the number of SCs at 50 NFPs.

proposed SMBDA outperforms the $(\textbf{DM})^2\textbf{S}$.

As one can see from Fig. (3.21), as the number of SCs increases the total number of associated SCs decreases. However, the number of SCs associate with NFPs in our algorithms are very close to the number of SCs associate with NFPs in the optimal case. Moreover, the number of associate SCs in our algorithms outperform the number of associate SCs in case of $(\textbf{DM})^2\textbf{S}$.

As one can see from the previous examples both HBCA and SMBDA outperform $(\textbf{DM})^2\textbf{S}$. As mentioned before $(\textbf{DM})^2\textbf{S}$ is a distributed algorithm, therefore, it has only a local information and this explain why HBCA outperform $(\textbf{DM})^2\textbf{S}$, since HBCA algorithm is a centralized algorithm. As discussed in 3.4.1, in the first step of $(\textbf{DM})^2\textbf{S}$ algorithm each SC sends a message to the NFP with the maximum SINR. Basically, each SC wants to connect NFP with the best SINR link. However, based on other constraints such as the number of links or the bandwidth each NFP can support, the NFP could send rejections to some SCs and these SCs will not attempt to associate with another NFP.

The SMBDA is also a distributed algorithm; however, the SMBDA tries to find the best association for each SC as explained in Section V-B taking into consideration all constraints. The SMBDA tries to find the best association by exploiting the idea of the stable marriage algorithm, which finds the stable match between two lists. This explains why the SMBDA outperforms the $(\textbf{DM})^2\textbf{S}$ algorithm.

Fig. 3.22 shows the total sum rate versus the number of SCs for the proposed HBCA, SMBDA, ILP, and $(\textbf{DM})^2\textbf{S}$ at 30 NFPs. In this scenario, the $\text{SINR}_{i,j}$ is given random values between -10 and 0 dB to put the proposed HBCA and SMBDA algorithm under a critical limitation. As it can be seen, in Fig. 3.22, the HBCA, and the SMBDA performances approach that of the optimal results of the ILP. Moreover, one can see from Fig. 3.22 that the proposed SMBDA outperforms the $(\textbf{DM})^2\textbf{S}$, which becomes clear as previously discussed. Fig. 3.23 shows the total number of associated SCs versus the number of SCs for the proposed HBCA, SMBDA, ILP, and $(\textbf{DM})^2\textbf{S}$ at 30 NFPs. As
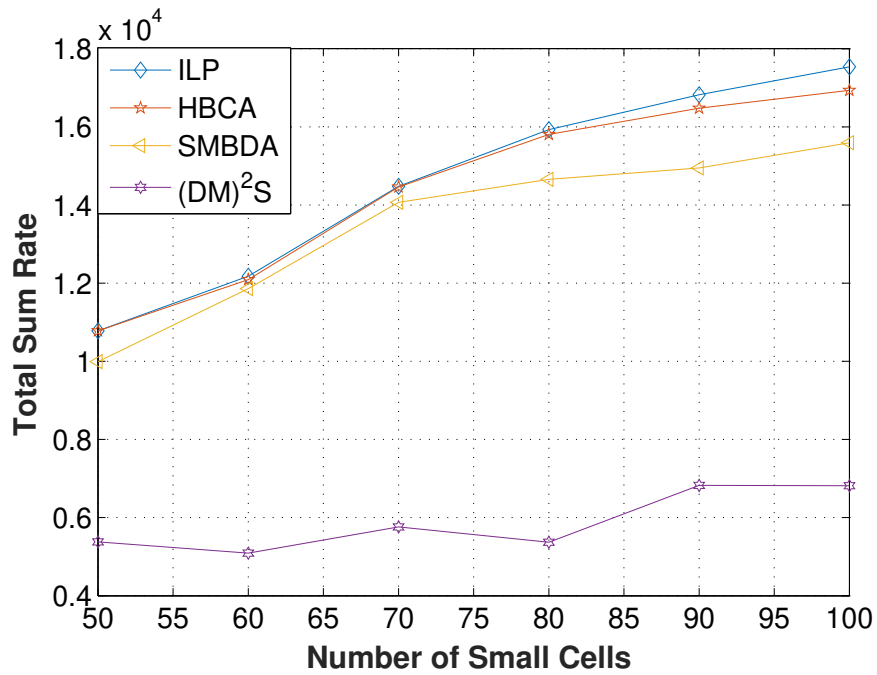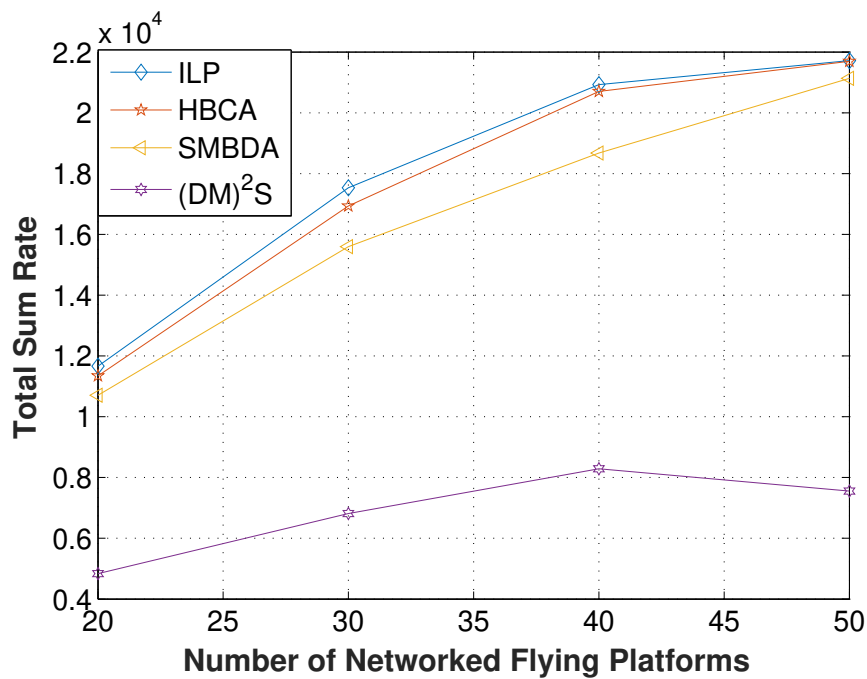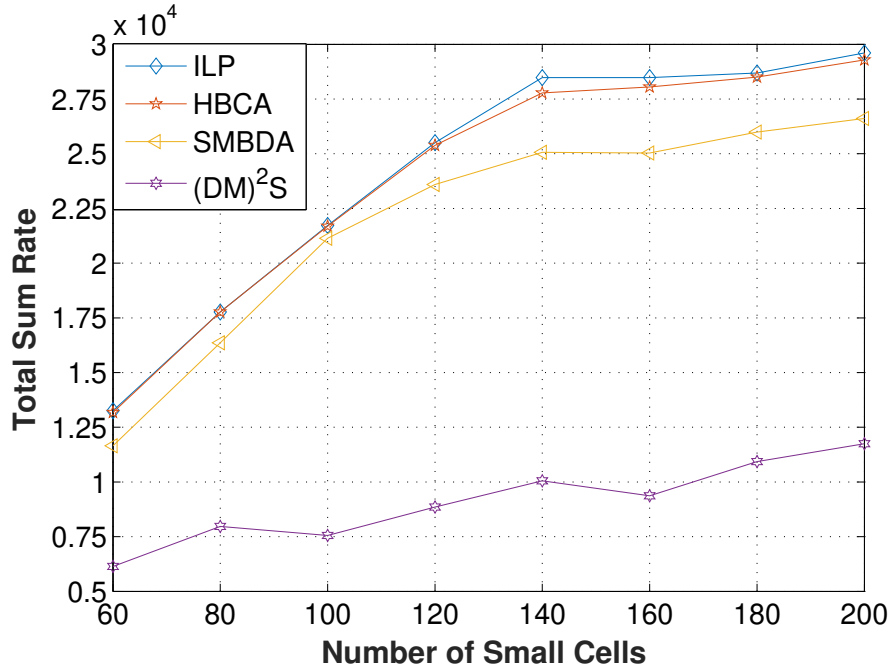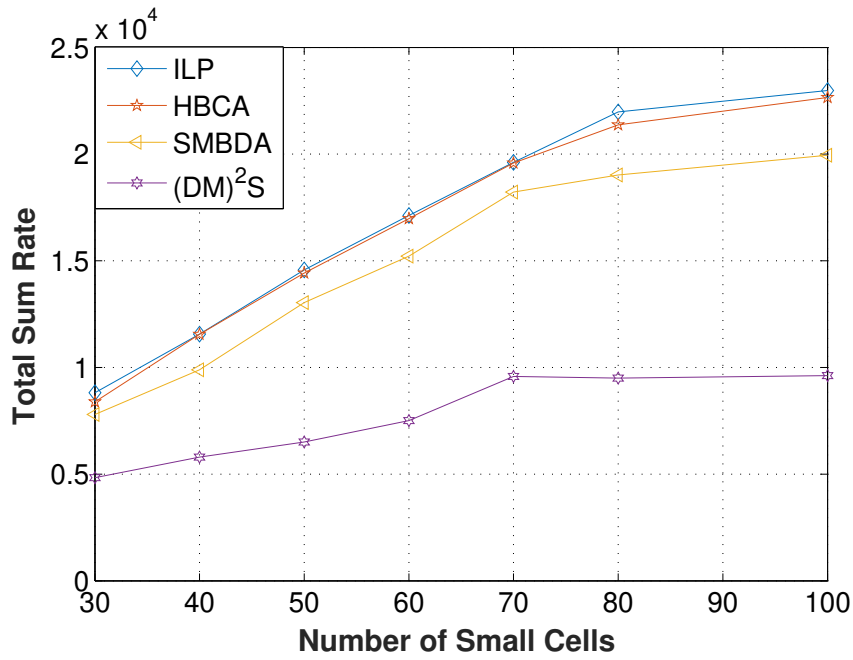
Figure 3.22: Total sum rate versus the number of SCs for the proposed HBCA, SMBDA, ILP, and $(\mathbf{DM})^2\mathbf{S}$ at 30 NFPs.
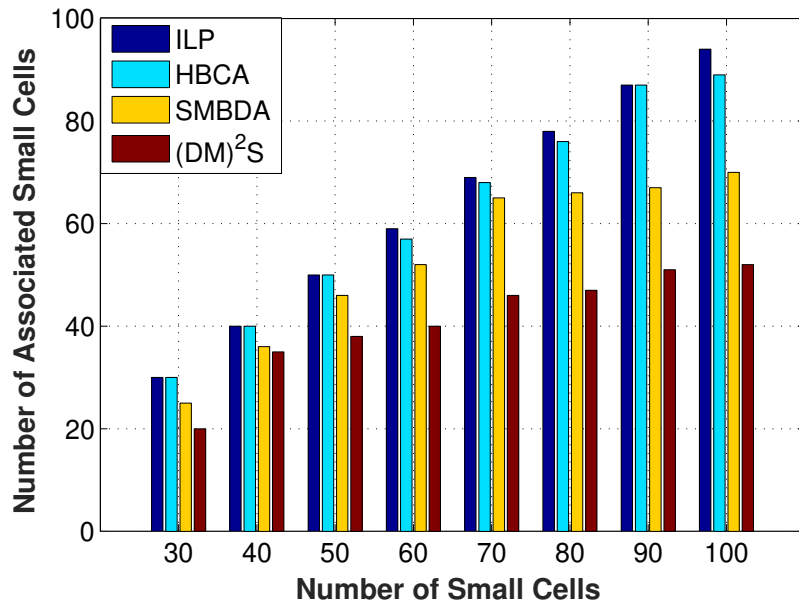
Figure 3.23: Total Number of associated SC versus the number of SCs for the proposed HBCA, SMBDA, ILP, and $(\mathbf{DM})^2\mathbf{S}$ at 30 NFPs.

can be seen the total number of associated SCs of the proposed HBCA and SMBDA algorithms approximated the total number of associated SCs of the ILP. However, the

number of associated SC of $(\mathbf{DM})^{\mathbf{2}}\mathbf{S}$ is less than SMBDA and HBCA. We find different results with different numbers of SCs and NFPs other than the previous one. We find that regardless the number of SCs or NFPs, the two proposed algorithms approach their counterparts obtained from the optimal solution of the integer linear program (ILP) of the problem in (3.8) and outperform the proposed distributed algorithm $(\mathbf{DM})^{\mathbf{2}}\mathbf{S}$ in [62].

3.7 Conclusion

In this chapter, the association problem of the NFPs with SCs of future cellular network is studied to maximize the system sum rate while taking into consideration each NFP bandwidth, the number of supported links, and minimum required SINR. We proposed a centralized (HBCA) and a distributed (SMBDA) algorithm to find a sub-optimal association between the SCs and NFPs, at reduced computational complexity. The numerical evaluation of the considered case study has shown that the performance of the proposed algorithms outperform the performance of the existing algorithm in terms of the number of connected SCs and the total sum rate.

Chapter 4

Interference Minimization Algorithms for Fifth Generation and Beyond Systems

4.1 Introduction

Interference minimization is an important research problem in 5G+ systems. The research community has been aware of these issues including the total sum rate and totally consumed power. 5G+ systems need to provide high data rates for an ultra-dense network of small cells (SCs) along with low interference and widespread coverage. Recently, NFPs systems have started to attract both industry and academia. The focus of research should be on spectral efficiency, network throughput, communication delays, and quality. The algorithms of NFPs association with SCs is rarely proposed [62, 12, 68].

An ultra-dense SCs network is an approach to serve 5G and 5G+ systems requirements including higher data rate, energy efficiency and spectrum utilization. However, this large number of SCs will increase the overall system interference. Therefore, achieving a target data rate with minimal total interference is an important research problem. The research

community has been aware of 5G+ issues, such as the total sum rate, totally consumed power and coverage. However, they overlooked the interference minimization problem. 5G+ systems need to provide high data rates for an ultra-dense network of small cells (SCs) along with low interference and widespread coverage. Interference minimization is an important research problem in the 5G+ systems.

This chapter proposes two algorithms where each NFPs associates with one or more SCs depending on the NFPs limitations (NFPs bandwidth and number of links). Our goal is to minimize the total interference along with achieving a target data rate.

The main contributions of this chapter can be summarized as follows.

- We formulate the association problem of SCs with NFPs to achieve a minimized total interference. This chapter studies two variants, with the first minimizing the total interference and satisfying each SC data rate target. The second minimizes the total interference while maintaining the system total sum rate target.

- We solved the proposed problems numerically to obtain the optimal solution. However, it is not practical, as it takes a high time complexity. We hence propose a heuristic solution.

- For the first variant, when each SC has a data rate target, we check the feasibility. If the problem is feasible, then the system attempts to obtain the minimum total interference along with attaining the data rate target.

- This chapter proposes a heuristic algorithm or ILP to find the maximum total number of associated SCs that the system can accomplish and compares it with the number of SCs. We use this result to determine the feasibility of the problem.

- We design a resource allocation algorithm based on a weighted bipartite matching algorithm (Hungarian algorithm) and local search. This is completed in order to find the best association between NFPs and SCs minimizing the system's total interference subject to QoS constraints (the SINR) while also satisfying each SC data

64

rate target [76, 77]. This guarantees the performance and satisfies all constraints, as well as outperforming other existing algorithms.

- This chapter proposes another variant when the system has a total sum rate target: we propose a heuristic algorithm or ILP to find the maximum total sum rate of the system and compare it with the system data rate target to check feasibility.

- We design a local search based algorithm to find the minimum total interference.

- Finally, we provide extensive simulation results to estimate the performance of the proposed algorithms in realistic conditions.

4.2 Related Work

The higher required bandwidth in order to satisfy the greater data rate demands of 5G+ communication network will be largely recognised by the deployments of small cells. The small cells utilization delivers various advantages such as high data rate and low signal delay. However, it also suffers from various issues such as high interference. The visions and demands of 5G cellular wireless systems was described in [78]. They outlined the challenges for interference management in 5G multi-tier networks taking into consideration its requirements and key features. Furthermore, they combined resource-aware user association with conventional cell association methods to satisfy the objectives.

However, the work in [79] presented an overview of interference management. Where two classes of interference management technologies were discussed: UE-side interference management by advanced receivers with interference joint detection/decoding and network-side interference management by joint scheduling. The authors in [79] discussed the requirements and practical aspects related to these technologies, such as the transmitter coordination tactics and receiver architecture, as well as, the theoretical basis. On the other hand, Zhang *et al.* [80] including interference mitigation studied the handover management in the het-erogeneous cloud small cell network (HCSNet), where a cloud

radio access network was combined with small cells.

An coordinated multi-point (CoMP) transmission/reception clustering scheme using propagation was presented to decrease cell interference. Then the authors in [80] presented a handover management scheme and analyzed handover signaling procedures for HCSNet. They showed that the proposed network architecture, CoMP cluster scheme, and handover management scheme increased the capacity of HCSNet while maintaining the users' quality of service.

The increased interference in the network is one of the difficulties faced by NFPs when connected through an existing cellular network. Moreover, the increased altitude and the propagation of the NFPs increases the interference to the neighboring cells. At the same time, it encounters more interference from the down-link transmissions (the transmission going from a NFP to BS) of the adjacent base stations. Terrestrial UEs degrades performance and produces the up-link (the transmission going from a BS to NFP) interference problem. In [81], they extended the existing power control framework to reduce up-link and down-link interference. They used some down-link physical channels, like a Synchronization Channel (SCH) and Physical Broadcast Channel (PBCH) for cell acquisition.

In like manner, a user association design to minimize the down-link co-channel interference was proposed in [82], where they proposed a mobile station (MS) association system where an active MS needs to associate itself with a particular cell in multi-tier networks while also maintaining the QoS specifications. Their contributions were the introduction of a transmission power normalization model (TPNM) for examining the performance of multi-tier eterogeneous cellular networks (HCN). Based on TPNM, Their results confirmed that the proposed system could reduce the down-link interference under the predefined QoS requirements. Meanwhile, the emergence of Self-interference cancellation (SIC) invalidated the assumption in wireless network design that radios can only operate in half-duplex mode on the same channel [83].

Hence, SIC tremendously simplified spectrum management. It rendered entire ecosystems and enabled future networks to leverage the fragmented spectrum. This technology offered the potential to facilitate the evolution of future networks toward heterogeneous small cell networks. SIC eliminated the backhaul problem by enabling the small cell to reuse LTE radio resources. It provided throughput improvements comparable to out-of-band backhaul solutions by achieving high spectral efficiencies.

This chapter adopts the idea of associating NFPs with SCs, while minimizing the total interference along with satisfying a minimum data rate target. In this chapter we discuss two variants. First, minimizing total interference while satisfying each SC target data rate, in case we need to satisfy each SC fairness. Second, minimizing total interference while maintaining the system target total sum rate to demonstrate effective performance for overall network based on operator view point. For the first variant, when each SC has a target data rate either a heuristic algorithm or integer linear programming approach will be utilized to find the maximum total number of associated SCs that the system can accomplish and compare it with the number of SCs. We used this result to decide whether the problem is feasible or not.

After that, a centralized resource allocation algorithm is designed based on the Hungarian algorithm and local search to solve the problem. For the second variant when the system has a target total sum data rate, we propose an algorithm or integer linear programming to find the maximum total sum rate of the system. Then we compare it with the system target data rate to check feasibility. Then, an algorithm is designed based on local search to find the minimum total interference.

The rest of this chapter is organized as follows: Section 4.3 describes the used system model. Section 4.4 presents the proposed solution. Section 4.5 discusses the computational complexity of the proposed solution. The performance analysis and results for the proposed solution is discussed in Section 4.6. Finally, Section 4.7 concludes this chapter.
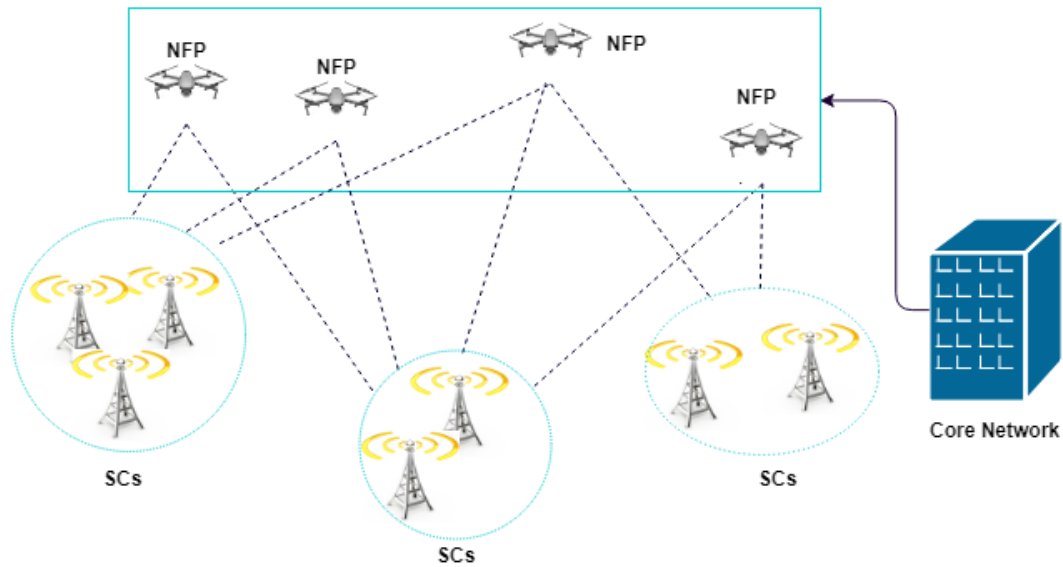
Figure 4.1: Graphical representation of NFPs and SCs in 5G+.

4.3   System Model

As can be seen in Fig. 4.1, this work examines a heterogeneous network which incorporates three classes of wireless nodes: 1) ground SCs which transfer the traffic between the core network and end users, 2) Ground core network, and 3) the NFPs serving as hubs to provide fronthaul connectivity between SCs and the ground core network. SCs allow the end-user to communicate with the core network depending on the fronthaul link of the NFPs. This leads to the association problem of SCs. An intelligent association between NFPs and SCs can minimize the total sum interference while simultaneously satisfying a target data rate.

Here we consider a 5G+ system where the NFPs and SCs are uniformly distributed within 4 km by 4 km area. We consider a system with J number of SCs and I number of NFPs ($J >>> I$), where the set of NFPs is represented as $F = \{f_1, f_2, ..., f_I\}$ and the set of SCs is expressed as $S = \{s_1, s_2, ..., s_J\}$.

For the remainder of this chapter NFPs are denoted as f_i for each $1 \leqslant i \leqslant I$ and SCs are denoted as s_j for each $1 \leqslant j \leqslant J$.

We use the air-to-ground path loss channel model. Thus, the wireless link between NFPs and SCs is mainly vertical. Hence, in the following subsection, the ATG path loss model is discussed.

4.3.1   Air-to-Ground Path Loss Model

This work adopts a widely adopted ATG path loss (PL) model in the NFP literature [62, 11]. ATG communication occurs in correspondence to two main propagation groups. The first group corresponds to SCs placing in a LoS or near-Line-of-Sight to the NFPs, while the second group corresponds to SCs with no LAP Line-of-Sight but still receiving coverage via strong reflections and diffractions. The probability of LoS depends on the orientation of NFPs and SCs, and the environment (urban, rural, etc.). The probability of LoS is a primary factor in finding the path loss in the ATG model. The probability of LoS is defined in [62] as:

$$P(\text{LoS}) = \frac{1}{1 + \alpha \exp[-\beta(\frac{180}{\pi}, \theta - \alpha)]} \tag{4.1}$$

where β and α are constants relying on the surrounding environmen, $\theta = \arctan(\frac{h_D}{s})$ is the angle between the NFP and SC, and $s = \sqrt{(x - x_D)^2 + (y - y_D)^2}$ is the horizontal distance between the NFP and the SC. The locations of the SCs and NFPs in the Cartesian coordinate are given as (x, y) and (x_D, y_D, h_D), respectively. The average PL is given as:

$$PL(d)|_{\text{dB}} = 10 \log \left(\frac{4\pi f_c d}{c} \right)^\gamma + \eta_{\text{LoS}} \, P(\text{LoS}) + \eta_{\text{NLoS}} \, P(\text{NLoS}), \tag{4.2}$$

where the free space path loss in dB is denoted as $PL(d)|_{\text{dB}}$, the carrier frequency is dented as f_c, the speed of light is represented as c, the PL exponent is represented as γ, and the distance between the NFP f_i and SC s_j is denoted as $d_i = \sqrt{h_D^2 + s^2}$. η_{LoS} and η_{NLoS}

69

represent the additional losses of the LoS and NLoS links, and $P(\text{NLoS}) = 1 - P(\text{LoS})$.

4.3.2 Problem Formulation

The association between SCs and NFPs is affected by some constraints: the maximum number of links supported by each NFP, the maximum bandwidth, the maximum number of links supported by each SC, etc. In this work there are two types of QoS: minimum target data rate per each SC and minimum target rate for the whole system. Therefore, we propose two problems. First, solving the association problem to minimize the total interference while taking into consideration each SC data rate target. Second, solving the association problem to minimize the total interference of the system while satisfying a total sum rate target

We denote the requested data rate of the SC s_j from the NFP f_i by $r_{i,j}$; hence, $r_{i,j}$ can be calculated as:

$$r_{i,j} = \eta_{i,j} b_{i,j}, \tag{4.3}$$

where $b_{i,j}$ is the bandwidth between f_i and s_j. $\eta_{i,j} = \log_2(1 + SINR_{i,j})$, where SINR is the signal to interference plus noise ratio and can be found using:

$$\text{SINR}_{i,j} = \frac{P_{i,j} PL(d_{i,j})}{\sum_{k=1, k \neq i}^{I} P_{k,j} PL(d_{k,j}) + \sigma_i^2}, \tag{4.4}$$

where $P_{k,j}$ is the transmit power from f_k to s_j, σ_i^2 denotes the noise power at the S_j and $d_{i,j}$ is the distance between f_i and s_j. The SINR relies on path loss in equation (4.2).

We denote the interference between f_i and s_j as $I_{i,j}$; hence, the interference between f_i and s_j can be represented as follows:

$$I_{i,j} = \sum_{k=1, k \neq i}^{I} Pr_{k,j}, \tag{4.5}$$

We denote the association between the s_j and the f_i by $A_{i,j}$ that can be formally defined as:

$$A_{i,j} = \begin{cases} 1, & \text{if } f_i \text{ is connected with } s_j, \\ 0, & \text{Otherwise.} \end{cases}$$

Taking the previously mentioned constrains into consideration for a particular time when SCs and NFPs have specified positions, the first objective is to determine the optimal/sub-optimal association between the SCs and the NFPs. This is based on minimizing the total interference of the system while satisfying each SC data rate target. This problem can be formulated as:

$$\min_{A_{i,j}} \sum_{i=1}^{I} \sum_{j=1}^{J} I_{i,j}.A_{i,j} \tag{4.6a}$$

subject to

$$\sum_{i=1}^{I} r_{i,j}.A_{i,j} \geqslant r_{SC_j}, \quad \forall\, j, \tag{4.6b}$$

$$\sum_{j=1}^{J} b_{i,j}.A_{i,j} \leqslant B_i, \quad \forall\, i, \tag{4.6c}$$

$$\sum_{j=1}^{J} A_{i,j} \leqslant Nl_i, \quad \forall\, i, \tag{4.6d}$$

$$\sum_{i=1}^{I} A_{i,j} \leqslant 1, \quad \forall\, j, \tag{4.6e}$$

$$A_{i,j} \in \{0,1\}, \quad \forall\, i,j, \tag{4.6f}$$

where r_{SC_j} is each SC's j data rate target (SCs can have the same or different data rate target). B_i is the maximum bandwidth allocated by the f_i, Nl_i is the number of links

supported by each f_i, $A_{i,j}$ is the optimization parameter that indicates the association between s_j and f_i, and we call it minimizing interference while sustaining each SC target data rate problem (MIETDR).

The proposed problem is an integer linear program and the optimal solution can be solved numerically. However, this is also an NP-hard problem.

Lemma 1: The interference minimization problem while maintaining a target data rate per each SC is NP-hard.

Proof: Examine a scenario where there exists a J number of SCs $(s_1, s_2, ...s_J)$, one NFPs f_1 and B_1 is equal to infinity. $I_{1,j}$ is the weight of the links between f_1 and any s_j, where the objective of the problem to minimize the cost (total interference). Therefore, this problem can be reduced to a minimum knapsack problem, which is also an NP-hard problem.

In the optimization problems, the sub-optimal solution is a feasible solution for which the objective function attains its maximum or minimum value depending on the profit or the cost problems. The solution required to solve the problem must be in the feasible region [84]. To check the feasibility for the previous problem, this work finds the maximum number of associated SCs with NFPs for the system while taking into account all constraints for a specific time. The problem formulation for finding the maximum total number of associated SCs can be formulated as follows:

$$\max_{A_{i,j}} \sum_{j=1}^{J} A_{i,j} \tag{4.7a}$$

$$\text{subject to} \quad (4.6b), (4.6c), (4.6d), (4.6e), (4.6f).$$

We call it maximum total SCs problem (MTSCs).

Taking all constraints into consideration for a specific time when NFPs and SCs have

a particular location, the second objective of this work is to determine the sub-optimal association between the SCs and the NFPs. This is based on minimizing total interference of the system while satisfying a total target sum rate. This problem can be formulated as:

$$\min_{A_{i,j}} \sum_{i=1}^{I} \sum_{j=1}^{J} I_{i,j}.A_{i,j} \tag{4.8a}$$

$$\text{subject to} \quad (4.6c), (4.6d), (4.6e), (4.6f),$$

$$\sum_{i=1}^{I} \sum_{j=1}^{J} r_{i,j}.A_{i,j} \geqslant r_m , \tag{4.8b}$$

where r_m is the total sum rate target, and we call it minimizing interference while sustaining the target total sum rate problem (MITTSR).

To check the feasibility for the previous problem, this work finds the maximum total sum rate for the system while taking into account all constraints. The problem of finding the maximum total sum rate can be formulated as follows:

$$\max \sum_{i=1}^{I} \sum_{j=1}^{J} r_{i,j}.A_{i,j} \tag{4.9a}$$

$$\text{subject to} \quad (4.6c), (4.6d), (4.6e), (4.6f),$$

we call it finding the maximum total sum rate problem (FMTSR).

4.4 The Proposed Solutions

We proposed the the ILP solution with exponential complexity using the Gurobi optimization tool [75]. On the other hand, we propose heuristic solutions to solve the proposed

---

Algorithm 8 : Number of Associated SCs (NOAS)

1: **procedure** ALGORITHM$(S, F, B, Nl, b, r, SL, r_{SC_j})$
2:     Sort $\{f_1, f_2, ..., f_i\}$ set based on B_i from max to min
3:     Sort edge between f_i and s_j based on $(\frac{r_{i,j}}{b_{i,j}})$ from max to min
4:     **Select** the case that maximize the total sum rate
5:     **Case** 1:
6:     **for** each f_i starting from max to min B_i **do**
7:         **for** each s_j starting from max to min $(\frac{r_{i,j}}{b_{i,j}})$ **do**
8:             **if** $SL_j > 0$ & $L_i > 0$ & $B_i - b_{i,j} \geq 0$ & $r_{i,j} \geq r_{SC_j}$ **then**
9:                 $A_{i,j} = 1$
10:                $B_i = B_i - b_{i,j}$
11:                $L_i = L_i - 1$
12:                $SL_j = SL_j - 1$
13:            **end if**
14:        **end for**
15:    **end for**
16:    **Case** 2:
17:    **for** each f_i starting from min to max B_i **do**
18:        **for** each s_j starting from max to min $(\frac{r_{i,j}}{b_{i,j}})$ **do**
19:            **if** $SL_j > 0$ & $L_i > 0$ & $B_i - b_{i,j} \geq 0$ & $r_{i,j} \geq r_{SC_j}$ **then**
20:                $A_{i,j} = 1$
21:                $B_i = B_i - b_{i,j}$
22:                $L_i = L_i - 1$
23:                $SL_j = SL_j - 1$
24:            **end if**
25:        **end for**
26:    **end for**
27:    Select the case that maximizes the total number of associated SCs
28:    Find Total Number of Associated SCs with NFPs
29: **end procedure**

---

problems with polynomial complexity. The position of NFPs will be fixed when we run the algorithms. However, if the NFPs location changes then we need to rerun the algorithms again.

4.4.1   The Proposed Solution for MIETDR

This work presents the number of associated SCs algorithm (number of associated SCs algorithm (NOAS)) to find the sub-optimal maximum total number of associated SCs. Furthermore, it uses an integer linear programming method to get the optimal maximum total number of associated SCs for maximum total SCs (MTSCs) problem.

The Proposed Algorithm To Check Feasibility "The Total Number of Associated SCs With NFPs (NOAS)
The proposed NOAS can be elucidated as follows.

- NOAS starts by sorting the NFPs $\{f_1, f_2, ..., f_i\}$ based on B_i and edge between f_i and s_j based on $\left(\frac{r_{i,j}}{b_{i,j}}\right)$ from max to min (lines 2-3).

- The NOAS algorithm then starts to associate SCs with NFPs depending on the sorted lists. It applies two sorting methods: either the sorting starts from minimum to maximum B_i or the opposite from maximum to minimum B_i(lines 6-26).

- After that, the NOAS algorithm selects the sorting method that maximizes the total number of associated SCs, then checks whether all constraints are satisfied and updates A, B, Nl, and SL (lines 27).

- Finally, the NOAS algorithm finds the number of associated SCs (line 28).

The retrieved total number of associated SCs from NOAS is compared with the number of SCs J. If the retrieved value from NOAS is equal to J, then the solution for MIETDR is feasible and can be found. Otherwise, if the retrieved value from NOAS is less than J, we find the maximum total number of associated SCs by ILP using Gurobi optimization tool [75]. If the retrieved value from ILP is less than J, then the solution is infeasible.

Minimize Total Interference based on Hungarian Algorithm and Local Search

We present an algorithm to find an initial solution for the minimum total interference based on the Hungarian algorithm. After that we used local search to find a sub-optimal solution for the association MIETDR. In the following, we present a Hungarian based initial minimum total interference (HBIMTI) algorithm.

The HBIMTI can be clarified as follows:

- The HBIMTI algorithm checks if there are still available NFPs (has links and sufficient bandwidth), then starts filling the Wt matrix based on the constraints with $I_{i,j}$ or ∞ (lines 6).

- HBIMTI uses the Hungarian algorithm, which first requests a squared (n × n)

Algorithm 9 : Hungarian Based Initial Minimum Total Interference (HBIMTI)

1: **Input:** $(F, S, I, SL, Nl, B, b, r, r_{SC_j})$
2: Let $Wt_{J \times J}$ be a new Matrix $\quad \triangleright Wt_{i,j}$ is the edge weight between f_i and s_j and it is initialised to ∞
3: **while** there is available $f_i \in F$ **do**
4:     **for** each $f_i \in F$ **do**
5:         **for** each $s_j \in S$ **do**
6:             **if** $SL_j > 0$ && $L_i > 0$ && $B_i - b_{i,j} \geq 0$ && $r_{i,j} \geq r_{SC_j}$ **then**
7:                 $Wt_{i,j} = I_{i,j}$
8:             **end if**
9:         **end for**
10:     **end for**
11:     **for** each f_i in $J - I$ dummy NFPs **do**
12:         $Wt_{i,j} = \infty$
13:     **end for**
14:     Let $H_{J \times J}$ be a new boolean matrix $\quad \triangleright H = \textsc{Hungarian}(Wt)$, if f_i is assigned to s_j then a true value is
        assigned to H_{ij} index $\quad\quad\quad\quad\quad\quad\quad\quad \triangleright$ Hungarian Algorithm is a matching algorithm
15:     **for** each $f_i \in F$ **do**
16:         **for** each $s_j \in S$ **do**
17:             **if** $H_{i,j} = 0$ **then**
18:                 Associate s_j with f_i
19:                 $L_i = L_i - 1$
20:                 $B_i = B_i - bi, j$
21:                 $SL_j = SL_j - 1;$
22:             **end if**
23:         **end for**
24:     **end for**
25: **end while**

---

matrix as input. However, the number of SCs in our problem is much higher than the number of NFPs. Therefore, a dummy NFPs is added (lines 11).

- After that, the Hungarian algorithm is used to obtain the initial association between NFPs and SCs. Then all related factors for each associated SCs and non-dummy NFPs are deleted respectively (lines 17-22).

- HBIMTI algorithm repeats this process until there are no free NFPs or all SCs are assigned.

The minimizing total interference algorithm (MTI) proposes to enhance the HBIMTI solution. The MTI algorithm considers all cases of swapping, and changes the association as follow:

- Swap association: both SCs swapped their associated NFPs $(f_j s_i, f_i s_j)$ (line 4)

76

Algorithm 10 : Minimizing Total Interference MTI

1: **procedure** ALGORITHM(S, F)
2:   **while** Improve **do**
3:     **for** each pair $(f_i, f_j) \in F$ **do**   ▷ where $i \neq j$ ▷ s_i, s_j are assigned with f_i and f_j respectively $\in S$
4:       **set** $= \{(f_j s_i, f_i s_j), (f_j s_i, f_j s_j), (f_i s_i, f_i s_j)\}$
5:       Select from the **set** an element that minimize the total interference along with satisfying each SC
   data rate target
6:         **if** such element found **then**
7:           Update the system association accordingly
8:         **end if**
9:     **end for**
10:   **end while**
11: **end procedure**

- Move association: associates SC s_i with another NFPs f_j and keeps SC s_j association with NFPs f_j or vice versa, $(f_j s_i, f_j s_j), (f_i s_i, f_i s_j)$ (line 4)

- The algorithm selects from the **set** the case that minimize the total interference. After that, the algorithm updates the SCs and NFPs association (lines 6-7)

4.4.2   The Proposed Solution for MITTSR Problem

In this subsection we presents an algorithm to find the maximum total sum rate for FMTSR problem. We propose the same solution as in algorithm NOAS to find the total sum rate while eliminating the $(r_{i,j} \geq r_{SC_j})$ constraint from the if statement in line (8) and call it maximum total sum rate (MTSR). Moreover, it presents minimize total interference based on local search (MTIBLS) that is designed to solve the minimizing interference while sustaining the target total sum rate (MITTSR) problem.

Minimize Total Interference based on Local Search (MTIBLS)

To achieve an efficient association with a lower time complexity for the proposed NP-hard association MITTSR problem, this work presents MTIBLS algorithm based on local search to solve the problem.

First, either the MTSR algorithm or the ILP is used to find the maximum total sum rate, which provides the initial association between the SCs and the NFPs. At the

Algorithm 11 : Minimize Total Interference based on Local Search (MTIBLS)

1: **procedure** ALGORITHM(S, F)
2:    **while** Improve **do**
3:       **for** each pair $(f_i, f_j) \in F$ **do**   ▷ where $i \neq j$ ▷ s_i, s_j are assigned with f_i and f_j respectively $\in S$
4:          $set = \{(f_j s_i, f_i s_j), (f_\phi s_i, f_j s_j), (f_j s_i, f_\phi s_j), (f_j s_i, f_j s_j),$
             $(f_\phi s_i, f_i s_j), (f_i s_i, f_i s_j), (f_i s_i, f_\phi s_j), (f_\phi s_i, f_\phi s_j)\}$
5:          Select from the **set** an element that minimize the total interference along with satisfying the minimum sum rate target
6:             **if** such element found **then**
7:                Update the system association accordingly
8:             **end if**
9:       **end for**
10:    **end while**
11: **end procedure**

---

same time, the MTSR algorithm checks whether the minimum total sum rate target is achievable or not, and initializes the association between the SCs and the NFPs. After that, the MTIBLS algorithm is used to minimize the total interference while satisfying a minimum total sum rate target.

MTIBLS algorithm considers all cases for dropping, swapping, and change association as follow:

- Drops the associated SC from the NFPs $(f_\phi s_i, f_j s_j)$ and $(f_i s_i, f_\phi s_j)$.

- Swap association: both SCs swapped their associated NFPs $(f_j s_i, f_i s_j)$.

- Move association: associates SC s_i with another NFPs f_j and drops SC s_j association from NFPs f_j or vice versa, $(f_j s_i, f_\phi s_j)$ and $(f_\phi s_i, f_i s_j)$.

- Move association: associates SC s_i with another NFPs f_j and keeps SC s_j association with NFPs f_j or vice versa, $(f_j s_i, f_j s_j)$ and $(f_i s_i, f_i s_j)$.

- Drop both SCs s_i, s_j association from NFPs f_i, f_j respectively $(f_\phi s_i, f_\phi s_j)$.

The algorithm calculates the total interference and the total sum rate for all cases. The algorithm then selects the one that minimizes the total interference along with satisfying the total sum rate target. Following this, the algorithm updates all related variables. Subsequently, it changes the SC and NFPs association according to the selected case. In the end, the total interference is minimized while maintaining the total sum rate target.
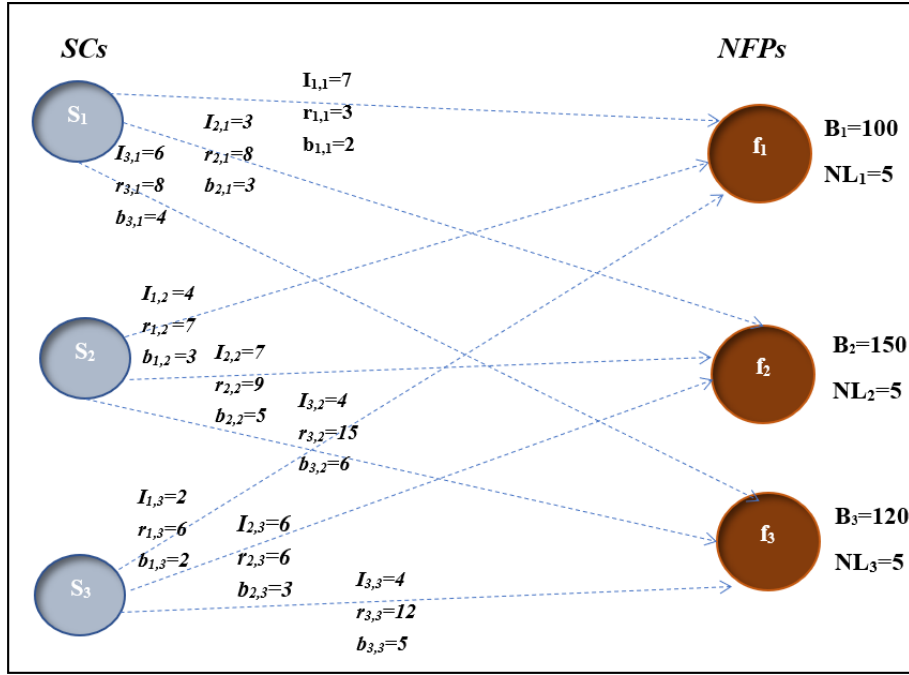
Figure 4.2: Example of the interference, data rate and bandwidth between SCs and NFPs.

4.4.3 HBIMTI and MTILBS Algorithms Examples

Fig. 4.2 shows an example that helps expound the NOAS and HBIMTI algorithms more clearly. In this example, we have three NFPs f_1, f_2 and f_3, where each has 5 links. We have three SCs as well, each SC demands a particular data rate from each NFPs as shown in Fig. 4.2. The NFPs supported a specific bandwidth, each SC requires a particular bandwidth, and the interference of the links between the SCs and NFPs are shown in Fig. 4.2. Finally, all SCs have the same data rate target equal to 2.

The NOAS algorithm starts by sorting the NFPs based on the bandwidth ascending (f_1, f_3, f_2) and descending (f_2, f_3, f_1). As shown in Fig. 4.3, the NOAS algorithm then sorts the links between the SCs and NFPs based on the ratio of the data rate over the bandwidth between the SCs and the NFPs in descending order. The NOAS finds the maximum total number of associated SCs in two methods. In the first method, since f_1 has the least bandwidth, the NOAS algorithm checks the link to one of the SCs with the largest rate to bandwidth ratio. In this example it is between f_1 and s_3; the NOAS algorithm

79
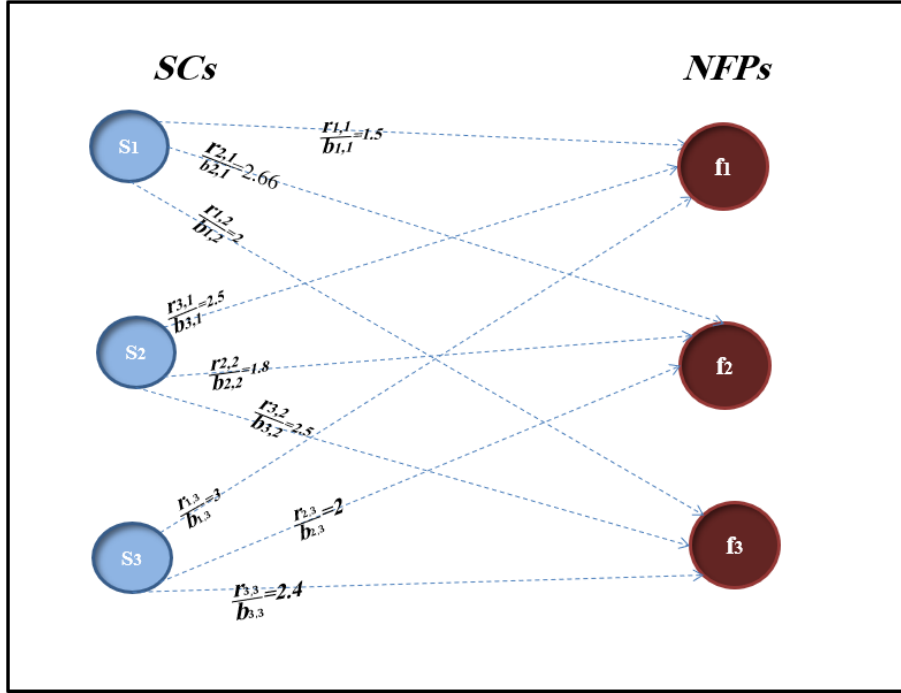
Figure 4.3: The ratio between data rate and the bandwidth

checks if the other constraints like f_1 bandwidth and the number of links supported by f_1 are satisfied or if the data rate provided from f_1 to s_3 is larger than s_3 data rate target r_{SC_3}. Since f_1 has 5 links and r_{SC_3} is equal to 2, the NOAS algorithm associates s_3 with f_1. It then checks the second largest ratio which is between f_1 and s_2, and verifies whether the other constraints are satisfied. Indeed f_1 has 5 links and it has enough bandwidth. Moreover, the requested data rate by s_2 from f_1 is more than 2; therefore, the NOAS algorithm associates s_2 with f_1. Finally the third and last maximum ratio is between f_1 and s_1. Since all constraints are satisfied, the NOAS algorithm associates s_1 with f_1. Hence, the total number of associated SCs is 3.

In the second method, since f_2 has the maximum bandwidth, the NOAS algorithm checks the link to one of the SCs with the largest rate to bandwidth ratio. In this example it is between f_2 and s_1 ; therefore, the NOAS algorithm associates s_1 with f_2 after checking all other constrains. Moreover, since f_2 after associating with s_1 still has 5 links and has enough bandwidth, the NOAS algorithm checks the second and third largest ratio which

are between f_2 and s_3 and between f_2 and s_2. Therefore, the NOAS algorithm associates s_3 and s_2 with f_2. In this case the total number of associated SCs is 3. The returned total number of SCs from the ILP using Gurobi tool is also equal to 3. However, since the total number of associated SCs returned from NOAS equals 3 (which is equal to J) this problem is feasible and we don't need to check the retrieved value from the Gurobi optimizer.

Since the problem is feasible, as shown in Fig. 4.4, the HBIMTI uses the Hungarian algorithm and local search to associate the SCs with NFPs. The Hungarian algorithm accepts only a square matrix. The HBIMTI starts by adding a dummy NFPs if needed; however, in this case the number of NFPs equals the number of SCs. HBIMTI creates and fills a $3X3$ W matrix with the $I_{i,j}$ if all constraints are satisfied and with ∞ otherwise.

After that, HBIMTI sends the matrix to the Hungarian algorithm to get the optimal one-to-one match between the SCs and the NFPs. Each SC that has a real association with an NFPs drops from the W matrix. This process repeats until all the NFPs links are used, all the NFPs bandwidth are used, or all SCs are associated.

Since we have an initial solution we can use the local search algorithm to look for better solution if it exists. At the end, HBIMTI associates f_1 with s_3, f_2 with s_1 and f_3 with s_2. Therefore, the total interference is 9. On the other hand, the returned total interference from the ILP using Gurobi is equal to 9. Therefore, in this case HBIMTI returns the optimal result.

We used the example in Fig. 4.2 to help clarify the MTSR and MTILBS algorithms. The total sum rate target in this example is 18. The MTSR algorithm starts by sorting the NFPs based on the bandwidth ascending (f_1, f_3, f_2) and descending (f_2, f_3, f_1). Then, the MTSR algorithm sorts the links between the SCs and NFPs based on the ratio of the data rate over the bandwidth between the SC and the NFPs in descending order. The MTSR finds the total sum rate in two methods. First, since f_1 has the least bandwidth, the MTSR algorithm checks the link to the SCs with the largest rate to bandwidth ratio
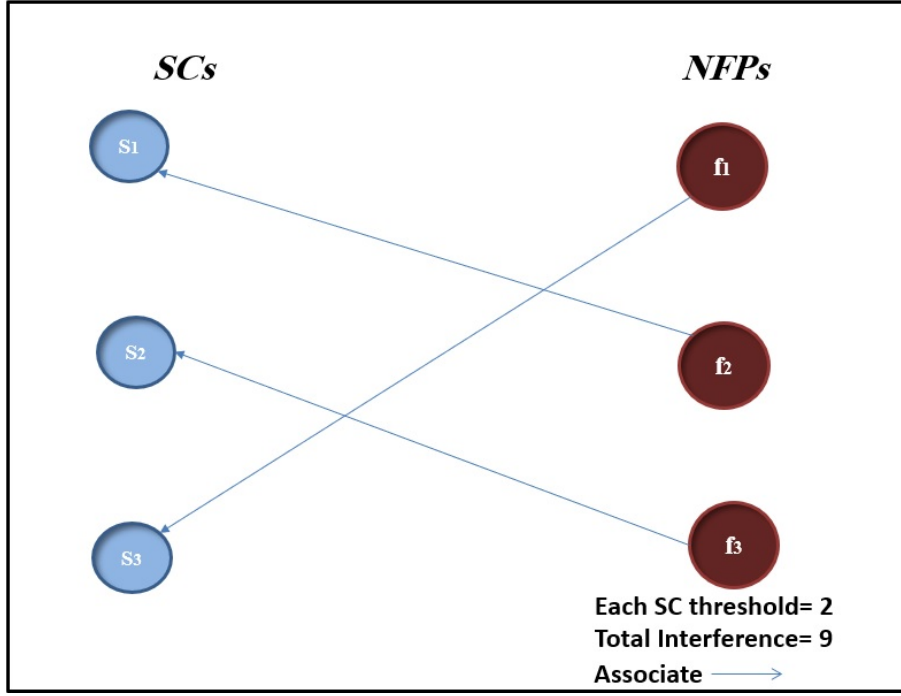
Figure 4.4: HBIMTI algorithm result

which, in this example is between f_1 and s_3. Therefore, the MTSR algorithm associates s_3 with f_1. Since f_1 has 5 links, the MTSR algorithm checks the second and third largest ratio which are between f_1 and s_2 and between f_1 and s_1. Therefore, the MTSR algorithm associates s_2 and s_1 with f_1. Hence, the total sum rate equals 16.

Since f_2 has the maximum bandwidth, the MTSR algorithm checks the link to the SCs with the largest rate to bandwidth ratio which in this example is between f_2 and s_1. Therefore, the MTSR algorithm associates s_1 with f_2. Since f_2 has 5 links, the MTSR algorithm checks the second and third largest ratio which are between f_2 and s_3 and between f_2 and s_2. This means the MTSR algorithm associates s_3 and s_2 with f_2. Hence, the total sum rate equals to 23. The MTSR algorithm selects the case with the largest total sum rate; therefore, it selects the second case.

The returned total sum rate from the ILP using Gurobi tool is equal to 35. However, since the retrieved value from MTSR algorithm is 23, which is greater than 18, we use the MTSR algorithm association as the initial association between SCs and NFPs.
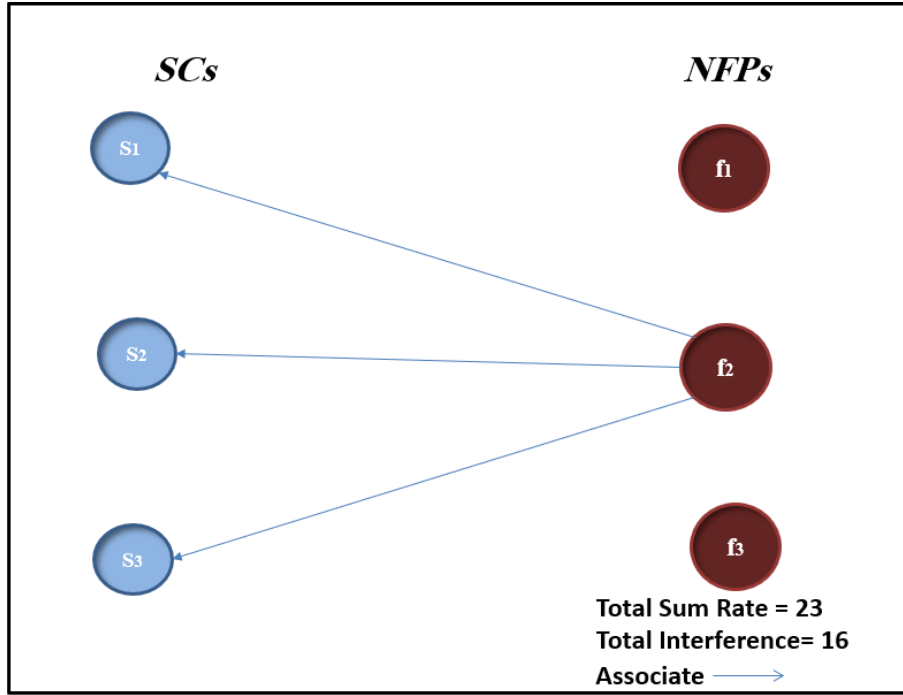
Figure 4.5: Initial association between SCs and NFPs.

As can be seen in Fig. 4.5, the initial association between SCs and NFPs is f_2 with s_1, f_2 with s_3, and f_2 with s_2; where the total interference in this case is 16.

MTILBS algorithm drops the association between f_2 and s_2 and associates f_3 with s_2 to minimize the total interference. Then, the MTILBS algorithm based on the local search drops the association between f_2 and s_3. In the end, the total sum rate is 23 and the total interference is 7, meaning that the total interference was reduced.

4.5   Complexity Analysis

In this section, we analyze the worst case time complexity of the proposed algorithms.

The worst case time complexity of the NOAS algorithm is $O(IJ)$ and can be explained as follows:

- Sorting in lines 2 and 3 requires a complexity of $O(IJ)$.

- The for loops in lines (7- 15) requires a complexity of $O(IJ)$.
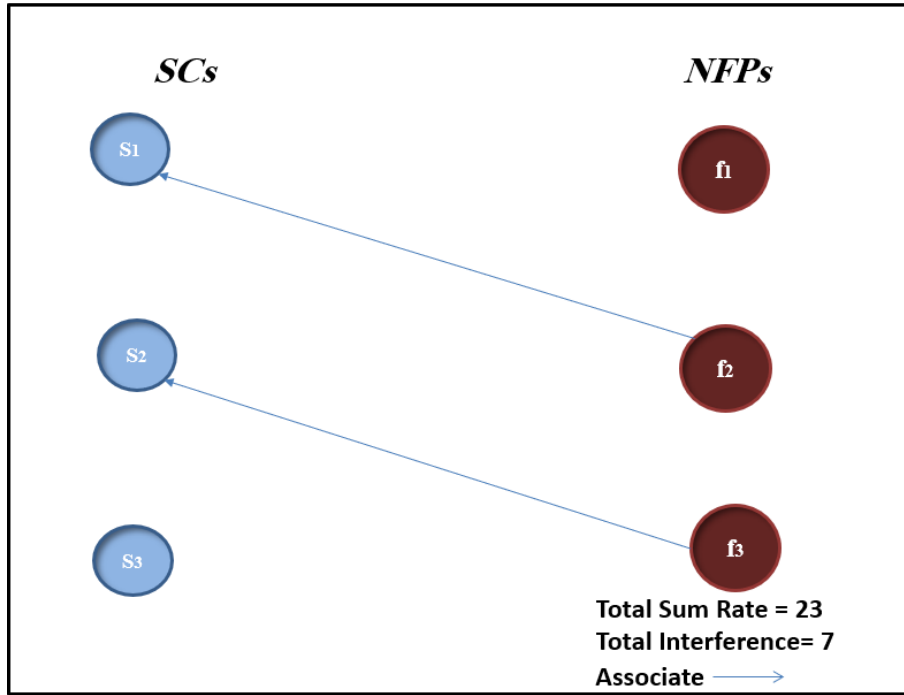
Figure 4.6: MTIBLS algorithm result

- The for loops in lines (18- 26) requires a complexity of $O(IJ)$.

Therefore, the overall complexity for NOAS algorithm will be $O(IJ)+O(IJ)+O(IJ) = O(IJ)$.

The worst case complexity of HBIMTI algorithm is $O(IJ^3)$. We can expound it as follows:

- The complexity of the while loop in line (3) is $O(I)$

- The complexity for the loops in lines (4) and (5) are $O(I)$ and $O(J)$, respectively.

- The complexity for the loop in line (11) is $O(J-I)$, and the complexity for the Hungarian algorithm in line (14) is $O(J^3)$.

- The complexity for the loops in lines (15) and (16) are $O(I)$ and $O(J)$, respectively.

Hence, the complexity of HBIMTI is $O(I)\left(O(IJ) + O(J-I) + O(J^3) + O(IJ)\right) = O(IJ^3)$.

Table 4.1: Computational time complexity of the proposed algorithms.

Algorithm	Time Complexity Order
HBIMTI	$O(IJ^3)$
MTIBLS	$O(WI^2J^2)$
NOAS	$O(IJ)$

The worst case complexity of the proposed algorithm MTIBLS is $O(WI^2J^2)$, and it can be explained as follows:

- The proposed MTSR algorithm requires a complexity of $O(IJ)$

- The complexity for the while loop in line 2 is $O(W)$ where $W = \sum_{i=1}^{I} \sum_{j=1}^{J} I_{i,j}$.

- The complexity for the loop in line 3 is $O(IJ)$.

- Selecting the element which minimizes the total interference along with satisfying the minimum sum rate target in line 5 requires a complexity of $O(IJ)$.

Hence, the worst case complexity for MTIBLS algorithm is $O(WI^2J^2)$.

Table 4.1 summarizes the worst case time complexity of the proposed algorithms. It is clear that it has a polynomial time complexity, indicating that it can be practically implemented.

4.6   Performance Results

In this section, we investigate the performance of the proposed algorithms that minimize the total interference. After that, we compare the results with its counterparts obtained from the Gurobi optimization tool [75] which achieves optimal results from the ILP for MIETDR and MITTSR problems.

We assumed that all NFPs have the same height, $h_{d_i} = 300$ m $\forall i$. NFPs have the different bandwidths. All NFPs have the same number of links which is $J/5$ or $J/3$. The SC data rate target is set to be equal to one of two selections: 50 or each SC can has

Table 4.2: Simulation Parameters

Parameter	Value	Parameter	Value
B_i	200-500 MHz	h_d	300 m
J	(30, 40, 50, 60)	I	(20)
J	(60, 70, 80, 90, 100)	I	(50)
P_t	5 Watts	Nl	J / 5 , J / 3

it own threshold for MIETDR problem. On the other hand, for the MITTSR problem, the total sum rate target is equal to one of three selections: the half of the maximum sum rate (MSR) retrieved from ILP, the third of the MSR, or in between the retrieved value from MTSR and MSR. The system parameters are defined in Table 4.2. Finally, all needed parameters are passed to the algorithms to find the best association between SCs and NFPs.

Here Min_{TI} represents the ILP optimal minimum total interference, and HBIMTI represents total interference returned from the proposed algorithm HBIMTI. The total interference in the following result is in μWatt.

Fig. 4.7, shows the total interference of the proposed HBIMTI with the minimum total interference obtained from Gurobi optimization tool with 50 NFPs. In HBIMTI all SCs are associated with NFPs (if in total we have 60 SCs then each SC is associated with an NFPs). SC_{rm_j} has different values ranging between $30 - 50$ Mbps. The number of each NFPs links is equal to the number of $J/5$. As can be seen in Fig. 4.7, the total interference of both HBIMTI and Min_{TI} is very close. Although each SC has it own target data rate, the proposed algorithm succeed to minimize the total interference of the system while satisfying each SC target data rate.

Fig. 4.8, shows the total interference of the proposed algorithm HBIMTI along with the minimum total interference with 50 NFPs. The target data rate equals 50 Mbps. The number of each NFPs links is equal to $J/5$. Fig. 4.8 shows that the total interference of HBIMTI is approaching the total interference of Min_{TI}. Thus, even when the number of SCs and NFPs increase the proposed algorithm approximates . As can be seen from
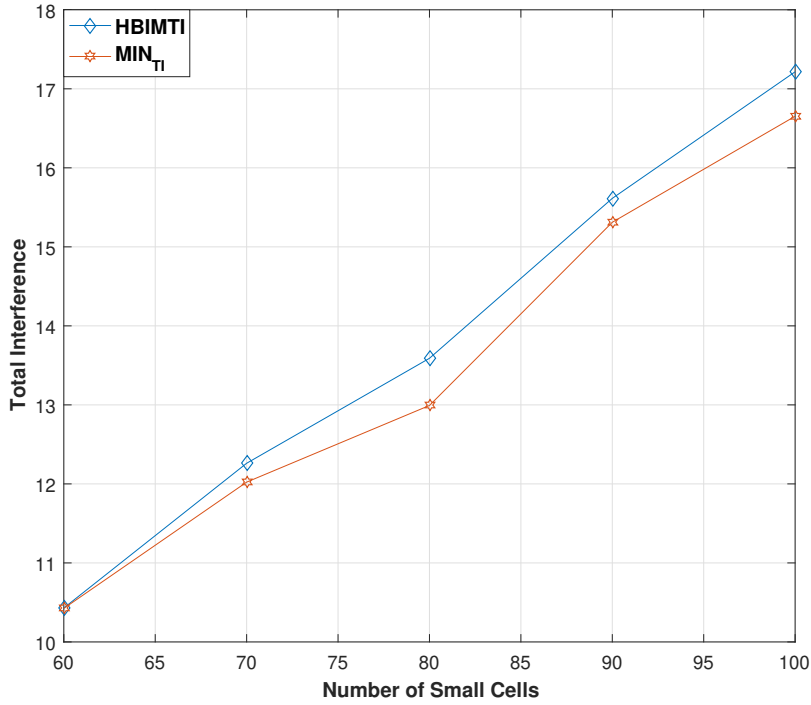
Figure 4.7: Total interference with $SC_{rm_j} = $ (30-60) Mbps and $NL_i = J/5$.

Fig. 4.8, increasing the number of SCs will increase the number of associated SCs and the total interference will increase.

Since, most of the related works have different system models and different objectives, we compare our results with the ones obtained from theHBCA [85]. HBCA is an algorithm that uses almost the same system model with an objective of maximizing the total sum rate subject to some constraints such as the maximum bandwidth, the number of links supported by each NFPs, and the minimum allowed SINR. The reason for which we do not compare the HBIMTI algorithm result with HBCA, as mentioned before, the HBIMTI associates each SC with an NFPs. However, in HBCA, each SC does not necessarily have an association with an NFPs. Therefore, it will not be a fair comparison. Moreover, we compare the MTIBLS algorithm result with the optimal result derived from ILP.

Fig. 4.9, shows the total interference of the proposed algorithm MTIBLS along with the minimum total interference obtained from ILP and initial total interference with 50
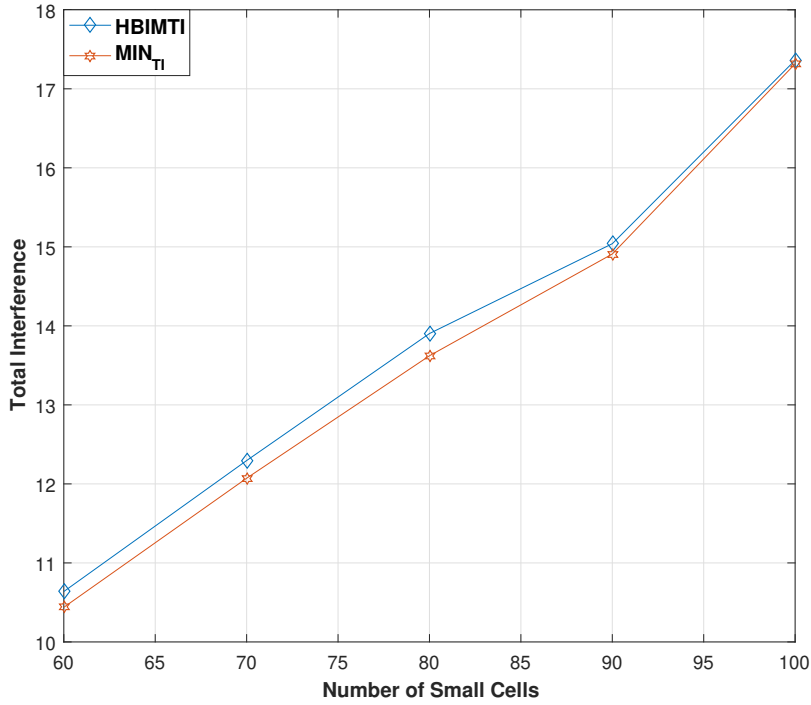
Figure 4.8: Total interference with SC_{rm_j}=50 Mbps and $Nl_i = J/5$.

NFPs. The total sum rate target equals half of MSR. The number of each NFPs links equal to $J/3$. Here $MTSR_{TI}$ in Fig. 4.9 represents the total interference obtained from the initial association between SCs and NFPs, MTIBLS represents total interference returned from the proposed algorithm, and HBCA$_{TI}$ represent the total interference retrieved from HBCA algorithm. Fig. 4.9 shows that the total interference of MTIBLS is less than HBCA$_{TI}$ total interference, and it is approximating the total interference of Min_{TI}. On the other hand, the total interference of MTIBLS is much less than the total interference of $MTSR_{TI}$. Thus, the proposed algorithm minimized the total interference of the system.

Fig. 4.10 displays the total interference of the proposed algorithm along with the one obtained from ILP and the minimum total interference with 50 NFPs. The total sum rate target equals one-third of the MSR. The number of each NFPs links is equal to $J/3$. Fig. 4.10 shows that the total interference of MTIBLS is much less than HBCA$_{TI}$ total interference. Moreover, the total interference of MTIBLS is emulating the total interference
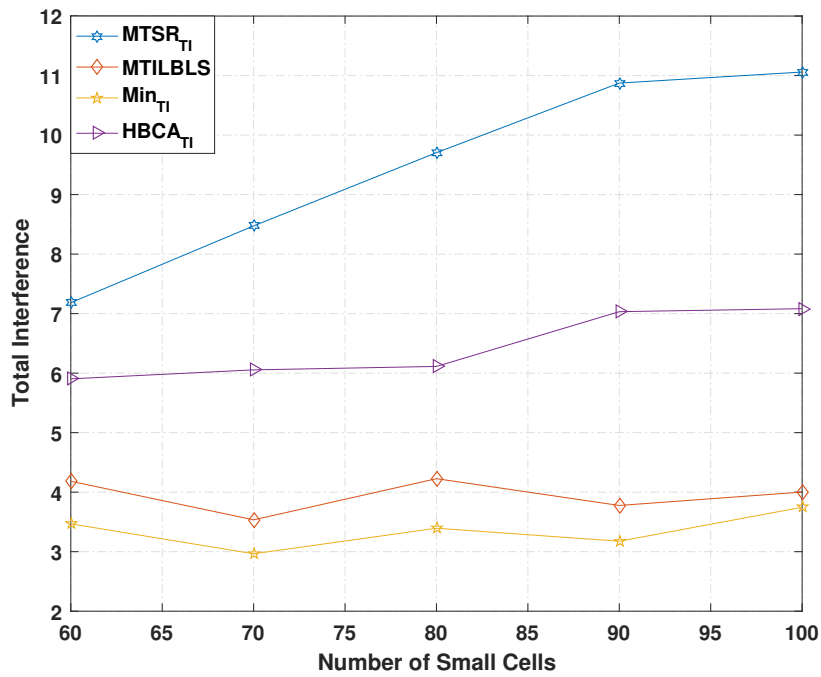
Figure 4.9: Total interference with $r_m=$ MSR/2 and $Nl_i = J/3$.
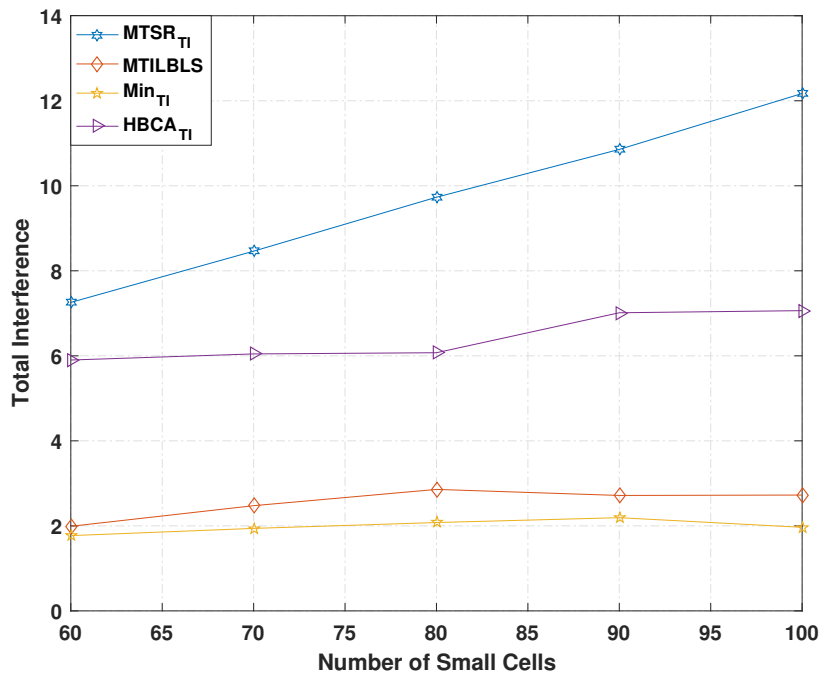
Figure 4.10: Total interference with $r_m=$ MSR/3 and $Nl_i = J/3$.
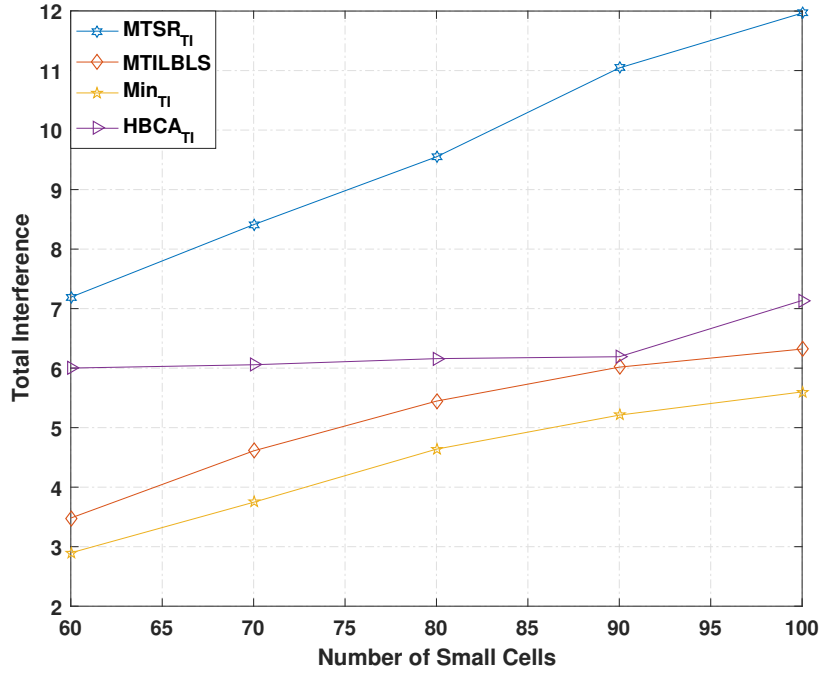
Figure 4.11: Total interference with MTSR$< r_m <$MSR and $Nl_i = J/3$.

of Min_{TI}. On the other hand, the difference between the total interference of MTIBLS and the total interference of $MTSR_{TI}$ indicates that the total system interference has decreased.

Fig. 4.11 demonstrates the total interference of the proposed algorithm along with the one obtained from initial association and the minimum total interference with 50 NFPs. The total sum rate target is between MTSR and MSR, and the number of each NFPs links is equal to $J/3$. As can be seen from Fig. 4.11, even though the total interference is increased (based on the increasing of total sum rate target), the total interference of MTIBLS is still approaching the total interference of Min_{TI}. Therefore, MTIBLS is still better than HBCA$_{\text{TI}}$ total interference. This means that regardless of the increased number of SCs, the proposed algorithms provides the sup-optimal solutions of the proposed problems.

One can observe, that the total interference in the MIETDR results is higher than the one returned from MITTSR problem, which is normal and expected. This is because in the

Table 4.3: Algorithms Uses

Algorithm	Uses
HBIMTI	Satisfy each SC fairness
MTIBLS	Satisfy a good overall network performance based on operator view point

MIETDR all SCs should be associated to the NFPs. On the other hand, not all SCs should be associated to the NFPs for MITTSR problem, where the number of associated SCs to the NFPs depends on the total sum rate target. Overall, minimizing total interference will enhance energy efficacy and increase reliability. Table 4.3, is explained where one of the algorithms will be preferable over the other one.

4.7 Conclusion

In this chapter, we examined the problem of associating SCs with NFPs while taking into consideration all related constraints (NFPs number of links, NFPs maximum bandwidth, maintaining a target data rate, etc.). We proposed two variants: First, the variant of associating SCs with NFPs to minimize the total interference while taking into consideration each SC target data rate. The NOAS algorithm that checks its feasibility. Following this, we proposed the HBIMTI algorithms (which is based on the Hungarian algorithm and local search techniques) to obtain sub-optimal solutions with reduced complexity. This chapter, also proposed the Min_{TI} which represents the ILP minimum total interference optimal result to solve this variant. As has been shown in the simulation results, the proposed HBIMTI algorithm approaches the optimal solution derived from Min_{TI} in term of minimizing the total interference.

The second variant associates SCs with NFPs to minimize the total interference of the system while sustaining a target total sum rate. We presented the MTSR algorithm to check its feasibility, then proposed the MTIBLS algorithm to solve the problem. The ILP of the problems was also examined to compare the proposed solutions results with the ILP derived bounds. Moreover, we compared the obtained result from the MTIBLS with

HBCA$_{\text{TI}}$ which represented the total interference retrieved from the HBCA algorithm. The proposed MTIBLS outperforms HBCA$_{\text{TI}}$ and approaches Min$_{\text{TI}}$. One can see that the total system interference of the proposed algorithms approached the total interference of Min_{TI}. Thus, the proposed algorithms are successful in enhancing the system total interference.

Chapter 5

Joint User Association and Power Allocation with Trajectory Optimization for Multi-UAVs Enabled Wireless Networks

5.1 Introduction

New technologies can be used in next wireless systems to satisfy the expected performance and overcome the existing terrestrial cellular systems limitations. One of these technologies is unmanned aerial vehicles (UAVs). UAVs can be used as a flying BSs in wireless communication network scenarios. Thus, flying aerial base stations can be used to support the connectivity of existing terrestrial wireless networks [86, 87].

UAVs have garnered great attention from the research community over the past few years due to their mobility, flexibility, and wide range of application fields (e.g. surveillance, monitoring, delivery of medical supplies, rescue operations, and telecommunications) [88]. UAVs can even be used as aerial BSs that can deliver reliable, cost-effective,

and on-demand wireless communications to desired areas.

When UAVs are used as aerial BSs, they ultimately extend the connectivity of the terrestrial wireless networks [89]. Relaying in wireless communication systems is an efficient technique for improving throughput, reliability and coverage [90, 91]. UAVs can be implemented as a new relaying technique, where the relay nodes are capable of moving at relatively high speeds to improve the connectivity and coverage of ground wireless devices.

The association problem of SCs with UAVs to minimize total interference was investigated in [92] by taking a look at the number of UAVs links, the UAV's maximum bandwidth, and target data rates constraints. In [85], distributed and centralized algorithms were proposed to connect air drones and balloons with traditional SCs of the cellular network, with the goal of maximizing system capacity. The performance of the works in [92] and [85] can be improved if the transmit power of users and/or the UAVs trajectory is further optimized. The authors in [93] proposed a UAV-supported system to maximize the uplink average sum rate of QoS terminals by planning UAV trajectory and resource allocation while satisfying the uplink sum rate and the UAV mobility constraints. They also proposed a sub-optimal iterative algorithm which alternatively optimized resource allocation and UAV trajectory until convergence.

In this chapter, we study a multi-UAV enabled wireless communication system, where numerous UAVs serve a group of UEs on the ground. To this end, we assume that all UAVs share the same frequency band for their communications with the UEs. By focusing on the up-link transmission from the ground UEs to the UAVs, our goal is to maximize the total uploaded rate among all users by jointly optimizing the UEs association with the UAVs, the UEs transmit power, and the UAVs trajectory in a given period.

The main contributions of this chapter can consequently be enumerated as follows.

- We formulate the total rate maximization problem to optimize the association between the UAVs and UEs, the UAVs trajectories, and the UEs transmit power allocations when subject to minimum data rate, maximum UAVs speed, maximum

UAV flying energy, maximum UEs transmit power, and minimum distance between
the drones to avoid collision.

- We consider two scenarios, namely, offline and online. In the offline scenario, we maximize the rate over all the time slots; while in the online scenario, we maximize the rate on a time-slot by time-slot basis.

- In the offline scenario, we propose an iterative algorithm to optimize the UAVs-UEs association using a modified Hungarian algorithm. Next, the UEs transmit power is optimized using a logarithmic approximation and the Lagrange equation. Finally, the UAVs trajectory is optimized using the UAVs trajectory in an interior-point algorithm alternately over all the time slots.

- In the online scenario, we assume fixed transmit power of UEs and find closed-form expressions of the optimal UAVs-UEs associations.

- We provide extensive simulation results to assess the performance of the proposed algorithms.

5.2 Related Work

A single UAV was employed to enhance the performance of wireless networks in [90, 94, 95, 96]. Likewise, the authors in [97] proposed a single UAV-aided mobile edge computing system, where the problem of user association, UEs uploading power, and the UAV trajectory was proposed to maximize the sum bits of offloaded tasks. They used integer programming and successive convex optimization methods to solve the proposed problem.

Moreover, the trajectory optimization of a single UAV has been studied for data offloading in the edge area of multiple cells in [98]. The authors considered a single UAV and three adjacent cells. The UAV trajectory was optimized to maximize the sum rate of edge users while taking into account the interference between ground BSs and UAV and satisfying all the mobile users required rate. They solved this non-convex problem

by divided it into two convex sub-problems. Then, they propose an iterative algorithm to obtain sub-optimal solution by optimizing the UAV trajectory and edge user scheduling alternately.

Similarly, the authors in [99] considered a fixed-wing UAV transmission communication problem, where an aerial BS is flying based on an optimized trajectory to cover the maximum number of ground users before draining its energy. Thus, they designed the initial UAV trajectory to enhance the coverage and proposed an iterative iterative algorithm to optimize the users communication scheduling, UAV flying parameters, UAV completion time, communication time among users, and transmit power in each iteration. Moreover, the authors in [100] studied the problem of maximizing the throughput for a UAV-enabled wireless powered communication network by jointly optimizing the UAV trajectory and the resource allocation in both the downlink and uplink. The throughput maximization problem was constrained by the UAV's maximum speed as well as the users' energy. However, a single UAV has limited capabilities due to its size, weight, and power constraints. This motivates the deployment of multiple UAVs that collaborate to serve ground users and further improve the performance of communication systems.

Therefore, the multi-UAV enabled wireless networks was investigated in [101], where the user association, the transmit power, and the UAV trajectories were jointly optimized in order to maximize the minimum average rate among all users. They proposed an iterative algorithm to solve the problem, and when compared to the case with static BSs, their numerical results showed that the mobility of UAVs help to achieve better air-to-ground channels and to enhance the system throughput.

The authors in [102] studied UAVs-enabled interference channel (UAV-IC). They considered the UAVs trajectory and power control (TPC) optimization problem to maximize the total sum rate of the UAV-IC for a given flying period of time, while taking into account the UAV flying speed, altitude, and collision avoidance. In particular, they proposed a successive convex approximation based algorithm to achieve a sub-optimal

96
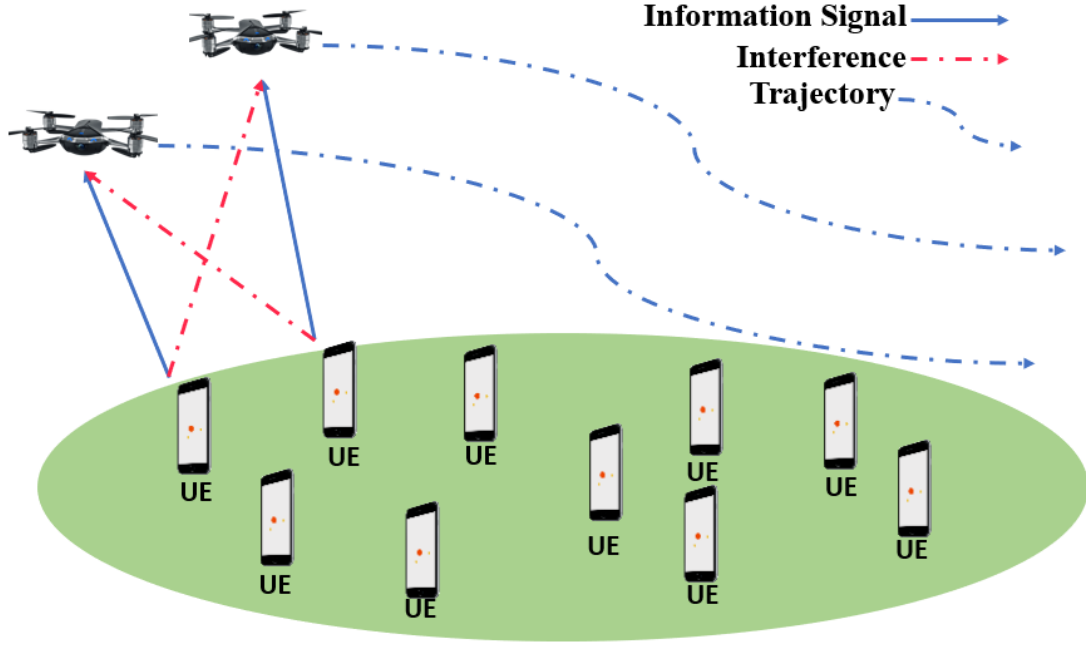
Figure 5.1: A multi-UAVs enabled wireless network.

solution of the problem. Their proposed algorithm jointly updated the UAVs trajectory and transmission power in each iteration.

The rest of this chapter is organized as follows. The system model is proposed in section 5.3. Next, in sections 5.4 and 5.5, we propose two efficient iterative algorithms to solve both the "offline" and "online" scenarios. Then, in section 5.6, we analysed the complexity of the proposed algorithms. The numerical results to demonstrate the performance of the proposed algorithms is presented in section 5.7. Finally, we conclude the chapter in Section 5.8.

5.3 System Model

As shown in Fig. 5.1, we consider a wireless communication system where I (≥ 1) UAVs are used to provide communication services for J (≥ 1) ground UEs. We assume that the UEs are distributed randomly over a 2-D coordinate plane, where each ground UE j, $j \in \{1, 2, ..., J\}$, is located at $z_j = (x_j, y_j)$. All the UAVs share the same frequency

band to support communications over a duration $T > 0$. During this period, each UAV i, $i \in \{1, 2, ..., I\}$ departs from its origin location $q_{i,0} = (x_{i,0}, y_{i,0})$, serves its associated ground UEs, and finally stops at its final destination $q_{i,T} = (x_{i,T}, y_{i,T})$.

The period T is divided into N equal time slots indexed by $n \in \{1, 2, ..., N\}$. The slot length $\delta_t = \frac{T}{N}$ is chosen to be sufficiently small such that each UAV's location is approximately unchanged within each one. Thus, the UAV location in the nth time slot is $q_{i,n} = (x_{i,n}, y_{i,n})$. Note that $q_{i,N} = q_{i,T}$, guaranteeing that each UAV at time slot N reaches the final destination.

We defined $\mathbf{Q}$ as an $I \times N$ matrix whose elements are represented as $q_{i,n}, \forall i, n$, to include all the UAVs trajectory at all time slots. All UAVs are considered to fly at a fixed altitude H above the ground, and the ith UAV velocity denoted by $v_{i,n}$ in the nth time slot is constrained by the maximum allowed velocity $\mathrm{V_{max}}$ as follows

$$v_{i,n} = \frac{||q_{i,n} - q_{i,n-1}||}{\delta_t} \leq \mathrm{V_{max}}. \tag{5.1}$$

To avoid collision between UAVs, a minimum distance, $\mathrm{d_{min}}$, should be ensured as follows

$$||q_{m,n} - q_{i,n}||^2 \geq \mathrm{d}^2_{\min}, \quad \forall i, m \in I, m \neq i. \tag{5.2}$$

For the sake of simplicity, we consider that the communication links from the UAVs to the ground UEs are dominated by the LoS links where the UAV-UE distance determines the channel quality [97]. The channel gain between UE j and the UAV i at the nth time slot follows the free-space path loss model, which can be given as [97, 101]

$$h_{i,j,n} = \frac{\rho_0}{H^2 + ||q_{i,n} - z_j||^2}, \tag{5.3}$$

where ρ_0 is the channel gain at reference distance of $d_0 = 1$ m.

We defined $\mathbf{A}$ as an $I \times J \times N$ matrix whose elements are represented as $a_{i,j,n}, \forall i, j, n$. $a_{i,j,n}$ is a binary variable that indicates whether UE j is served by the UAV i in time

slot n. At each time slot n, each UAV i serves at most one ground UE, and this can be mathematically represented as follows

$$\sum_{j=1}^{J} a_{i,j,n} = 1, \quad \forall i, n. \tag{5.4}$$

Similarly, at each time slot n, each UE j is served by at most one UAV, yielding the following constraint

$$\sum_{i=1}^{I} a_{i,j,n} = 1, \quad \forall j, n. \tag{5.5}$$

We defined $\mathbf{P}$ as a $J \times N$ matrix and its elements are equal to $P_{j,n} \quad \forall j, n$. Thus, $p_{j,n}$ is the uplink transmit power of UE j in time slot n and is constrained as follows

$$0 \leq p_{j,n} \leq P_{\max}, \tag{5.6}$$

where $P_{\max}$ is the maximum UE uploading power. For the jth UE, the total uploading energy over all N time slots is limited by a maximum energy denoted as E_j as seen here

$$\sum_{n=1}^{N} P_{j,n} \delta_n \leq \mathrm{E}_j, \quad \forall j. \tag{5.7}$$

The received SINR at UAV i, assuming UE j is associated with UAV i in time slot n, can be expressed as

$$\mathrm{SINR}_{i,j,n} = \frac{P_{j,n} h_{i,j,n}}{\sigma_i^2 + \sum_{k=1, k \neq j}^{J} P_{k,n} h_{i,k,n}}, \tag{5.8}$$

where σ_i^2 is the power of MTSR at the UAV i and the $\sum_{k=1, k \neq j}^{J} P_{k,n} h_{i,k,n}$ in the denominator represents the interference caused by the transmissions of allthe other UEs at time slot n. If the UE is not associated, then its transmit power is zero in the interference term. The uploaded rate of UE j in time slot n to the UAV i in (bits/s/Hz), denoted by

99

$R_{i,j,n}$, can be expressed as

$$R_{i,j,n} = \log_2 \left(1 + \text{SINR}_{i,j,n}\right), \quad \forall i, j, n. \tag{5.9}$$

The uploaded data rate from UE j at time slot n to UAV i should satisfy a minimum-requested rate denoted by $R_{\min}$. The data rate uploaded from each UE over all N time slots is given by

$$S_j = \sum_{n=1}^{N} \sum_{i=1}^{I} a_{i,j,n} R_{i,j,n}. \tag{5.10}$$

Hence, the sum rate from all UEs over all time slots is defined as

$$\widehat{S} = \sum_{j=1}^{J} S_j. \tag{5.11}$$

The energy consumed by the UAVs is mostly used to support flight. We will consider an energy consumption model that has been widely adopted in the literature for both fixed and rotary wing UAV [103, 104]. This model takes into account only the kinetic energy based on the fact that constant-height flights require no change in the gravitational potential energy.

That said, the flying energy of UAV i at each time slot n depends only on the velocity $v_{i,n}$ and is given by

$$e_{F_{i,n}} = k_i v_{i,n}^2, \tag{5.12}$$

where $k_i = 0.5 M_i \delta_t$, and M_i is the UAV i mass including its payload. Therefore, the flight energy consumed by each UAV i over all time slots N can be represented by

$$E_{F_i} = \sum_{n=1}^{N} e_{F_{i,n}}, \quad \forall i. \tag{5.13}$$

Considering that the UAV is equipped with a battery of finite energy E_0, the energy consumption of UAV i is restricted since $E_{F_i} \leq E_0$.

5.3.1 Problem Formulation

This chapter aims to maximize the total uploaded rate from the ground UEs to the aerial BS by jointly optimizing the user association $\mathbf{A}$, the transmitted power $\mathbf{P}$, and the UAV trajectory $\mathbf{Q}$ over all time slots. This optimization problem can therefore be formulated as

$$\mathcal{P}: \max_{\mathbf{A},\mathbf{P},\mathbf{Q}} \quad \widehat{S}(\mathbf{A},\mathbf{P},\mathbf{Q}) \tag{5.14a}$$

$$\text{subject to} \quad E_{F_i}(q_i) \leq \mathrm{E}_0, \quad \forall i, \tag{5.14b}$$

$$a_{i,j,n}R_{i,j,n}(P_j,q_i) \geq \mathrm{R}_{\min}, \quad \forall i,j, \tag{5.14c}$$

$$v_{i,n}(q_i) \leq \mathrm{V}_{\max}, \quad \forall i,n, \tag{5.14d}$$

$$\sum_{n=1}^{N} P_{j,n}\delta_t \leq \mathrm{E}_j, \quad \forall j, \tag{5.14e}$$

$$\sum_{j=1}^{J} a_{i,j,n} = 1, \quad \forall i,n, \tag{5.14f}$$

$$\sum_{i=1}^{I} a_{i,j,n} = 1, \quad \forall j,n, \tag{5.14g}$$

$$0 \leq P_{j,n} \leq \mathrm{P}_{\max}, \quad \forall j,n, \tag{5.14h}$$

$$q_{i,N} = q_{i,T}, \quad \forall i, \tag{5.14i}$$

$$q_{i,0} = q_{i,T=0}, \quad \forall i, \tag{5.14j}$$

$$||q_{m,n} - q_{i,n}||^2 \geq \mathrm{d}^2_{\min}, \quad \forall m,i \in I, m \neq i, \tag{5.14k}$$

$$a_{i,j,n} \in \{0,1\}, \quad \forall i,j,n. \tag{5.14l}$$

Solving problem $\mathcal{P}$ is quite challenging due to the integer constraints, the non-convex objective, and data rate constraint (5.14c) with respect to the UAVs trajectory variables and transmit power variables. It can be viewed as a mixed-integer non-convex problem, which is generally difficult to be optimize.

Towards this end, we propose two solutions for solving problem $\mathcal{P}$. The offline solu-

tion assumes global network information availability and the less-complex online solution assumes only the availability of local network information.

5.4 The Proposed Solution for The Offline Scenario

In the offline scenario, we jointly optimize the UAVs-UEs association, power allocation, and UAVs trajectory over all time slots simultaneously. We apply the following iterative approach, which transacts with user association, power optimization, and UAVs trajectory separately

$$\underbrace{\mathbf{A}^0 \to \mathbf{P}^0 \to \mathbf{Q}^0}_{\text{Initialization}} \to \dots \underbrace{\mathbf{A}^r \to \mathbf{P}^r \to \mathbf{Q}^r}_{\text{Iteration } r} \to \dots \underbrace{\mathbf{A}^{\text{SubOpt}} \to \mathbf{P}^{\text{SubOpt}} \to \mathbf{Q}^{\text{SubOpt}}}_{\text{SubOptimal \quad Solution}}. \qquad (5.15)$$

Therefore, for given UAVs trajectory and UEs transmit power, we optimize the UAVs-UEs association. Similarly, for given UAVs-UEs association and UAVs trajectory, we optimize the UE transmit power. Then, for given UAVs-UEs association and UEs transmit power, we optimize the UAVs trajectory.

This iterative process repeats until convergence; however it is worth mentioning that arriving at the global optimal solution cannot be guaranteed in this case. The overall algorithm to find the sub-optimal solution for the offline scenario is summarized at the end of this section. In the following subsections, we discuss the proposed solutions for UAVs-UEs association, UEs transmit power, and UAVs trajectory.

5.4.1 UAVs-UEs Association Optimization

In this subsection, given the UEs transmit power and UAVs trajectory at iteration $r-1$, i.e., $\mathbf{P}^{r-1}$ and $\mathbf{Q}^{r-1}$, respectively, we find the UAVs-UEs association to maximize the sum

---

Algorithm 12 : Modified Hungarian Algorithm (MHA)

1: **Input:** $(UEs, UAVs, \mathbf{P}, \mathbf{Q}, R)$
2: Let $W_{J \times J \times N}$ be a new Matrix ▷ $W_{i,j,n}$ is the weight of the edge between ith UAV and jth UE.
3: **for** each $n \in N$ **do**
4:    **for** each UAV i **do**
5:       **for** each UE j **do**
6:          $W_{i,j,n} = R_{i,j,n}$
7:       **end for**
8:    **end for**
9:    **for** each $J - I$ virtual UAVs pair **do**
10:       **for** each UE **do**
11:          $W_{i,j,n} = 0$
12:       **end for**
13:    **end for**
14:    Let $H_{J \times J}$ be a new matrix   ▷ a Boolean matrix, a true value in i, j index depicts, ith UAV is assigned to sth UE, $H = $ HUNGARIAN(W) ▷ Hungarian Algorithm is the bipartite matching algorithm which will return a Boolean matrix
15:    **for** each UAV $i \in I$ **do**
16:       **for** each UE $j \in J$ **do**
17:          **if** $H_{i,j} = 0$ **then**
18:             Associate jth UE with ith UAV
19:          **end if**
20:       **end for**
21:    **end for**
22: **end for**

---

rate. Hence, the optimization problem $\mathcal{P}$ can be formulated as

$$\mathcal{P}_1 : \quad \max_{\mathbf{A}} \quad \sum_{n=1}^{N} \sum_{j}^{J} \sum_{i=1}^{I} a_{i,j,n} R_{i,j,n} \tag{5.16a}$$

$$\text{subject to} \quad (5.14c), (5.14f), (5.14g), (5.14l), \tag{5.16b}$$

where the constraints in (5.14b), (5.14e), (5.14h), (5.14i), (5.14j), and (5.14k) are not functions of the association variable $\mathbf{A}$ and are consequently treated as constants. The problem $\mathcal{P}_1$ is an integer linear program and can be solved using the branch and bound algorithm [19], however, at the cost of high computational complexity. Therefore, we propose a Hungarian-based algorithm to find the sub-optimal solution for problem $\mathcal{P}_1$ at reduced computational complexity.

The original Hungarian algorithm performs one-to-one matching of two lists of same length. In our system model, each UAV associates with one UE at each time slot; however, the number of UEs is greater than the number of UAVs. Hence, the original Hungarian algorithm cannot be directly used. We therefore propose a modified Hungarian algorithm that can handle the differing numbers of UAVs and UEs. The basic idea of the MHA is to add virtual UAVs to compensate for the difference between the UAVs and UEs numbers. The proposed MHA can be explained as follows.

- The proposed MHA adds a number of virtual UAVs equal to the difference between the UEs and the UAVs. Then, it checks if there are any free non-virtual UAVs, and fills the element $W_{i,j,n}$ of a matrix $\mathbf{W}$ with $R_{i,j,n}$, otherwise $W_{i,j,n}$ is filled with zero (lines 4-13).

- The Hungarian algorithm takes $\mathbf{W}$ as input and outputs a matrix $\mathbf{H}$, indicating if there is an association between the ith UAV and the jth UE if $H_{i,j,n} = 0$, and hence, the association matrix $\mathbf{A}$ is updated accordingly. (lines 14- 21).

5.4.2 UEs Transmit Power Optimization

In this subsection, given the optimized UAVs-UEs association at iteration r and UAVs trajectory at iteration $r-1$, i.e., $\mathbf{A}^r$ and $\mathbf{Q}^{r-1}$, respectively, we optimize the UEs transmit power allocation to maximize the sum rate. As a result, the optimization problem $\mathcal{P}$ can be written as

$$\mathcal{P}_2: \quad \max_{\mathbf{p}} \quad \sum_{j}^{J} \sum_{n=1}^{N} \sum_{i=1}^{I} a_{i,j,n} R_{i,j,n}(\mathbf{p}) \tag{5.17a}$$

$$\text{subject to} \quad (5.14c), (5.14e), (5.14h), \tag{5.17b}$$

where the constraints in (5.14b), (5.14d), (5.14f), (5.14g), (5.14i), (5.14k), (5.14j), and (5.14l) are not functions of $\mathbf{P}$ and are treated as constants.

It is clear that problem $\mathcal{P}_2$ is not concave with respect to $\mathbf{P}$ because the rate function

is highly non-concave in $\mathbf{P}$. To overcome this difficulty, we employ a successive convex approximation (SCA) approach allocation [105, 106] using a logarithmic approximation to find the sub-optimal power.

Our approach considers a relaxation of the non-convex problem (5.17) to avoid dealing with the highly non-concave rate function in (5.9). We make use of the following lower bound on the logarithmic rate function [107]

$$\log(1+w) \geq \alpha \log(w) + \beta, \tag{5.18}$$

which is tight at $w = \bar{w} > 0$ when the approximation constants α and β are chosen such as

$$\alpha = \frac{\bar{w}}{1+\bar{w}}, \tag{5.19}$$

and

$$\beta = \log(1+\bar{w}) - \frac{\bar{w}}{1+\bar{w}} \log(\bar{w}). \tag{5.20}$$

Applying the approximation in (5.17) to (5.9) and utilizing the change of variable $\hat{p}_{j,n} = \log_2(p_{j,n})$, we obtain the following optimization problem

$$\mathcal{P}_3 : \quad \max_{\widehat{\mathbf{P}}} \quad \sum_{j}^{J} \sum_{n=1}^{N} \sum_{i=1}^{I} a_{i,j,n} \hat{R}_{i,j,n}(e^{\hat{p}_j}, \alpha, \beta) \tag{5.21a}$$

$$\sum_{n=1}^{N} e^{\hat{p}_j} \delta_t \leq \mathrm{E_j}, \quad \forall j, \tag{5.21b}$$

$$0 \leq e^{\hat{p}_j} \leq \mathrm{P_{max}}, \quad \forall j, n, \tag{5.21c}$$

$$\hat{R}_{i,j,n}(e^{\hat{p}_j}, \alpha, \beta) \geq \mathrm{R_{min}}, \quad \forall j, \tag{5.21d}$$

where $\widehat{\mathbf{P}}$ is defined as $J \times N$ matrix and its elements are equal to $\widehat{P}_{j,n}$ $\forall j, n$, and $\widehat{R}_{i,j,n}(e^{\hat{p}_j}, \alpha, \beta) = \sum_{j=1}^{J} (\alpha_j \log_2(\mathrm{SINR}_{i,j}) + \beta_j)$ is a lower bound of $R_{i,j,n}(\mathbf{P})$.

Since the log-sum-exp function is convex [108], it is clear that $\mathcal{P}_3$ is a concave maximization problem. Let $\lambda_j \geq 0$ and $\phi_j \geq 0$ be the Lagrangian multipliers of sub-problem

105

Algorithm 13 : Power Allocation based on logarithmic approximation for overall n

1: Initialize: $t_{in} := 0$, $t_o := 0$.
2: For each UE j initialize: $\phi_j > 0$, $\lambda_j > 0$ $\alpha_j = 1$ and $\beta_j = 0$.
3: **Repeat**{To solve (5.17)}
4: **Repeat**{To solve (5.21)}
5: UE j computes its power $P_{j,n}$ using equation (5.23)
6: UE j updates λ_j by (5.24)
7: UE j updates ϕ_j by (5.25)
8: Set $t_{in} = t_{in} + 1$
9: **Until** ϕ and λ_j converges
10: Set $P^*[t_o] = P[t_{in}]$
11: UE j updates $\alpha_j[t_o + 1]$ and $\beta_j[t_o + 1]$
12: Set $t_o = t_o + 1$
13: **Until P** converges

in $\mathcal{P}_3$ associated with (5.21b) and (5.21d), respectively. The Lagrangian function of $\mathcal{P}_3$ is defined as

$$\mathcal{L}(\hat{P}, \lambda, \phi) = \sum_{j=1}^{J} \widehat{R}_{i,j,n}(e^{\hat{p}_j}, \alpha, \beta) + \sum_{j=1}^{J} \lambda_j \left(\widehat{R}_{i,j,n}(e^{\hat{p}_j}, \alpha, \beta) - R_{\min} \right) - \sum_{j=1}^{J} \phi_j \left(\sum_{n=1}^{N} e^{\hat{p}_{j,n}} \delta_t - E_j \right).$$

(5.22)

By solving the stationary condition $\partial \mathcal{L}((\hat{P}, \lambda, \phi)/\partial \widehat{p}_{j,n} = 0$ and turning the result back as $p_{j,n} = e^{\hat{p}_{j,n}}$, the following equation can be derived

$$p_{j,n} = \left[\frac{\alpha_j(1 + \lambda_j)}{\frac{\alpha_j(1+\lambda_j)}{\sum_{\bar{k}=1, \bar{k} \neq j}^{J} p_{k,n} h_{i,\bar{k}} + \sigma^2} h_{i,j} + \phi_j} \right]_0^{P_{max}}.$$

(5.23)

The Lagrange multiplier λ_j and ϕ_j can be updated using the sub-gradient method as follows [109]

$$\lambda_j^{d+1} = \left[\lambda_j^d + \delta_\lambda(R_{\min} - R_{i,j,n}) \right]^+,$$

(5.24)

$$\phi_j^{d+1} = \left[\phi_j^d + \delta_\phi(\sum_{n=1}^{N} P_{j,n}\delta_t - E_j) \right]^+,$$

(5.25)

where $[.]^+ = \max(., 0)$, $\delta_\lambda > 0$ and $\delta_\phi > 0$ are step sizes. We tighten the bound in $\mathcal{P}_3$ by updating α and β values according to (5.19) and (5.20) [110]. We summarize the

106

procedure to find the UEs transmit power in Algorithm 13.

5.4.3 UAVs Trajectory Optimization

In this subsection, given the optimized UAVs-UEs association as well as the UE transmit power at iteration r, i.e., $\mathbf{A}^r$ and $\mathbf{P}^r$, respectively, we find the UAVs trajectory that maximizes the sum rate. Therefore, the optimization problem $\mathcal{P}$ can be written as follows

$$\mathcal{P}_4 : \quad \max_{\mathbf{Q}} \quad \sum_{j}^{J} \sum_{n=1}^{N} \sum_{i=1}^{I} a_{i,j,n} R_{i,j,n}(\mathbf{Q}) \tag{5.26a}$$

$$\text{subject to} \quad (5.14\text{b}), (5.14\text{c}), (5.14\text{d}), (5.14\text{i}), (5.14\text{j}), (5.14\text{l}), (5.14\text{k}), \tag{5.26b}$$

where the constraints in (5.14e), (5.14f), (5.14g), and (5.14h) are not functions of $\mathbf{Q}$ and are treated as constants.

One can note that problem $\mathcal{P}_4$ is a non-convex problem due to the non-convex expression $R_{i,j,n}$ with respect to $q_{i,n}$ and the non-convex constraints (5.14k). Following this, it becomes undoubtedly difficult to solve. Adopting a similar approach to what was done to handle problem $\mathcal{P}_3$, we use the successive convex optimization technique [105, 106, 19] to solve the problem $\mathcal{P}_4$.

In this chapter, we address these non-convex objective and constrains using their first order Taylor expansion. To this end, one can rewrite $R_{i,j,n}$ in (5.9) as follows

$$R_{i,j,n} = \widehat{R}_{i,j,n} - \log_2 \left(\sum_{k=1, k\neq j}^{J} \frac{P_{k,n}\rho_0}{H^2 + ||q_{i,n} - z_k||^2} + \sigma^2 \right), \tag{5.27}$$

where

$$\widehat{R}_{i,j,n} = \log_2 \left(\sum_{j=1}^{J} \frac{P_{j,n}\rho_0}{H^2 + ||q_{i,n} - z_j||^2} + \sigma^2 \right). \tag{5.28}$$

Despite the fact that $\widehat{R}_{i,j,n}$ is not concave with respect to $q_{i,n}$, it is convex with respect to $||q_{i,n} - z_k||^2$.

Algorithm 14 : Offline scenario iterative algorithm

1: Initialize: $\mathbf{Q}^{r-1}$, $\mathbf{P}^{r-1}$, Let $r = 1$
2: **Repeat** { to solve $\mathcal{P}$}
3: For given { $\mathbf{Q}^{r-1}$, $\mathbf{P}^{r-1}$}, solve problem $\mathcal{P}_1$ and find the optimal solution as $\mathbf{A}^r$.
4: For given { $\mathbf{Q}^{r-1}$, $\mathbf{A}^r$}, solve problem $\mathcal{P}_2$ and find the optimal solution as $\mathbf{P}^r$.
5: For given { $\mathbf{A}^r$, $\mathbf{P}^r$}, solve problem $\mathcal{P}_4$ and find the optimal solution as $\mathbf{Q}^r$.
6: Update $r = r + 1$
7: **Until** Convergence of $\mathbf{Q}$, $\mathbf{P}$, and $\mathbf{A}$

As commonly known, any convex function is globally lower-bounded by its first-order Taylor expansion at any point [111]. Hence, for a given point $q_{i,n}^r$ in iteration r, the lower bound for $\widehat{R}_{i,j,n}$ can be written as follows

$$\widehat{R}_{i,j,n} \geq \sum_{j=1}^{J} -D_{i,j,n}^r \left(||q_{i,n} - z_j||^2 - ||q_{i,n}^r - z_j||^2 \right) + C_{i,j,n}^r \triangleq \widehat{R}_{i,j,n}^{lb}, \tag{5.29}$$

where $D_{i,j,n}^r$ is a constant equal to the first order derivative of $\widehat{R}_{i,j,n}$ at a given point $q_{i,n}^r$, and $C_{i,j,n}^r$ is a constant equal to $\widehat{R}_{i,j,n}$ at $q_{i,n}^r$. The values of $D_{i,j,n}^r$ and $C_{i,j,n}^r$ are given as

$$D_{i,j,n}^r = 2 \frac{\sum_{j=1}^{J} \frac{P_{j,n}\rho_0 ||q_{i,n}^r - z_j||}{(H^2 + ||q_{i,n}^r - z_j||^2)^2} log_2(e)}{\sum_{l=1}^{J} \frac{P_{l,n}\rho_0}{H^2 + ||q_{i,n}^r - z_l||^2} + \sigma^2}, \quad \forall i, j, n \tag{5.30}$$

and

$$C_{i,j,n}^r = \log_2 \left(\sum_{j=1}^{J} \frac{P_{j,n}\rho_0}{H^2 + ||q_{i,n}^r - z_j||^2} + \sigma^2 \right), \quad \forall i, j, n. \tag{5.31}$$

Hence, $\widehat{R}_{i,j,n}^{lb}$ is convex with respect to $q_{i,n}$.

Note that the second term on the right hand side in (5.27) is non-convex in $\mathbf{Q}$. Thus, by introducing the slack variables $F = \{F_{i,k,n} = ||q_{i,n} - z_k||^2, \ \forall k \neq j, n\}$, we can rewrite equation (5.27) as follows

$$R_{i,j,n} \geq \widehat{R}_{i,j,n}^{lb} - \log_2 \left(\sum_{k=1,k\neq j}^{J} \frac{P_{k,n}\rho_0}{H^2 + F_{i,k}} + \sigma^2 \right) \triangleq \widehat{R}_{i,j,n}^{low,r}. \tag{5.32}$$

The new slack variable constraint should be added to problem $\mathcal{P}_4$ as $F_{i,k,n} \leq ||q_{i,n} -$

$z_k||^2$. Therefore, $\mathcal{P}_4$ can be rewritten as follows

$$\mathcal{P}_5: \quad \max_{\mathbf{Q}} \quad \widehat{S}^{low,r} \tag{5.33a}$$

$$\text{subject to} \quad a_{i,j,n} R_{i,j,n}^{low,r} \geq \mathrm{R_{min}}, \quad \forall i, \tag{5.33b}$$

$$F_{i,k,n} \leq ||q_{i,n} - z_k||^2 \quad \forall i \neq m, \tag{5.33c}$$

$$||q_{m,n} - q_{i,n}||^2 \geq \mathrm{d^2_{min}} \quad \forall i \neq m, \tag{5.33d}$$

$$(5.14\mathrm{b}), (5.14\mathrm{d}), (5.14\mathrm{i}), (5.14\mathrm{j}), \tag{5.33e}$$

where $\widehat{S}^{low,r} = \sum_{n=1}^{N} \sum_{i=1}^{I} a_{i,j,n} R_{i,j,n}^{low,r}$.

Since, $||q_{i,n} - z_k||^2$ is a convex function with respect to $q_{i,n}$, $||q_{i,n} - z_k||^2$ is lower bounded by its first order Taylor expansion at point $q_{i,n}^r$ as follows

$$||q_{i,n} - z_k||^2 \geq ||q_{i,n}^r - z_k||^2 + 2(q_{i,n}^r - z_k)^T (q_{i,n} - z_k), \quad \forall j \neq m, n. \tag{5.34}$$

For constraint (5.33d), by applying the first-order Taylor expansion at the given point $q_{m,n}$ and $q_{i,n}$ to $||q_{m,n} - q_{i,n}||^2$, we obtain the following inequality

$$||q_{m,n} - q_{i,n}||^2 \geq - ||q_{m,n}^r - q_{i,n}^r||^2 + 2(q_{m,n}^r - q_{i,n}^r)^T (q_{m,n} - q_{i,n}), \quad \forall j \neq m, n. \tag{5.35}$$

Therefore, we can rewrite problem $\mathcal{P}_5$ as

$$\mathcal{P}_6: \quad \max_{\mathbf{Q}} \quad \widehat{S}^{low,r} \tag{5.36a}$$

$$\text{subject to} \quad a_{i,j,n} R_{i,j,n}^{low,r} \geq \mathrm{R_{min}}, \quad \forall i, \tag{5.36b}$$

$$F_{i,k,n} \leq ||q_{i,n}^r - z_k||^2 + 2(q_{i,n}^r - z_k)^T (q_{i,n} - z_k) \quad \forall i \neq m, \tag{5.36c}$$

$$\mathrm{d^2_{min}} \leq - ||q_{m,n}^r - q_{i,n}^r||^2 + 2(q_{m,n}^r - q_{i,n}^r)^T (q_{m,n} - q_{i,n}) \quad \forall i \neq m, \tag{5.36d}$$

$$(5.14\mathrm{b}), (5.14\mathrm{d}), (5.14\mathrm{i}), (5.14\mathrm{j}). \tag{5.36e}$$

Since, all constraints in problem $\mathcal{P}_6$ are either concave or linear, problem $\mathcal{P}_6$ is concave and can be effectively solved by standard convex optimization solvers such as CVX [106, 108, 19].

5.4.4 Overall Algorithm

In this subsection, we summarize the overall iterative approach used to solve problem $\mathcal{P}$ by applying the alternating optimization method shown in Algorithm 14. Specifically, the algorithm starts by finding the UAVs-UEs association based on the given $\mathbf{P}$ and $\mathbf{Q}$ in the previous iteration using Algorithm 12. Then, for the given $\mathbf{Q}$ and optimized $\mathbf{A}$, the power allocation $\mathbf{P}$ is found using Algorithm 13. Finally, based on the optimized $\mathbf{A}$ and $\mathbf{P}$, the UAV trajectory $\mathbf{Q}$ is optimized using any standard CVX. The process repeats until $\mathbf{A}$, $\mathbf{P}$, and $\mathbf{Q}$ converge or there is no further improvement in the sum rate.

5.5 The Proposed Solution for The Online Scenario

In the online scenario, we jointly optimize the UAVs-UEs association $\mathbf{A}_n$. We define $\mathbf{A}_n$ as an $I \times J$ matrix whose elements are represented as $a_{i,j}, \forall i, j$. Looking at the UEs power allocation $\mathbf{P}_n$, we define $\mathbf{P}_n$ as J vector whose elements are represented as $p_j, \forall j$. Next, when investigating UAV locations $\mathbf{Q}_n$, we define a I vector whose elements are represented as $q_i, \forall i$, on a time slot by time slot basis. We apply the next iterative approach to optimize the UAVs-UEs association, the UEs power allocation, and the UAV locations at each time slot separately.

$$\underbrace{\mathbf{A}_n^0 \rightarrow \mathbf{P}_n^0 \rightarrow \mathbf{Q}_n^0}_{\text{Initialization}} \rightarrow .... \underbrace{\mathbf{A}_n^r \rightarrow \mathbf{P}_n^r \rightarrow \mathbf{Q}_n^r}_{\text{Iteration} \quad r} \rightarrow .... \underbrace{\mathbf{A}_n^{\text{SubOpt}} \rightarrow \mathbf{P}_n^{\text{SubOpt}} \rightarrow \mathbf{Q}_n^{\text{SubOpt}}}_{\text{SubOptimal} \quad \text{Solution}} \quad (5.37)$$

Hence, for the nth time slot UAVs locations and nth time slot UEs transmit power, we optimize the nth time slot UAVs-UEs association. In a similar fashion, for a given nth time slot UAVs-UEs association and the nth time slot UAVs locations, we optimize the nth time slot UEs transmit power. Afterwards, for the nth time slot UAVs-UEs

association and UEs transmit power, the nth time slot UAVs locations are optimized. This iterative process is repeated until convergence. We summarize the overall algorithm to find the sub-optimal solution for the online scenario at the end of this section. In the coming subsections, we discuss the proposed solutions for the online scenario.

5.5.1   UEs Transmit Power Optimization

For the online scenario, we assume that the UEs have a fixed transmit power for each time slot as follows

$$P_{j,n} = \mathrm{E}_j/(N\delta_t), \quad \forall j, n. \tag{5.38}$$

Note that fixing the transmit power can be useful in some IoT applications, where the sensor nodes may not have complex circuitry to support adaptive power.

5.5.2   UAVs-UEs Association Optimization

In this subsection, given the nth time slot UEs fixed transmit power and nth time slot UAVs location at iteration $r-1$, i.e., $\mathbf{P}_n^{r-1}$ and $\mathbf{Q}_\mathrm{n}^{\mathrm{r}-1}$, respectively, we find the nth time slot UAVs-UEs association to maximize the sum rate. Hence, the optimization problem $\mathcal{P}$ can be written as

$$\mathcal{P}_7: \quad \max_{\mathbf{A}_n} \quad \sum_{n=1}^{N} \sum_{j}^{J} \sum_{i=1}^{I} a_{i,j,n} R_{i,j,n} \tag{5.39a}$$

$$\text{subject to} \quad (5.14c), (5.14f), (5.14g), (5.14l), \tag{5.39b}$$

where the constraints in (5.14b), (5.14e), (5.14h), (5.14i),(5.14j), and (5.14k) are not function of $\mathbf{A}_n$ and are therefore treated as constants.

Problem $\mathcal{P}_7$ is a integer linear program and can be solved using branch and bound algorithm with a high time complexity [19] and of course at the cost of high computational complexity. We exploit the fact that in $\mathcal{P}_7$, the UEs transmit power is fixed to obtain the UAVs-UEs association in low complexity as discussed in the following proposition.

Proposition: When the optimal solution of $\mathcal{P}_7$ is found, each UE is assigned to the

111

UAV that offers the highest data rate.

Proof: Suppose that when the optimal solution of (5.39) is found, at time slot n, we assume without loss of generality that the UAV 1 is assigned to UE j, $j \in J \setminus j^*$, $d \in D \setminus d^*$, implying that d can be any element in D excluding d^*, where UE j^* denotes the UE with the highest data rate to UAV 1 at time slot n. As a result, we can present the following

$$\text{SINR}_{1,j,n} = \frac{P_{j,n} h_{1,j,n}}{\sigma_1^2 + P_{j^*,n} h_{1,j^*,n} + \sum_{k=1, k \neq j, j^*}^{J} P_{k,n} h_{1,k,n}}. \tag{5.40}$$

Assume that the UAV 1 at n instead assigned to UE j^*, then the SINR from UE j^* to UAV 1 can be given as

$$\text{SINR}_{1,j^*,n} = \frac{P_{j^*,n} h_{1,j^*,n}}{\sigma_1^2 + P_{j,n} h_{1,j,n} + \sum_{k=1, k \neq j, j^*}^{J} P_{k,n} h_{1,k,n}}. \tag{5.41}$$

Note that the two terms $\sum_{k=1, k \neq j, j^*}^{J} P_{k,n} h_{1,k,n}$ and $\sum_{k=1, k \neq j, j^*}^{J} P_{k,n} h_{1,k,n}$ have the same value. Therefore, based on the assumption that UE j^* denotes the UE with the highest data rate at time slot n, then either the numerator of $\text{SINR}_{1,j^*,n}$ is larger than the numerator of $\text{SINR}_{1,j,n}$ or the denominator of $\text{SINR}_{1,j^*,n}$ is less than the denominator of $\text{SINR}_{1,j,n}$. Based on our assumption that all UE transmit power is fixed, the higher SINR at the j^*th UE concludes that $h_{1,j^*,n} > h_{1,j,n}$. Therefore, the interference will be decreased, and the total sum rate will be increased. This contradicts the initial optimal assumption; thus, UAV 1 at time slot n must always be given to UE J^*. ∎

5.5.3 Online Trajectory Optimization

In this subsection, given the nth time slot-optimized UAVs-UEs association as well as nth time UE transmit power at iteration r, i.e., $\mathbf{A}_n^r$ and $\mathbf{P}_n^r$, respectively, we find the nth time slot UAVs location to maximize the sum rate. Therefore, the optimization problem $\mathcal{P}$ can be written as follows

$$\mathcal{P}_8 : \max_{\mathbf{Q}_n} \quad \widehat{S}(\mathbf{Q}_n) \tag{5.42a}$$

$$\text{subject to} \quad (5.14b), (5.14c), (5.14d), (5.14i), (5.14j), (5.14l), (5.14k), \tag{5.42b}$$

Algorithm 15 : Online scenario iterative algorithm

 1: Initialize: $\mathbf{Q}_n^{r-1}$, $\mathbf{P}_n^{r-1}$. Let $r = 1$
 2: **Repeat** { to solve $\mathcal{P}$}
 3: **Repeat** for each n in N
 4: For given { $\mathbf{Q}_n^{r-1}$, $\mathbf{A}_n^r$}, use (5.38) to find $\mathbf{P}_n^r$.
 5: For given { $\mathbf{Q}_n^{r-1}$, $\mathbf{P}_n^r$}, solve problem $\mathcal{P}_7$ and find the optimal solution as $\mathbf{A}_n^r$}.
 6: For given {$\mathbf{A}_n^r$, $\mathbf{P}_n^r$}, solve problem $\mathcal{P}_8$ and find the optimal solution as $\mathbf{Q}_n^r$.
 7: Update $r = r + 1$
 8: **Until** Convergence of $\mathbf{Q}$, $\mathbf{P}$, and $\mathbf{A}$
---

where the constraints in (5.14e), (5.14f), (5.14g), and (5.14h) are not functions of $\mathbf{Q}_n$ and are treated as constants.

We solved the online trajectory problem in a way that was similar to the offline one. The only difference between them is that in the former, we were looking to find the next location in the trajectory at each n time slot $\mathbf{Q}_n$. However, in the latter, we wanted to determine the trajectory of overall UAV time slots $\mathbf{Q}$, where the number of decision variables $\mathbf{Q}_n$ is smaller than $\mathbf{Q}$, lead into a lower complexity as well.

5.5.4   Overall Algorithm

In this subsection, we summarize the overall iterative approach to solve problem $\mathcal{P}$ by using the alternating optimization method presented in Algorithm 15. Specifically, the algorithm starts by finding the UEs transmit power using equation (5.38). Then, using the given $\mathbf{P}_n^r$ and $\mathbf{Q}_n^{r-1}$ in the previous iteration, the UAVs-UEs association is found through the implementation of the proposition in 5.5.2. Finally, based on the optimized $\mathbf{A}_n^r$ and calculated $\mathbf{P}_n^r$, the UAVs location $\mathbf{Q}_n^r$ is optimized using CVX. The process repeats until $\mathbf{A}$, $\mathbf{P}$, and $\mathbf{Q}$ converge or until there can be no further improvement in the sum rate.

5.6   Complexity Analysis

In this section, we provide the worst-case complexity analysis of the proposed solutions for both offline and online scenarios.

5.6.1 Offline Scenario Algorithms Complexity Analysis

The worst possible time complexity for Algorithm 12 is $O(NIJ^3)$. This can be justified as follows

- The for loop in line 3 requires a complexity of $O(N)$

- The for loops in lines 4 and 5 require complexities of $O(I)$ and $O(J)$, respectively

- The for loop in line 9 requires a complexity of $O(J-I)$, and the Hungarian algorithm in line 14 requires a complexity of $O(J^3)$.

- The for loops in lines 15 and 16 require complexities of $O(I)$ and $O(J)$, respectively.

As a result, the worst-case complexity of Algorithm 12 is
$O(N)\left(O(IJ) + O(J-I) + O(J^3) + O(IJ)\right) = O(NIJ^3)$.

For Algorithm 13, time complexity can be analyzed as follows:

- The loop in line 3 requires a complexity of $O(I_{ot})$, where I_{ot} is the maximum number of iterations needed to solve (5.17).

- The loop in line 4 requires a complexity of $O(I_{in})$, where I_{in} is the maximum number of iterations needed to to solve (5.21).

- Lines 5-7 requires a complexity of $O(NIJ^3)$.

Hence, the time complexity of Algorithm 13 is $O(I_{ot})O(I_{in})O(NIJ^3) = O(I_{ot}I_{in}NIJ^3)$.

The overall time complexity for Algorithm 14 can be explained as follows:

- The loop in line 2 requires a complexity of $O(I_r)$, where I_r is the maximum number of iterations needed to to solve $\mathcal{P}$.

- As previously discussed, Algorithm 12 for UAVs-UEs association in line 3 requires a complexity of $O(NIJ^3)$.

- Algorithm 13 for finding power in line 4 requires a complexity of $O(I_{ot}I_{in}NIJ^3)$.

- The interior-point algorithm to find the UAVs trajectory requires a complexity of $O(I^3N^3)$ [112].

Hence, The overall time complexity for Algorithm 14 is

$O(I_r)(O(NIJ^3) + O(I_{ot}I_{in}NJ^3) + O(I^3N^3))$.

The overall complexity is of order 3 for the UEs.

5.6.2 Online Scenario Algorithms Complexity Analysis

The time complexity for Algorithm 15 can be evaluated as follows:

- The loop in line 2 requires a complexity of $O(I_n)$, where I_n is the maximum number of iterations needed to to solve $\mathcal{P}$.

- The loop in line 3 requires a complexity of $O(N)$.

- Finding the UAVs-UEs association in line 5 based on the proposition requires a complexity of $O(I^2J)$.

- The interior-point algorithm to find the UAVs trajectory requires a complexity of $O(I^3)$).

Therefore, the overall time complexity for Algorithm is

$O(I_n)O(N)(O(I^2J) + O(I^3))$.

It is obvious that the computational complexity in the online scenario is considerably reduced when compared with the offline scenario.

5.7 Numerical Results

In this section, we demonstrate the effectiveness of the proposed algorithms by providing extensive numerical examples. We consider a system with 2 or 3 UAVs and 10, 20 and 30

ground UEs that are randomly distributed within a 2D area of 500×500 m^2. The UEs can represent cluster heads (CHs), where each collects data from a number of nodes.

We make the following assumptions. All UAVs remain at a fixed height $H = 100$ m. The receiver noise power at ith UAV is assumed to be $\sigma^2 = -110$ dBm as in [101]. The maximum UEs transmit power $P_{\max} = 0.1$ W, the channel gain at the reference distance of $d_0 = 1$ m is set as $\rho_0 = -60$ dB. The maximum speed of UAVs is assumed to be $V_{\max} = 50$ m/s [101]. The threshold in Algorithm 14 is set as 10^{-4}. The minimum distance between UAVs $d_{\min} = 50, 75$, the period time $T = 50$ s.

Fig. 5.2 show the optimized trajectories for 2 UAVs for the offline and online scenarios (Fig. 5.2(a)) with the associated UEs transmit power (Fig. 5.2(b)) in the offline scenario. In Fig. 5.2(a) the green circles illustrate the locations of the UEs. The trajectory of the two UAVs in both scenarios tend to stay away from each other to satisfy the minimum required distance and avoid UAV collision. Moreover, the trajectory of the two UAVs in both scenarios tend to be as close as possible as to the associated ground UEs to maximize the uploaded sum rate. One can see that the UAV trajectory for the online scenario is close to that of its offline counterpart and with comparable sum rates (12.94 bits/sec/Hz for the online scenario vs. 15.06 bits/sec/Hz for the offline scenario).

Fig. 5.3 shows the optimized trajectories for 2 UAVs for the offline and online scenarios (Fig. 5.3(a)) with the associated UEs transmit power (Fig. 5.3(b)). As can be seen from Fig. 5.3(a), the trajectory of the two UAVs in both scenarios satisfy the minimum required distance to avoid UAVs collision. Furthermore, the trajectory of the two UAVs in both scenarios tend to be closer to the corresponding ground UEs to maximize the uploaded sum rate. It is evident that the online UAVs trajectory approaches the offline one with comparable sum rates (13.66 bits/sec/Hz for the online scenario vs. 15.43 bits/sec/Hz for the offline scenario). The trajectory of the UAVs is seen to be identical; however, this happens at different time slots and the minimum distance constraint is not violated. For instance, in Fig. 5.3(a), in the offline scenario, UAV 1 and UAV 2 start to have the same
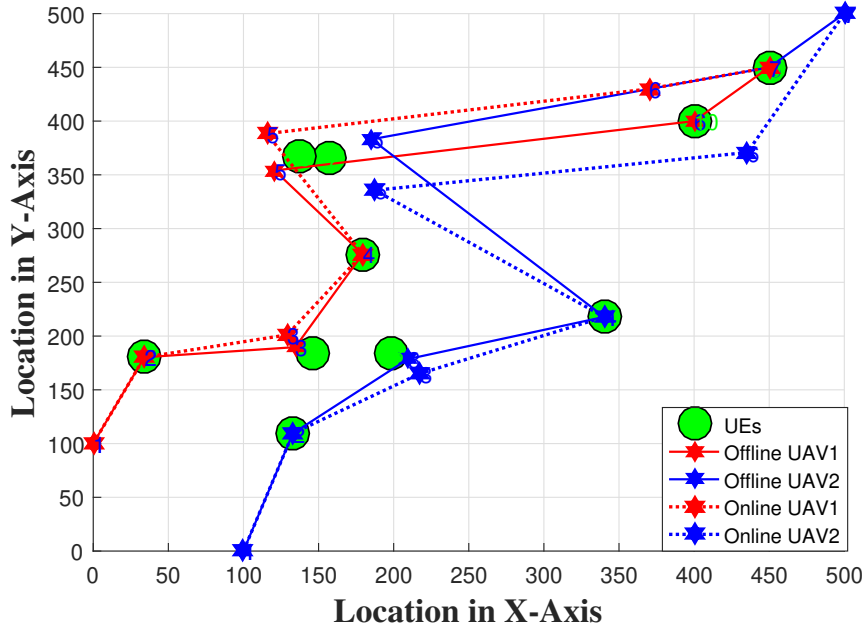
(a) UAVs Trajectory
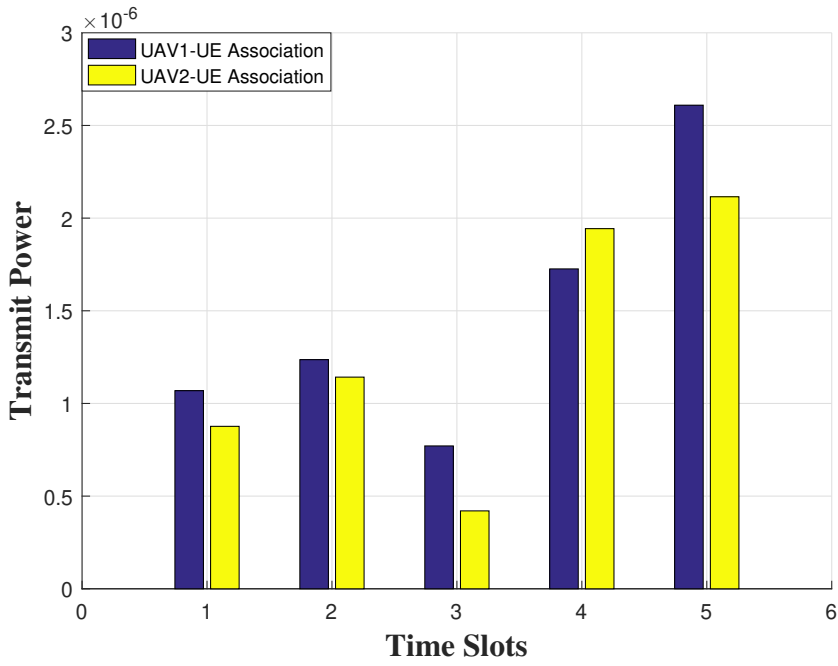
(b) UEs transmit power for the offline scenario.

Figure 5.2: The trajectory of 2 drones flying over 10 UEs for the offline and online scenarios with the associated UEs transmit power.
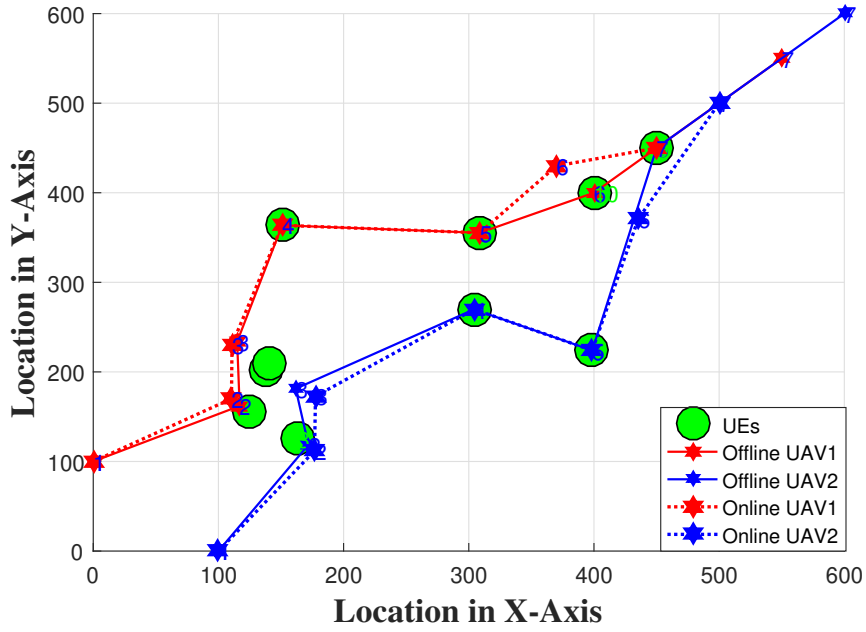
(a) UAVs Trajectory
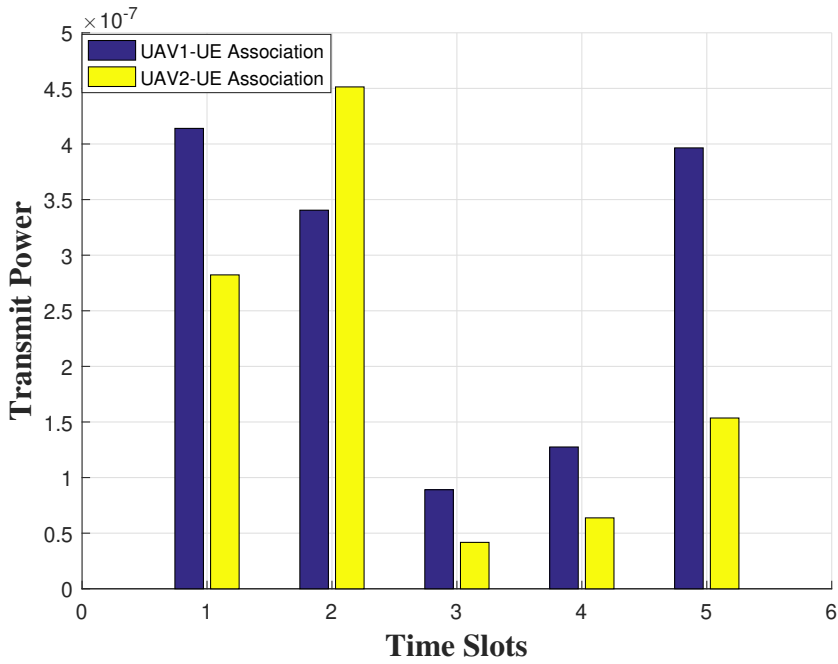

(b) UEs transmit power for the offline scenario.

Figure 5.3: The trajectory of 2 UAVs flying over 10 UEs for the offline and online scenarios with the associated UEs transmit power.

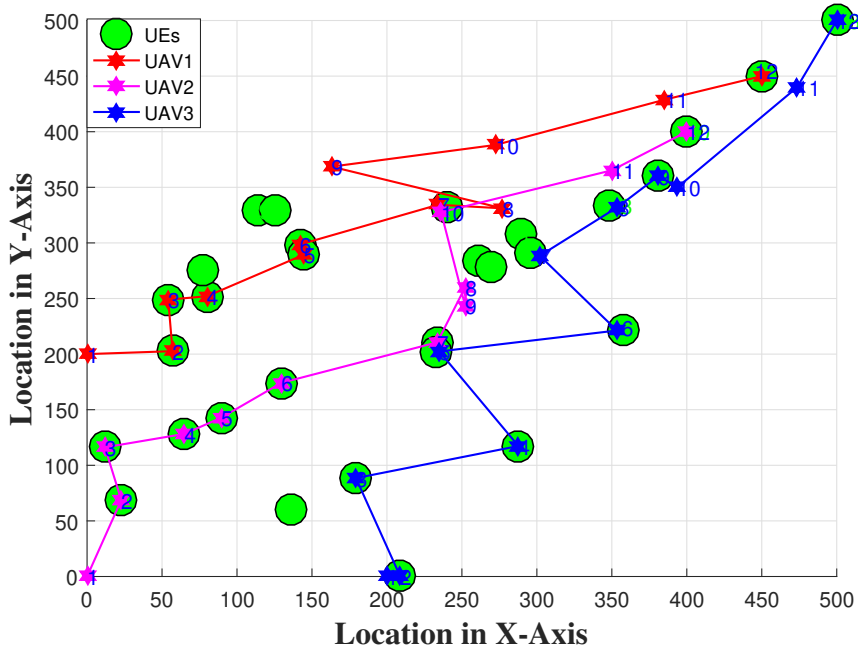trajectory at the 6th time slot of UAV 1 and 5th time slot of UAV 2.

Figure 5.4: The trajectory of 3 UAVs flying over 30 UEs for offline scenario.

Fig. 5.4 shows the optimized trajectories for 3 drones for offline scenario. The trajectory of the three UAVs tends to the ground UEs to reduce the needed transmit power as well as to maximize the total sum rate. Meanwhile, at each time slot, the UAVs trajectory keeps maintaining the minimum distance needed to prevent drone collision.

Fig. 5.5 shows the optimized trajectories for 3 drones in an online scenario. On one hand, the trajectories of the 3 UAVs seeks to be closer to the ground UEs to reduce the transmit power and maximize the total sum rate. Thus, we can notice that UAVs trajectory for the offline scenario in Fig. 5.4 is very close to the UAVs trajectory for the online scenario in Fig. 5.5.

One can see from the trajectory figures that on average the worst distance between the UAVs trajectory in the offline scenario and online scenario does not exceed 30 m. Fig. 5.6 presents a comparison between the offline scenario, and online scenario for 2 UAVs in terms of the average total sum rate in three different cases. First, with 10 UEs, second,
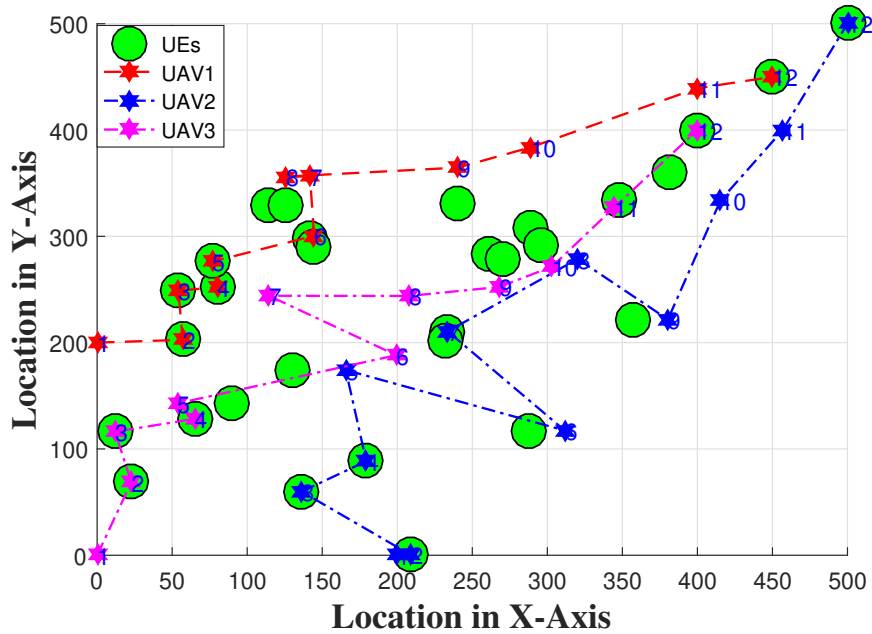
Figure 5.5: The trajectory of 3 UAVs flying over 30 UEs for online scenario.

20 UEs, and third 30 UEs. In all cases, the online scenario total sum rate approaches the offline ones. Thus, the online scenario can achieve comparable sum rates at reduced computational complexity.

5.8 Conclusion

In this chapter, the utilization of UAVs in wireless communication systems was examined using multiple UAVs to serve a group of ground UEs. Our goal was to maximize the total uploaded rate of ground users. This chapter proposed two scenarios (offline and online) for optimizing the UAVs-UEs association jointly with the UEs transmit power and UAVs trajectory. In the offline scenario, we decompose the problem into three sub-problems and found the optimized UAVs-UEs association, UEs transmit power, and UAVs trajectory for all the time slots. In the online scenario, and to further reduce the complexity, we assume fixed transmit power of UEs and derived the optimal UAV-UEs association on a time-slot by time-slot basis. The performance of the proposed algorithm of the online
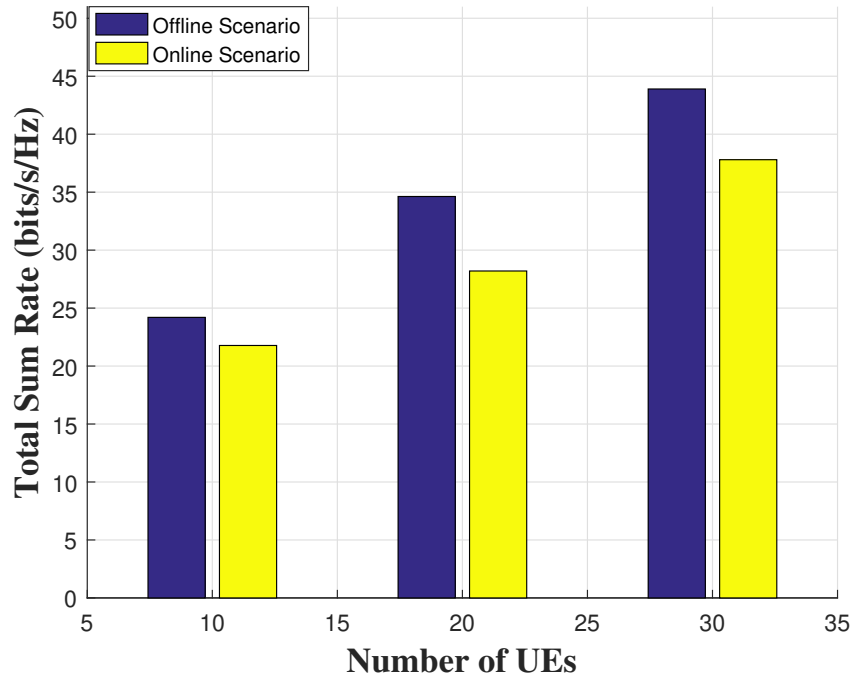
Figure 5.6: The total sum rate in offline and online scenarios with different number of UEs and UAVs.

scenario is found to approach that of its offline counterpart at reduced computational complexity.

Chapter 6

Conclusions and Future Work

6.1 Conclusions

5G+ systems has promised to provide better real-time services, efficient spectrum utilization, energy efficiency, and enhanced coverage. This thesis studied the employment of NFPs in wireless communication systems, where multiple NFPs were used as aerial BSs to serve a group of SCs or UEs. The utilization of NFPs in 5G+ faces undesirable challenges such as the association problem of NFPs and SCs or UEs to maximize the system total sum rate, minimize the system interference or optimize the UAVs trajectory.

This thesis started by studying the association problem between NFPs and SCs to maximize the system sum rate while taking into consideration some limitations such as each NFP bandwidth, the number of supported links, and minimum required SINR. The formulated optimization problem was an integer linear program and the optimal association between the NFPs and SCs is found using numerical solvers at the expense of high computational complexity. However, we proposed two algorithms (centralized and distributed) to reach a sub-optimal association at reduced complexity. The simulation results showed that the performance of the proposed algorithms approaches the counterpart of its optimal solution and outperforms the state-of-the-art techniques from the literature.

After that, this thesis studied the association problem of SCs with NFPs while taking into consideration the following constraints: the number of NFP links, the NFP's maximum bandwidth, whether a target data rate is maintained, in order to achieve a minimized total interference. Two variants were discussed in this work. Both variants were NP-hard problems that can be solved numerically using integer linear programming to obtain the optimal solution.

The first variant minimized total interference while satisfying each SC data rate target and the second variant was to minimize the total interference while maintaining the system total sum rate target. We proposed the bipartite matching and local search based algorithms to obtain sub-optimal solutions with reduced complexity. Integer linear programming based solution was examined to compare the performance of the proposed solutions. Simulation results showed lower interference levels which approaching the derived bound with minimum total interference.

Finally, this thesis examined the utilization of multiple UAVs to serve a group of UEs on the ground. With the aim of maximizing the total uploaded rate of overall ground users in the up-link transmission, we jointly optimized the NFPs-SCs association, the transmit power of the UEs, and the UAV's trajectory. The formulated problem was a mixed-integer non-convex optimization problem, which was challenging to solve.

We considered two scenarios, namely offline and online. With respect to the former, the optimization problem was solved for all time slots, while in the latter, the optimization problem was solved on a time-slot by time-slot basis. We used alternative optimization to find a reduced complexity solution to the offline scenario. For the online scenario, to further reduce the complexity, we assumed fixed UE transmit power and found a closed-form expression of the optimal UAVs-UEs associations. Simulations results showed that, on average, the total uploaded rate of the online scenario approached that of its offline counterpart.

This thesis showed that utilizing NFPs can help to enhance the existing terrestrial

cellular systems in urban areas and provide network coverage in hard-to-reach rural areas.

6.2 Future Work

There are several challenges that still need to be investigated on employing UAVs as flying wireless platforms. Resource management is a major challenge for UAVs networks, due to many factors such as 1) the interaction between the UAVs flight time, energy, path plan, and spectral efficiency, 2) The UAVs strict energy and flight limitations, 3) The UAVs high mobility, and 4) LoS interference produced from ATG and air-to-air links.

Therefore, optimizing and managing resource allocation in UAV-assisted wireless networks is an important issue. Flying UAVs have a limited energy that used for transmission, mobility, control, data processing, and payloads purposes[113]. Hence, the UAVs have a short flight duration that is insufficient for providing long-term, continuous wireless coverage.

Moreover, there is a lot of factors that affect the UAVs energy consumption such as the UAVs mission, navigation path, and the weather conditions. Thus, this energy limitation leads to reduce the flight and hover time durations. Therefore, the UAVs energy and flight constraints should be taken into consideration while designing UAV communication systems. Furthermore, the limited energy is a key constraint for the UAVs deployment and mobility in various applications.

An important future issue is the coverage enhancement of beyond 5G wireless cellular networks by utilizing NFPs. The coverage of existing wireless cellular networks was brought to its limits, which leads to the emergence of a new wireless technologies such as NFPs to enhance the wireless cellular networks coverage. The high-altitude NFPs can achieve 3D coverage in the future communication networks, and it can help to improve the area spectrum efficiency measured in $bits/s/Hz/m^3$ and the area energy efficiency measured in $bits/s/Hz/W/m^3$.

Another issue to be addressed that related to the previous one is to study the three

dimensional (3D) deployment of NFPs. The deployment of the NFPs is a key factor in enhancing wireless cellular networks coverage. Thus, the optimal 3D deployment of NFPs is a challenging issue, as it depends on the locations of ground users, the deployment environment, and NFP's maximum and minimum altitude limitation.

Indeed, the deployment of NFPs is more challenging than that of ground base stations, due to the fact that employing multiple NFPs leads to rising the inter-cell interference on the system performance. In contradict to the terrestrial base stations NFPs need to be deployed in 3D space while taking into consideration the effect of altitude, the NFPs flight time and energy constraints as they impact the network performance.

One more issue is optimizing the 3D UAVs trajectory. In this thesis, we optimized the UAVs trajectory with fixed height. However, working on optimizing the 3D trajectory will enhance the overall wireless networks. Commonly, optimizing the 3D flight path of UAVs is a challenging issue as it requires taking into account many parameters and physical constraints. Such as flight time, energy constraints, UEs demands, and collision avoidance.

Therefore, while finding the 3D UAVs trajectory, various key factors needs to be considered such as channel variation due to the mobility, UAV's dynamics, energy consumption of UAVs, and flight constraints. Moreover, optimizing a continuous UAVs trajectory is an challenging problem as it includes finding infinite numbers of optimization variables (UAV's locations) [114]. In addition, 3D UAVs trajectory optimization requires compatibility between the UAVs mobility and the QoS metrics in wireless communication.

We can explore the use of Machine learning (ML) to enhance UAVs-based wireless communication systems. Thus, ML can help UAVs to dynamically adjust their trajectories to provide better service to the ground users. Moreover, by utilizing neural networks techniques and analyze the data, UAVs can be deployed based on the ground users' behavior prediction (such as users' mobility and their traffic distribution). In addition, the use of ML can help to support large numbers of UAVs and SCs with a reasonable

computational complexity (due to the fact that the computational complexity of the ML at training is normally very high, however, the computational complexity of the machine learning at inference can be low).

Bibliography

[1] J. G. Andrews, S. Buzzi, W. Choi, S. V. Hanly, A. Lozano, A. C. K. Soong, and J. C. Zhang, "What Will 5G Be?," *IEEE Journal on Selected Areas in Communications*, vol. 32, no. 6, pp. 1065–1082, Jun. 2014.

[2] A. Pizzinat, P. Chanclou, F. Saliou, and T. Diallo, "Things you should know about fronthaul," *Journal of Lightwave Technology*, vol. 33, no. 5, pp. 1077–1083, Jan. 2015.

[3] A. Gupta and R. K. Jha, "A Survey of 5G Network: Architecture and Emerging Technologies," *IEEE Access*, vol. 3, pp. 1206–1232, 2015.

[4] W. V. WS, R. Schober, D. W. K. Ng, and L. Wang, *Key technologies for 5G wireless systems.* Cambridge university press, 2017.

[5] "Microwave towards 2020," *Ericsson*, Sep. 2015, accessed on May 18, 2017.

[6] "Buisness case elements for small cell virtualization," *Real Wireless Ltd.*, Jun. 2015, accessed on May 18, 2017.

[7] M. Zuckerberg, "Connecting the world from the sky," *Facearticle Technical Report*, 2014.

[8] I. Bucaille, S. Héthuin, A. Munari, R. Hermenier, T. Rasheed, and S. Allsopp, "Rapidly Deployable Network for Tactical Applications: Aerial Base Station with Opportunistic Links for Unattended and Temporary Events ABSOLUTE Example," in *MILCOM 2013 - 2013 IEEE Military Communications Conference*, pp. 1116–1120, Nov. 2013.

[9] K. Kamnani and C. Suratkar, "A review paper on Google Loon technique," *International Journal of Research In Science & Engineering*, vol. 1, no. 1, pp. 167–171, Mar. 2016.

[10] Q. Wu, J. Xu, and R. Zhang, "UAV-enabled aerial base station (BS) III/III: Capacity characterization of UAV-enabled two-user broadcast channel," *available online: arxiv. org/abs/1801.00443*, Jan. 2018.

[11] M. Alzenad, M. Z. Shakir, H. Yanikomeroglu, and M. Alouini, "FSO-Based Vertical Backhaul/Fronthaul Framework for 5G+ Wireless Networks," *IEEE Communications Magazine*, vol. 56, no. 1, pp. 218–224, Jan. 2018.

[12] H. Ahmadi, K. Katzis, and M. Z. Shakir, "A Novel Airborne Self-Organising Architecture for 5G+ Networks," in *2017 IEEE 86th Vehicular Technology Conference (VTC-Fall)*, pp. 1–5, Sep. 2017.

[13] S. Meng, X. Su, Z. Wen, X. Dai, Y. Zhou, and W. Yang, "Robust drones formation control in 5G wireless sensor network using mmWave," *Wireless Communications and Mobile Computing*, May 2018.

[14] A. Al-Fuqaha, M. Guizani, M. Mohammadi, M. Aledhari, and M. Ayyash, "Internet of things: A survey on enabling technologies, protocols, and applications," *IEEE communications surveys & tutorials*, vol. 17, no. 4, pp. 2347–2376, Jun. 2015.

[15] T. Park, N. Abuzainab, and W. Saad, "Learning How to Communicate in the Internet of Things: Finite Resources and Heterogeneity," *IEEE Access*, vol. 4, pp. 7063–7073, 2016.

[16] A. Zanella, N. Bui, A. Castellani, L. Vangelista, and M. Zorzi, "Internet of Things for Smart Cities," *IEEE Internet of Things Journal*, vol. 1, no. 1, pp. 22–32, Feb. 2014.

[17] A. Ferdowsi and W. Saad, "Deep Learning-Based Dynamic Watermarking for Secure Signal Authentication in the Internet of Things," in *2018 IEEE International Conference on Communications (ICC)*, pp. 1–6, May 2018.

[18] S. Lim and J. Zhu, "Integrated data envelopment analysis: Global vs. local optimum," *European Journal of Operational Research*, vol. 229, no. 1, pp. 276–278, Aug. 2013.

[19] L. A. Wolsey, *Integer programming*, vol. 52. John Wiley & Sons, Sep. 1998.

[20] H. Marchand, A. Martin, R. Weismantel, and L. Wolsey, "Cutting planes in integer and mixed integer programming," *Discrete Applied Mathematics*, vol. 123, no. 1, pp. 397–446, 2002.

[21] J. Clausen, "Branch and bound algorithms-principles and examples," *Department of Computer Science, University of Copenhagen*, pp. 1–30, 1999.

[22] M. Fischetti and D. P. Williamson, *Integer Programming and Combinatorial Optimization*, vol. 4513. Springer, Jun. 2007.

[23] D. S. Johnson, C. H. Papadimitriou, and M. Yannakakis, "How easy is local search?," vol. 37, no. 1, pp. 79–100, Aug. 1988.

[24] E. Aarts, H. Aarts, and K. J. Lenstra, *Local search in combinatorial optimization*. Princeton University Press, 2003.

[25] H. W. Kuhn, "The Hungarian method for the assignment problem," *Naval research logistics quarterly*, vol. 2, no. 1-2, pp. 83–97, 1955.

[26] D. Gale and L. S. Shapley, "College admissions and the stability of marriage," *The American Mathematical Monthly*, vol. 69, no. 1, pp. 9–15, 1962.

[27] S. D. Silvey, "The Lagrangian multiplier test," *The Annals of Mathematical Statistics*, vol. 30, no. 2, pp. 389–407, Jun. 1959.

[28] L. Tang and G. Shao, "Drone remote sensing for forestry research and practices," *Journal of Forestry Research*, vol. 26, no. 4, pp. 791–797, Dec. 2015.

[29] P. Fahlstrom and T. Gleason, *Introduction to UAV systems*. John Wiley & Sons, 2012.

[30] A. Al-Hourani and K. Gomez, "Modeling Cellular-to-UAV Path-Loss for Suburban Environments," *IEEE Wireless Communications Letters*, vol. 7, no. 1, pp. 82–85, Feb. 2018.

[31] K. Nonami, F. Kendoul, S. Suzuki, W. Wang, , and D. Nakazawa, *Autonomous flying robots: unmanned aerial vehicles and micro aerial vehicles*. Springer Science & Business Media, 2010.

[32] A. Al-Hourani, S. Kandeepan, and S. Lardner, "Optimal LAP Altitude for Maximum Coverage," *IEEE Wireless Communications Letters*, vol. 3, no. 6, pp. 569–572, Dec. 2014.

[33] Y. Zeng, R. Zhang, and T. J. Lim, "Wireless communications with unmanned aerial vehicles: opportunities and challenges," *IEEE Communications Magazine*, vol. 54, no. 5, pp. 36–42, May 2016.

[34] M. Ding, P. Wang, D. López-Pérez, G. Mao, and Z. Lin, "Performance Impact of LoS and NLoS Transmissions in Dense Cellular Networks," *IEEE Transactions on Wireless Communications*, vol. 15, no. 3, pp. 2365–2380, Mar. 2016.

[35] T. Ding, M. Ding, G. Mao, Z. Lin, D. López-Pérez, and A. Y. Zomaya, "Uplink Performance Analysis of Dense Cellular Networks With LoS and NLoS Transmissions," *IEEE Transactions on Wireless Communications*, vol. 16, no. 4, pp. 2601–2613, Apr. 2017.

[36] M. Ding and D. Lopez Perez, "Please Lower Small Cell Antenna Heights in 5G," in *2016 IEEE Global Communications Conference (GLOBECOM)*, pp. 1–6, Dec. 2016.

[37] "Performance Impact of Base Station Antenna Heights in Dense Cellular Networks," *IEEE Transactions on Wireless Communications*, vol. 16, no. 12, pp. 8147–8161, Dec. 2017.

[38] S. A. P. Quintero, F. Papi, D. J. Klein, L. Chisci, and J. P. Hespanha, "Optimal UAV coordination for target tracking using dynamic programming," in *49th IEEE Conference on Decision and Control (CDC)*, pp. 4541–4546, Dec. 2010.

[39] A. Fotouhi, M. Ding, and M. Hassan, "Understanding autonomous drone maneuverability for Internet of Things applications," in *2017 IEEE 18th International Symposium on A World of Wireless, Mobile and Multimedia Networks (WoWMoM)*, pp. 1–6, Jun. 2017.

[40] J. Morley, "A World of Proliferated Drones: A Technology Primer," *Arms Control Today*, vol. 45, no. 6, p. 7, Jun. 2015.

[41] Skyfront, "RECORD ENDURANCE."

[42] M. Dudek, P. Tomczyk, P. Wygonik, M. Korkosz, P. Bogusz, , and B. Lis, "Hybrid fuel cell-battery system as a main power unit for small unmanned aerial vehicles (UAV)," *Int. J. Electrochem. Sci*, vol. 8, no. 6, pp. 8442–8463, Jun. 2013.

[43] M. Shaheed, A. Abidali, J. Ahmed, S. Ahmed, I. Burba, P. J. Fani, G. Kwofie, K. Wojewoda, and A. Munjiza, "Flying by the Sun only: The Solarcopter prototype," *Aerospace Science and Technology*, vol. 45, pp. 209–214, Sep. 2015.

[44] S. Sekander, H. Tabassum, and E. Hossain, "Multi-Tier Drone Architecture for 5G/B5G Cellular Networks: Challenges, Trends, and Prospects," *IEEE Communications Magazine*, vol. 56, no. 3, pp. 96–103, Mar. 2018.

[45] H. Wang, G. Ding, F. Gao, J. Chen, J. Wang, and L. Wang, "Power Control in UAV-Supported Ultra Dense Networks: Communications, Caching, and Energy Transfer," *IEEE Communications Magazine*, vol. 56, no. 6, pp. 28–34, Jun. 2018.

[46] M. Ding, D. Lopez-Pérez, G. Mao, and Z. Lin, "Performance Impact of Idle Mode Capability on Dense Small Cell Networks," *IEEE Transactions on Vehicular Technology*, vol. 66, no. 11, pp. 10446–10460, Nov. 2017.

[47] B. Liu, M. Ding, T. Zhu, Y. Xiang, and W. Zhou, "Using Adversarial Noises to Protect Privacy in Deep Learning Era," in *2018 IEEE Global Communications Conference (GLOBECOM)*, pp. 1–6, Dec. 2018.

[48] R. L. Finn, D. Wright, L. Jacques, and P. D. Hert, "Study on privacy, data protection and ethical risks in civil Remotely Piloted Aircraft Systems operations," *Final Report, Luxembourg: Publications Office of the European Union*, vol. 39, Feb. 2014.

[49] B. Canis, "Unmanned aircraft systems (UAS): Commercial outlook for a new industry," Sep. 2015.

[50] C. Stöckera, R. B. andF. Nex, M. Gerke, and J. Zevenbergen, "Review of the current state of UAV regulations," *Remote sensing*, vol. 9, no. 5, p. 459, May 2017.

[51] S. Onoe, "1.3 Evolution of 5G mobile technology toward 1 2020 and beyond," in *2016 IEEE International Solid-State Circuits Conference (ISSCC)*, pp. 23–28, Jan. 2016.

[52] S. Patel, M. Chauhan, and K. Kapadiya, "5G: Future mobile technology-vision 2020," *International Journal of Computer Applications*, vol. 54, no. 17, 2012.

[53] X. Liu, M. Qiu, X. Wang, W. Liu, and K. Cai, "Energy efficiency optimization for communication of air-based information network with guaranteed timing constraints," *Journal of Signal Processing Systems*, vol. 86, no. 2-3, pp. 299–312, Apr. 2016.

[54] M. Mozaffari, W. Saad, M. Bennis, and M. Debbah, "Drone Small Cells in the Clouds: Design, Deployment and Performance Analysis," pp. 1–6, Dec. 2015.

[55] A. L. Rezaabad, H. Beyranvand, J. A. Salehi, and M. Maier, "Ultra-Dense 5G Small Cell Deployment for Fiber and Wireless Backhaul-Aware Infrastructures," *IEEE Transactions on Vehicular Technology*, vol. 67, no. 12, pp. 12231–12243, Dec. 2018.

[56] M. S. Boosters, "drones vs bad weather."

[57] R. Harrison, "All Things Unmanned: The Impact of Weather on UAS."

[58] M. Mozaffari, W. Saad, M. Bennis, Y. Nam, and M. Debbah, "A Tutorial on UAVs for Wireless Networks: Applications, Challenges, and Open Problems," *IEEE Communications Surveys Tutorials*, vol. 21, no. 3, pp. 2334–2360, Mar. 2019.

[59] M. Erdelj and E. Natalizio, "UAV-assisted disaster management: Applications and open issues," pp. 1–5, Feb. 2016.

[60] A. Restas, "Drone applications for supporting disaster management," *World Journal of Engineering and Technology*, vol. 3, no. 03, p. 316, Oct. 2015.

[61] T. J. Tanzi, M. Chandra, D. C. J. Isnard, O. Sébastien, and F. Harivelo, "Towards" drone-borne" disaster management: future application scenarios," in *XXIII ISPRS Congress, Commission VIII (Volume III-8)*, vol. 3, pp. 181–189, Copernicus GmbH, Jul. 2016.

[62] S. A. W. Shah, T. Khattab, M. Z. Shakir, and M. O. Hasna, "A Distributed Approach for Networked Flying Platform Association with Small Cells in 5G+ Networks," in *GLOBECOM 2017-2017 IEEE Global Communications Conference*, pp. 1–7, Dec. 2017.

[63] M. Mozaffari, W. Saad, M. Bennis, and M. Debbah, "Optimal transport theory for power-efficient deployment of unmanned aerial vehicles," in *2016 IEEE International Conference on Communications (ICC)*, pp. 1–6, May 2016.

[64] I. AlQerm and B. Shihada, "Energy-Efficient Power Allocation in Multitier 5G Networks Using Enhanced Online Learning," *IEEE Transactions on Vehicular Technology*, vol. 66, no. 12, pp. 11086–11097, Jul. 2017.

[65] M. Mozaffari, W. Saad, M. Bennis, and M. Debbah, "Wireless Communication Using Unmanned Aerial Vehicles (UAVs): Optimal Transport Theory for Hover Time Optimization, year=2017," *IEEE Transactions on Wireless Communications*, vol. 16, no. 12, pp. 8052–8066.

[66] R. Ghanavi, E. Kalantari, M. Sabbaghian, H. Yanikomeroglu, and A. Yongacoglu, "Efficient 3D aerial base station placement considering users mobility by reinforcement learning," in *2018 IEEE Wireless Communications and Networking Conference (WCNC)*, pp. 1–6, 2018.

[67] E. Kalantari, M. Z. Shakir, H. Yanikomeroglu, and A. Yongacoglu, "Backhaul-aware robust 3D drone placement in 5G+ wireless networks," in *2017 IEEE International Conference on Communications Workshops (ICC Workshops)*, pp. 109–114, 2017.

[68] S. A. W. Shah, T. Khattab, M. Z. Shakir, and M. O. Hasna, "Association of net-worked flying platforms with small cells for network centric 5G+ C-RAN," in *2017 IEEE 28th Annual International Symposium on Personal, Indoor, and Mobile Radio Communications (PIMRC)*, pp. 1–7, Oct. 2017.

[69] Z. Mlika, E. Driouch, W. Ajib, and H. Elbiaze, "A completely distributed algorithm for user association in HetSNets," in *2015 IEEE International Conference on Communications (ICC)*, pp. 2172–2177, Jun. 2015.

[70] S. A. W. Shah, M. G. Khafagy, T. Khattab, M. O. Hasna, and K. Abualsaud, "ICIC-Enabled Association and Channel Selection for UAV-BSs Based on User Locations and Demands," in *2019 IEEE Wireless Communications and Networking Conference Workshop (WCNCW)*, pp. 1–7, 2019.

[71] H. Lewis, "Computers and intractability. A guide to the theory of NP-completeness," 1983.

[72] S. Shah, T. Khattab, M. Shakir, M. Khafagy, and M. Hasna, "Small cell association with networked flying platforms: Novel algorithms and performance bounds," *arXiv preprint arXiv:1802.01117*, Feb. 2018.

[73] E. Balas and E. Zemel, "An algorithm for large zero-one knapsack problems," *operations Research*, vol. 28, no. 5, pp. 1130–1154, Oct. 1980.

[74] D. Gusfield and R. W. Irving, *The stable marriage problem: structure and algorithms*. MIT press, 1989.

[75] Gurobi, "Gurobi Optimizer."

[76] W. Kuhn, "The Hungarian method for the assignment problem," *Naval research logistics quarterly*, vol. 2, no. 1-2, pp. 83–97, Mar. 1955.

[77] E. Aarts and J. karel Lenstra, *Local search in combinatorial optimization*. Princeton University Press, 2003.

[78] E. Hossain, M. Rasti, H. Tabassum, and A. Abdelnasser, "Evolution toward 5G multi-tier cellular wireless networks: An interference management perspective," *IEEE Wireless Communications*, vol. 21, no. 3, pp. 118–127, Jun. 2014.

[79] W. Nam, D. Bai, J. Lee, and I. Kang, "Advanced interference management for 5G cellular networks," *IEEE Communications Magazine*, vol. 52, no. 5, pp. 52–60, May 2014.

[80] H. Zhang, C. Jiang, J. Cheng, and V. C. M. Leung, "Cooperative interference mitigation and handover management for heterogeneous cloud small cell networks," *IEEE Wireless Communications*, vol. 22, no. 3, pp. 92–99, Jul. 2015.

[81] V. Yajnanarayana, Y. . Eric Wang, S. Gao, S. Muruganathan, and X. Lin Ericsson, "Interference Mitigation Methods for Unmanned Aerial Vehicles Served by Cellular Networks," in *2018 IEEE 5G World Forum (5GWF)*, pp. 118–122, Jul. 2018.

[82] T. Han, G. Mao, L. W. Q. Li, and J. Zhang, "Interference Minimization in 5G Heterogeneous Networks," *Mobile Networks and Applications*, vol. 20, no. 6, pp. 756–762, Dec. 2015.

[83] S. Hong, J. Brand, J. I. Choi, M. Jain, J. Mehlman, S. Katti, and P. Levis, "Applications of Self-Interference Cancellation in 5G and Beyond," *IEEE Communications Magazine*, vol. 52, no. 2, pp. 114–121, Feb. 2014.

[84] A. Törn and A. Žilinskas, "Global optimization," Mar. 1989.

[85] H. Y. Alsheyab, S. Choudhury, E. Bedeer, and S. S. Ikki, "Near-Optimal Resource Allocation Algorithms for 5G+ Cellular Networks," *IEEE Tran. on Veh. Tech.*, vol. 68, no. 7, pp. 6578–6592, Jul. 2019.

[86] H. Peng, C. Chen, C. C. Lai, L. C. Wang, and Z. Han, "A Predictive On-Demand Placement of UAV Base Stations Using Echo State Network," in *2019 IEEE/CIC International Conference on Communications in China (ICCC)*, pp. 36–41, 2019.

[87] M. Z. Noohani and K. U. Magsi, "A Review Of 5G Technology: Architecture, Security and wide Applications," vol. 07, pp. 3440–3471, 05 2020.

[88] K. P. Valavanis and G. J. Vachtsevanos, *Handbook of Unmanned Aerial Vehicles.* New Delhi, India: Springer Netherlands, 2015.

[89] Y. Liu, K. Xiong, Q. Ni, P. Fan, and K. B. Letaief, "UAV-Assisted Wireless Powered Cooperative Mobile Edge Computing: Joint Offloading, CPU Control, and Trajectory Optimization," *IEEE Internet of Things Journal*, vol. 7, no. 4, pp. 2777–2790, Apr. 2020.

[90] T. M. Cover and A. A. E. Gamal, "Capacity theorems for the relay channel," *IEEE Trans. Inf. Theory*, vol. 25, no. 5, pp. 572–584, Sep. 1979.

[91] Y. W. Hong, W. J. Huang, F. H. Chiu, and C. C. J. Luo, "Cooperative communications in resource-constrained wireless networks," *IEEE Signal Process. Mag.*, vol. 24, no. 3, pp. 47–57, May 2007.

[92] H. Y. AlSheyab, S. Choudhury, E. Bedeer, and S. S. Ikki, "Interference Minimization Algorithms for Fifth Generation and Beyond Systems," *Computer Communications*, vol. 156, pp. 145–158, Apr. 2020.

[93] Z. Na, Y. Liu, J. Shi, C. Liu, and Z. Gao, "UAV-supported Clustered NOMA for 6G-enabled Internet of Things: Trajectory Planning and Resource Allocation," *IEEE Internet of Things Journal*, pp. 1–1, Jun. 2020.

[94] W. Zhao, M. Ammar, and E. Zegura, "A message ferrying approach for data delivery in sparse mobile ad hoc networks," in *Proceedings of the 5th ACM International Symposium on Mobile ad hoc Networking and Computing*, pp. 187–198, May 2004.

[95] Z. Han, A. L. Swindlehurst, and K. J. R. Liu, "Optimization of MANET connectivity via smart deployment/movement of unmanned air vehicles," *IEEE Trans. Veh. Technol.*, vol. 58, no. 7, pp. 3533–3546, Sep. 2009.

[96] T. A. Johansen, A. Zolich, T. Hansen, and A. J. Sørensen, "Unmanned aerial vehicle as communication relay for autonomous underwater vehicle — Field tests," in *Proceeding 2014 IEEE Globecom Workshops (GC Wkshps)*, pp. 1469–1474, Dec. 2014.

[97] Y. Qian, F. Wang, L. S. J. Li, K. Cai, and F. Shu, "User Association and Path Planning for UAV-Aided Mobile Edge Computing with Energy Restriction," *IEEE Wireless Commun. Letters*, vol. 8, no. 5, pp. 1312–1315, Apr. 2019.

[98] F. Cheng, S. Zhang, Z. Li, Y. Chen, N. Zhao, F. R. Yu, and V. C. M. Leung, "UAV Trajectory Optimization for Data Offloading at the Edge of Multiple Cells," *IEEE Transactions on Vehicular Technology*, vol. 67, no. 7, pp. 6732–6736, 2018.

[99] X. Jing, J. Sun, and C. Masouros, "Energy aware trajectory optimization for aerial base stations," *IEEE Transactions on Communications*, pp. 1–1, 2021.

[100] L. Xie, J. Xu, and R. Zhang, "Throughput Maximization for UAV-Enabled Wireless Powered Communication Networks," *IEEE Internet of Things Journal*, vol. 6, no. 2, pp. 1690–1703, Apr. 2019.

[101] Q. Wu, Y. Zeng, and R. Zhang, "Joint Trajectory and Communication Design for Multi-UAV Enabled Wireless Networks," *IEEE Transactions on Wireless Communications*, vol. 17, no. 3, pp. 2109–2121, Jan. 2018.

[102] C. Shen, T. Chang, J. Gong, Y. Zeng, and R. Zhang, "Multi-uav interference coordination via joint trajectory and power control," *IEEE Transactions on Signal Processing*, vol. 68, pp. 843–858, 2020.

[103] C. Borst, F. Sjer, M. Mulder, M. Van Paassen, and J. Mulder, "Ecological approach to support pilot terrain awareness after total engine failure," *Journal of Aircraft*, vol. 45, no. 1, pp. 159–171, Jan. 2008.

[104] A. Chakrabarty and J. W. Langelaan, "Energy-based long-range path planning for soaring-capable unmanned aerial vehicles," *Journal of Guidance, Control, and Dynamics*, vol. 34, no. 4, pp. 1002–1015, Jul. 2011.

[105] Y. Zeng and R. Zhang, "Energy-efficient UAV communication with trajectory optimization," *IEEE Trans. Wireless Commun.*, vol. 16, no. 6, pp. 3747–3760, Jun. 2017.

[106] Y. Zeng, R. Zhang, and T. J. Lim, "Throughput maximization for UAV-enabled mobile relaying systems," *IEEE Trans. Commun.*, vol. 64, no. 12, pp. 4983–4996, Dec. 2016.

[107] J. Papandriopoulos and J. S. Evans, "SCALE: A Low-Complexity Distributed Protocol for Spectrum Balancing in Multiuser DSL Networks," *IEEE Transactions on Information Theory*, vol. 55, no. 8, pp. 3711–3724, Jul. 2009.

[108] S. Boyd and L. Vandenberghe, *Convex Optimization*. Cambridge, U.K.: Cambridge Univ. Press, 2004.

[109] W. Yu and R. Lui, "Dual methods for nonconvex spectrum optimization of multicarrier systems," *IEEE Transactions on Communications*, vol. 54, no. 7, pp. 1310–1322, Jul. 2006.

[110] D. T. Ngo, S. Khakurel, and T. Le-Ngoc, "Joint subchannel assignment and power allocation for OFDMA femtocell networks," *IEEE Transactions on Wireless Communications*, vol. 13, no. 1, pp. 342–355, Jan. 2014.

[111] D. P. Bertsekas, W. Hager, and O. Mangasarian, *Nonlinear programming*. Athena Scientific Belmont, MA, 1998.

[112] J. Umenberger and I. R. Manchester, "Specialized Interior-Point Algorithm for Stable Nonlinear System Identification," *IEEE Transactions on Automatic Control*, vol. 64, no. 6, pp. 2442–2456, Jun. 2019.

[113] B. Uragun, "Energy Efficiency for Unmanned Aerial Vehicles," in *2011 10th International Conference on Machine Learning and Applications and Workshops*, vol. 2, pp. 316–320, Dec. 2011.

[114] Y. Zeng, R. Zhang, and T. J. Lim, "Wireless communications with unmanned aerial vehicles: opportunities and challenges," *IEEE Communications Magazine*, vol. 54, no. 5, pp. 36–42, May 2016.